10 The MOS model, level 903

10.1 Introduction

General Remarks

MOS Model 9 is a compact MOS-transistor model, intended for the simulation of circuit behaviour with emphasis on analogue applications. The model gives a complete description of all transistor-action related quantities: nodal currents and charges, noise-power spectral densities and weak-avalanche currents. The equations describing these quantities are based on the gradual-channel approximation with a number of first-order corrections for small-size effects. The consistency is maintained by using the same carrier-density and electrical-field expressions in the calculation of all model quantities. Model 9 only provides a model for the intrinsic transistor. Junction charges and leakage currents are not included. They are covered by the separate **Juncap** model. Similarly, interconnect capacitances are deferred to the **Intcap** or **ConnectDPEM** model.

Structural Elements of Model 9

Model 9 is separable into a number of relatively independent parts, namely

- **Preprocessing:** The complete set of all the parameters, as they occur in the equations for the various electrical quantities, is denoted as the set of actual parameters, usually called the "miniset". Each of these actual parameters can be determined by purely electrical measurements. Since most of these parameters scale with geometry and temperature the process as a whole is characterized by an enlarged set of parameters, which is denoted as the set of reference and scaling parameters, usually called the "maxiset". This set of parameters contains most of the actual parameters for a reference device, a large set of sensitivity coefficients and the reference conditions. From this, the actual parameters for an arbitrary transistor under non-reference conditions are obtained by applying a set of transformation rules to the reference parameters. The transformation rules describe the dependencies of the actual parameters on the length, width, and temperature. This procedure is called preprocessing, as it is normally done only once, prior to the actual electrical simulation.

- **Clipping:** For very uncommon geometries or temperatures, the preprocessing rules may generate parameters that are outside a physically realistic range or that may create difficulties in the numerical evaluation of the model, for example division by zero. In order to prevent this, all parameters are limited to a pre-specified range directly after the preprocessing. This procedure is called clipping.

- **Current equations:** These are all expressions needed to obtain the nodal currents as a function of the bias conditions. They are segmentable in equations for the channel current and for the bulk current. For the channel current many auxiliary equations are needed, e.g. equations for the threshold voltage including back-bias dependency and small-size corrections, for the channel-conductance including mobility reduction and velocity saturation effects, and for the subthreshold region. These finally lead to an expression for the channel current I_{DS}. Due to the small device dimensions, high electrical fields occur, in particular in the vicinity of the drain. The carriers that are responsible for the channel current, can gain sufficient energy from this electrical field to induce electron-hole-pair creation. In turn, for an n-channel device, these extra electrons contribute to the channel current as do the holes to the bulk current. Vice versa, the same holds for p-channel devices.

- **Charge equations:** These are all the equations that are used to calculate the charge quantities Q_D, Q_G, Q_S, and Q_B, which are assigned to the nodes. To a large degree the same auxiliary expressions are used as for the current equations. In a few instances deviations were necessary for numerical reasons.

- **Noise equations:** The total noise output of a transistor consists of a thermal- and a flicker-noise part. They create fluctuations in the channel current. Because of the capacitive coupling between gate and channel region, also current fluctuations in the gate current are induced. These two aspects are covered in Model 9 by assigning two correlated noise-current sources, one connected between drain and source, the other one between gate and source, and an uncorrelated noise-current source between drain and source. The correlated current sources are directional!

- **Embedding model 9:** The electrical model only describes the behaviour of an n-channel device. Therefore, any p-channel device and its bias conditions have to be mapped onto those of an equivalent n-channel transistor. This mapping comprises a number of sign-changes. Also, the model describes a symmetrical device, i.e. the source and drain nodes can be interchanged without changing the electrical properties. The assignment of source and drain to the channel nodes is based on the voltages of these nodes: for an n-channel transistor the node at the highest potential is called the drain. In a circuit simulator the nodes are denoted by their network numbers, based on the circuit configuration. Again, a transformation is necessary involving a number of sign changes, including the directional noise-current sources.

Structure of the Documentation

After this introductory section, first the nomenclature as it is used in this model is defined. Next, there is a separate section on the physical background of the model.

Then, each of the structural elements of model 9 is discussed in detail. Finally, a chapter on the general validity range is added. More precise information on the accuracy for a certain type of transistor can be found in the appropriate process document, because such a discussion only makes sense in combination with a specific parameter set. One is therefore referred to the various “Blue Books” (design rules, parameter sets etc.).

10.1.1 Changes from MOS level 902

- A new flicker noise model has been added, which can be selected by setting the switch NFMOD to 1. Selecting the default value NFMOD = 0 yields the previous level 902 flicker noise model. In this way backwards compatibility is achieved.

- The coefficients W_{DOG} and f_{θ_1} have been put in their logical position in the list of scaling parameters.

- In Pstar 4.0, two bugs have been fixed. First, the θ_3-clipping is removed and is circumvented by using suitable ‘hyp-functions’. Second, the back-bias range described by the model is extended from -0.5 ϕ_B to -0.9 ϕ_B .

New geometry scaling rules

- New scaling rules have been implemented in MOS Model 9 for the parameters in the electrical model indicated in the table below. These new scaling rules lead to a considerably improved modelling accuracy, especially for devices with pocket implantations.

Parameter description	Parameter electrical model	New parameter geometrical model
Gain factor	β	$f_{\beta,1}, L_{P,1}$
		$f_{\beta,2}, L_{P,2}$
Body effect at low back-bias	K_0	$S_{L2;K_0}$
Body effect at high back-bias	K	$S_{L2;K}$
Threshold voltage	V_{T0}	$S_{L3;V_{T0}}$
Drain-induced barrier-lowering	γ_{00}	$S_{L2;\gamma_{00}}$
Mobility reduction	θ_1	$g_{\theta 1}$

- The default values of the new parameters have been chosen in such a way that the adapted model is backwards compatible. If they are not specified, you won't notice the change.

10.2 Nomenclature

The symbolic representation and the programming names of the quantities listed in the following sections, have been chosen in such a way to express their purpose and relations to other quantities and to preclude ambiguity and inconsistency.

10.2.1 Glossary of used symbols

All parameters which refer to the reference transistor and/or the reference temperature have a symbol with the subscript R and a programming name ending with R. All characters 0 (zero) in subscripts of parameters are represented by the capital letter O in the programming name. Scaling parameters are indicated by S with a subscript where the variables on which the parameter depends, preceed a semicolon whereas the parameter succeeds it, e.g. $S_{\mathrm{T},L;\theta 1}$. Generally, voltages related to energy levels are indicated by ϕ, exponents by η, the small smoothing parameters by ε and the model constants by λ. In the programming names, the greek characters are abbreviated by the first three letters of their names, e.g. β by BET.

The drain, gate, source and bulk terminals are indicated by D, G, S and B respectively.

The electrical variables are split into the external electrical variables which represent the electrical quantities, observed at the nodes of the physical device, and the internal electrical variables.

External Electrical Variables

The definitions of the external electrical variables are illustrated in Fig. 43.

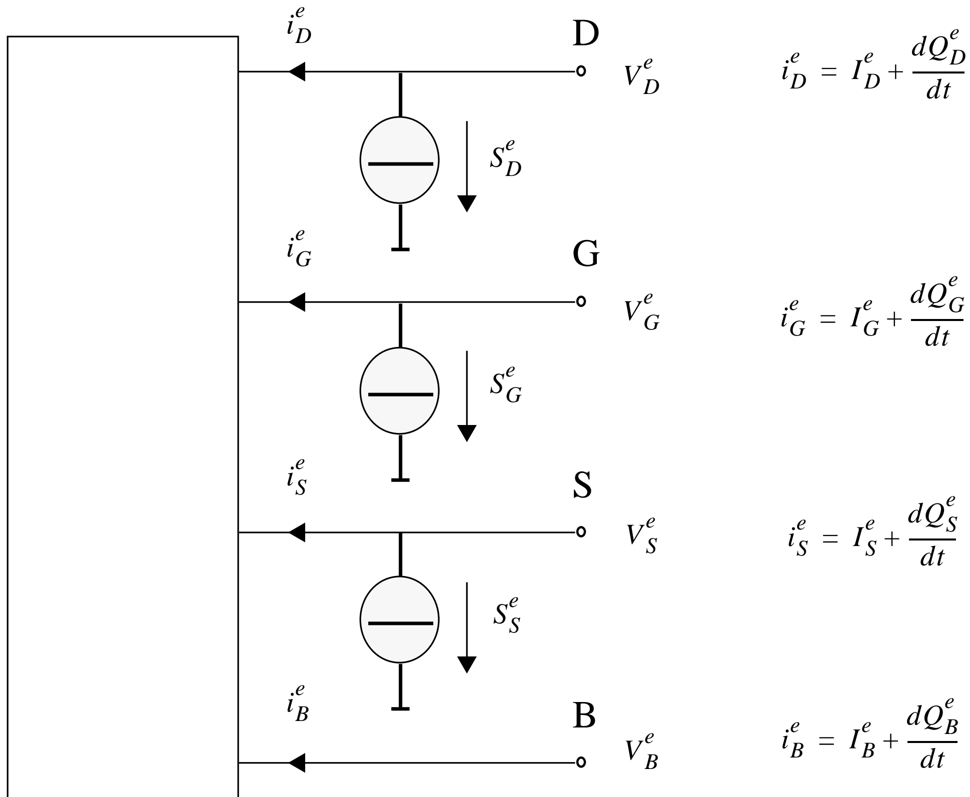

Figure 43: Definition of the external electrical variables

No.	Variable	Prog. Name	Units	Description
1	V_D^e	VDE	V	Potential applied to the drain node
2	V_G^e	VGE	V	Potential applied to the gate node
3	V_S^e	VSE	V	Potential applied to the source node
4	V_B^e	VBE	V	Potential applied to the bulk node
5	I_D^e	IDE	A	DC current into the drain
6	I_G^e	IGE	A	DC current into the gate
7	I_S^e	ISE	A	DC current into the source
8	I_B^e	IBE	A	DC current into the bulk
9	Q_D^e	QDE	C	Charge in the device attributed to the drain node
10	Q_G^e	QGE	C	Charge in the device attributed to the gate node
11	Q_S^e	QSE	C	Charge in the device attributed to the source node
12	Q_B^e	QBE	C	Charge in the device attributed to the bulk node
13	S_D^e	SDE	A^2s	Spectral density of the noise current into the drain
14	S_G^e	SGE	A^2s	Spectral density of the noise current into the gate
15	S_S^e	SSE	A^2s	Spectral density of the noise current into the source

No.	Variable	Prog. Name	Units	Description
16	S^{e}_{DG}	SDGE	A^2s	Cross spectral density of the noise current into the drain and the noise current into the gate
17	S^{e}_{GS}	SGSE	A^2s	Cross spectral density of the noise current into the gate and the noise current into the source
18	S^{e}_{SD}	SSDE	A^2s	Cross spectral density of the noise current into the source and the noise current into the drain

Internal Electrical Variables

No.	Variable	Progr. Name	Units	Description
1	V_{DS}	VDS	V	Drain-to-source voltage applied to the equivalent n-MOS
2	V_{GS}	VGS	V	Gate-to-source voltage applied to the equivalent n-MOS
3	V_{SB}	VSB	V	Source-to-bulk voltage applied to the equivalent n-MOS
4	I_{DS}	IDS	A	DC current through the channel flowing from drain to source
5	I_{AVL}	IAVL	A	DC current flowing from drain to the bulk due to the weak-avalanche effect
6	Q_D	QD	C	Charge in the equivalent n-MOS attributed to the drain node
7	Q_G	QG	C	Charge in the equivalent n-MOS attributed to the gate node
8	Q_S	QS	C	Charge in the equivalent n-MOS attributed to the source node
9	Q_B	QB	C	Charge in the equivalent n-MOS attributed to the bulk node
10	S_{th}	STH	A^2s	Spectral density of the thermal-noise current of the channel
11	S_{fl}	SFL	A^2s	Spectral density of the flicker-noise current of the channel
12	S_{ig}	SIG	A^2s	Spectral density of the noise current induced in the gate
13	S_{igth}	SIGTH	A^2s	Cross spectral density of the noise current induced in the gate and the thermal-noise current of the channel

10.2.2 Parameters

Parameters of the geometrical model

These parameters correspond to the geometrical model (MN, MP) in **Pstar.**

No.	Symbol	Progr. Name	Units	Description
1		LEVEL	-	Must be 903
2	L_{ER}	LER	m	Effective channel length of the reference transistor
3	W_{ER}	WER	m	Effective channel width of the reference transistor
4	ΔL_{PS}	LVAR	m	Difference between the actual and the programmed poly-silicon gate length
5	$\Delta L_{\mathrm{overlap}}$	LAP	m	Effective channel length reduction per side due to the lateral diffusion of the source/drain dopant ions
6	ΔW_{OD}	WVAR	m	Difference between the actual and the programmed field-oxide opening
7	$\Delta W_{\mathrm{narrow}}$	WOT	m	Effective reduction of the channel width per side due to the lateral diffusion of the channel-stop dopant ions
8	T_R	TR	°C	Temperature at which the parameters for the reference transistor have been determined
9	V_{T0R}	VTOR	V	Threshold voltage at zero back-bias for the reference transistor at the reference temperature
10	$S_{T;V_{T0}}$	STVTO	VK^{-1}	Coefficient of the temperature dependence V_{T0}
11	$S_{L;V_{T0}}$	SLVTO	Vm	Coefficient of the length dependence of V_{T0}
12	$S_{L2;V_{T0}}$	SL2VTO	Vm^2	Second coefficient of the length dependence of V_{T0}
13	$S_{L3;V_{T0}}$	SL3VTO	V	Third coefficient of the length dependence of V_{T0}

No.	Symbol	Progr. Name	Units	Description
14	$S_{W;V_{T0}}$	SWVTO	Vm	Coefficient of the width dependence of V_{T0}
15	K_{0R}	KOR	$V^{1/2}$	Low-backbias body factor for the reference transistor
16	$S_{L;K_0}$	SLKO	$V^{1/2}m$	Coefficient of the length dependence of K_0
17	$S_{L2;K_0}$	SL2KO	$V^{1/2}m^2$	Second coefficient of the length dependence of K_0
18	$S_{W;K_0}$	SWKO	$V^{1/2}m$	Coefficient of the width dependence of K_0
19	K_R	KR	$V^{1/2}$	High-backbias body factor for the reference transistor
20	$S_{L;K}$	SLK	$V^{1/2}m$	Coefficient of the length dependence of K
21	$S_{L2;K}$	SL2K	$V^{1/2}m^2$	Second coefficient of the length dependence of K
22	$S_{W;K}$	SWK	$V^{1/2}m$	Coefficient of the width dependence of K
23	ϕ_{BR}	PHIBR	V	Surface potential at strong inversion for the reference transistor at the reference temperature
24	V_{SBXR}	VSBXR	V	Transition voltage for the dual-k-factor model for the reference transistor
25	$S_{L;V_{SBX}}$	SLVSBX	Vm	Coefficient of the length dependence of V_{SBX}
26	$S_{W;V_{SBX}}$	SWVSBX	Vm	Coefficient of the width dependence V_{SBX}
27	β_{sq}	BETSQ	AV^{-2}	Gain factor for an infinite square transistor at the reference temperature
28	η_{β}	ETABET	-	Exponent of the temperature dependence of the gain factor
29	$L_{P,1}$	LP1	m	Characteristic length of first profile
30	$f_{\beta,1}$	FBET1	-	Relative mobility decrease due to first profile

No.	Symbol	Progr. Name	Units	Description
31	$L_{P,2}$	LP2	m	Characteristic length of second profile
32	$f_{\beta,2}$	FBET2	-	Relative mobility decrease due to second profile
33	θ_{1R}	THE1R	V^{-1}	Coefficient of the mobility reduction due to the gate-induced field for the reference transistor at the reference temperature
34	$S_{T;\theta_1,R}$	STTHE1R	$V^{-1}K^{-1}$	Coefficient of the temperature dependence of θ_1 for the reference transistor
35	$S_{L;\theta_1,R}$	SLTHE1R	$V^{-1}m$	Coefficient of the length dependence of θ_1 at the reference temperature
36	$S_{T,L;\theta_1}$	STLTHE1	$V^{-1}mK^{-1}$	Coefficient of the temperature dependence of the length dependence of θ_1
37	g_{θ_1}	GTHE1	-	Parameter that selects either the old ($g_{\theta_1} = 0$) or the new ($g_{\theta_1} = 1$) scaling rule of θ_1
38	$S_{W;\theta_1}$	SWTHE1	$V^{-1}m$	Coefficient of the width dependence of θ_1
39	W_{DOG}	WDOG	m	Characteristic drawn gate width, below which dogboning appears
40	f_{θ_1}	FTHE1	-	Coefficient describing the geometry dependence of θ_1 for $W < W_{DOG}$
41	θ_{2R}	THE2R	$V^{-1/2}$	Coefficient of the mobility reduction due to the back-bias for the reference transistor at the reference temperature
42	$S_{T;\theta_2,R}$	STTHE2R	$V^{-1/2}K^{-1}$	Coefficient of the temperature dependence of θ_2 for the reference transistor
43	$S_{L;\theta_2,R}$	SLTHE2R	$V^{-1/2}m$	Coefficient of the length dependence of θ_2 at the reference temperature
44	$S_{T,L;\theta_2}$	STLTHE2	$V^{-1/2}mK^{-1}$	Coefficent of the temperature dependence of the length dependence of θ_2

No.	Symbol	Progr. Name	Units	Description
45	$S_{W;\theta_2}$	SWTHE2	$V^{-1/2}m$	Coefficient of the width dependence of θ_2
46	θ_{3R}	THE3R	V^{-1}	Coefficient of the mobility reduction due to the lateral field for the reference transistor at the reference temperature
47	$S_{T;\theta_3,R}$	STTHE3R	$V^{-1}K^{-1}$	Coefficient of the temperature dependence of θ_3 for the reference temperature
48	$S_{L;\theta_3,R}$	SLTHE3R	$V^{-1}m$	Coefficient of the length dependence of θ_3 at the reference temperature
49	$S_{T,L;\theta_3}$	STLTHE3	$V^{-1}mK^{-1}$	Coefficient of the temperature dependence of the length dependence of θ_3
50	$S_{W;\theta_3}$	SWTHE3	$V^{-1}m$	Coefficient of the width dependence of θ_3
51	γ_{1R}	GAM1R	$V^{(1-\eta_{DS})}$	Coefficient for the drain induced threshold shift for large gate drive for the reference transistor
52	$S_{L;\gamma_1}$	SLGAM1	$V^{(1-\eta_{DS})}m$	Coefficient of the length dependence of γ_1
53	$S_{W;\gamma_1}$	SWGAM1	$V^{(1-\eta_{DS})}m$	Coefficient of the width dependence of γ_1
54	η_{DSR}	ETADSR	-	Exponent of the V_{DS} dependence of γ_1 for the reference transistor
55	α_R	ALPR	-	Factor of the channel-length modulation for the reference transistor
56	η_α	ETAALP	-	Exponent of the length dependence of α
57	$S_{L;\alpha}$	SLALP	m^{η_α}	Coefficient of the length dependence of α
58	$S_{W;\alpha}$	SWALP	m	Coefficient of the width dependence of α
59	V_{PR}	VPR	V	Characteristic voltage of the channel-length modulation for the reference transistor

No.	Symbol	Progr. Name	Units	Description
60	γ_{00R}	GAMOOR	-	Coefficient of the drain induced threshold shift at zero gate drive for the reference transistor
61	$S_{L;\gamma_{00}}$	SLGAMOO	m^2	Coefficient of the length dependence of γ_{00}
62	$S_{L2;\gamma_{00}}$	SL2GAMOO	-	Second coefficient of the length dependence of γ_{00}
63	$\eta_{\gamma R}$	ETAGAMR	-	Exponent of the back-bias dependence of γ_0 for the reference transistor
64	m_{0R}	MOR	-	Factor of the subthreshold slope for the reference transistor at the reference temperature
65	$S_{T;m_0}$	STMO	K^{-1}	Coefficient of the temperature dependence of m_0
66	$S_{L;m_0}$	SLMO	$m^{1/2}$	Coefficient of the length dependence of m_0
67	η_{mR}	ETAMR	-	Exponent of the back-bias dependence of m for the reference transistor
68	ζ_{1R}	ZET1R	-	Weak-inversion correction factor for the reference transistor
69	η_ζ	ETAZET	-	Exponent of the length dependence of ζ_1
70	$S_{L;\varsigma_1}$	SLZET1	m^{η_ζ}	Coefficient of the length dependence of ζ_1
71	V_{SBTR}	VSBTR	V	Limiting voltage of the V_{SB} dependence of m and γ_0 for the reference transistor
72	$S_{L;V_{SBT}}$	SLVSBT	Vm	Coefficient of the length dependence of V_{SBT}
73	a_{1R}	A1R	-	Factor of the weak-avalanche current for the reference transistor at the reference temperature
74	$S_{T;a_1}$	STA1	K^{-1}	Coefficient of the temperature dependence of a_1

No.	Symbol	Progr. Name	Units	Description
75	$S_{L;a_1}$	SLA1	m	Coefficient of the length dependence of a_1
76	$S_{W;a_1}$	SWA1	m	Coefficient of the width dependence of a_1
77	a_{2R}	A2R	V	Exponent of the weak-avalanche current for the reference transistor
78	$S_{L;a_2}$	SLA2	Vm	Coefficient of the length dependence of a_2
79	$S_{W;a_2}$	SWA2	Vm	Coefficient of the width dependence of a_2
80	a_{3R}	A3R	-	Factor of the drain-source voltage above which weak-avalanche occurs, for the reference transistor
81	$S_{L;a_3}$	SLA3	m	Coefficient of the length dependence of a_3
82	$S_{W;a_3}$	SWA3	m	Coefficient of the width dependence of a_3
83	t_{ox}	TOX	m	Thickness of the gate-oxide layer. t_{ox} is used for calculation of 1/f noise and C_{ox}, not for β !!!
84	C_{ol}	COL	Fm^{-1}	Gate overlap capacitance per unit channel width
85	N_{TR}	NTR	J	Coefficient of the thermal noise for the reference transistor
86	*NFMOD*	NFMOD	-	Switch that selects either old or new flicker noise model
87	N_{FR}	NFR	V^2	Flicker noise coefficient of the reference transistor (for NFMOD = 0)
88	N_{FAR}	NFAR	$V^{-1}m^{-4}$	First coefficient of the flicker noise of the reference transistor (for NFMOD = 1)
89	N_{FBR}	NFBR	$V^{-1}m^{-2}$	Second coefficient of the flicker noise of the reference transistor (for NFMOD = 1)
90	N_{FCR}	NFCR	V^{-1}	Third coefficient of the flicker noise of the reference transistor (for NFMOD = 1)
91	L	L	m	Drawn channel length in the lay-out of the actual transistor

No.	Symbol	Progr. Name	Units	Description
92	W	W	m	Drawn channel width in the lay-out of the actual transistor
93	ΔT_A	DTA	°C	Temperature offset of the device with respect to T_A
94	N_{MULT}	MULT	-	Number of devices in parallel

Remark: The parameters *L, W*, and *DTA* are used to calculate the electrical parameters of the actual transistor, as specified in the section on parameter preprocessing.

Parameters of the electrical model

These parameter correspond to the electrical model in **Pstar** (MNE, MPE).

No.	Symbol	Progr. Name	Units	Description
1		LEVEL	-	Must be 903
2	V_{T0}	VTO	V	Threshold voltage at zero back-bias for the actual transistor at the actual temperature
3	K_0	K0	$V^{1/2}$	Low-backbias body factor for the actual transistor
4	K	K	$V^{1/2}$	High-backbias body factor for the actual transistor
5	ϕ_B	PHIB	V	Surface potential at strong inversion for the actual transistor at the actual temperature
6	V_{SBX}	VSBX	V	Transition voltage for the dual-k-factor model for the actual transistor
7	β	BET	AV^{-2}	Gain factor for the actual transistor at the actual temperature
8	θ_1	THE1	V^{-1}	Coefficient of the mobility reduction due to the gate-induced field for the actual transistor at the actual temperature
9	θ_2	THE2	$V^{-1/2}$	Coefficient of the mobility reduction due to the back-bias for the actual transistor at the actual temperature
10	θ_3	THE3	V^{-1}	Coefficient of the mobility reduction due to the lateral field for the actual transistor at the actual temperature
11	γ_1	GAM1	$V^{(1-\eta_{DS})}$	Coefficient for the drain induced threshold shift for large gate drive for the actual transistor
12	η_{DS}	ETADS	-	Exponent of the V_{DS} dependence of γ_1 for the actual transistor
13	α	ALP	-	Factor of the channel-length modulation for the actual transistor

No.	Symbol	Progr. Name	Units	Description
14	V_P	VP	V	Characteristic voltage of the channel-length modulation for the actual transistor
15	γ_{00}	GAM00	-	Coefficient of the drain induced threshold shift at zero gate drive for the actual transistor
16	η_γ	ETAGAM	-	Exponent of the back-bias dependence of γ_0 for the actual transistor
17	m_0	MO	-	Factor of the subthreshold slope for the actual transistor at the actual temperature
18	η_m	ETAM	-	Exponent of the back-bias dependence m for the actual transistor
19	ϕ_T	PHIT	V	Thermal voltage at the actual temperature
20	ζ_1	ZET1	-	Weak-inversion correction factor for the actual transistor
21	V_{SBT}	VSBT	V	Limiting voltage of V_{SB} dependence of m and γ_0 for the actual transistor
22	a_1	A1	-	Factor of the weak-avalanche current for the actual transistor
23	a_2	A2	V	Exponent of the weak-avalanche current for the actual transistor
24	a_3	A3	-	Factor of the drain-source voltage above which weak-avalanche occurs for the actual transistor
25	C_{ox}	COX	F	Gate-to-channel capacitance for the actual transistor
26	C_{GDO}	CGDO	F	Gate-drain overlap capacitance for the actual transistor
27	C_{GSO}	CGSO	F	Gate-source overlap capacitance for the actual transistor
28	N_T	NT	J	Coefficient of the thermal noise for the actual transistor
29	*NFMOD*	NFMOD	-	Switch that selects either old or new flicker noise model

No.	Symbol	Progr. Name	Units	Description
30	N_F	NF	V^2	Flicker noise coefficient of the actual transistor (for NFMOD = 0)
31	N_{FA}	NFA	$V^{-1}m^{-4}$	First coefficient of the flicker noise of the actual transistor (for NFMOD = 1)
32	N_{FB}	NFB	$V^{-1}m^{-2}$	Second coefficient of the flicker noise of the actual transistor (for NFMOD = 1)
33	N_{FC}	NFC	V^{-1}	Third coefficient of the flicker noise of the actual transistor (for NFMOD = 1)
34	t_{ox}	TOX	m	Thickness of the gate-oxide layer ✓
35	$MULT$	MULT	-	Number of devices operating in parallel

✓ Note

t_{ox} is used for calculation of 1/f noise, not for β !!!

10.2.3 Model constants

The following is a list of constants hardcoded in **Pstar**.

No.	Constant	Units	Description
1	T_0	K	Offset for conversion from Celsius to Kelvin temperature scale (273.15)
2	k	JK^{-1}	Boltzmann constant $(1.3806226 \cdot 10^{-23})$
3	q	C	Elementary unit charge $(1.6021918 \cdot 10^{-19})$
4	ε_{ox}	Fm^{-1}	Absolute permittivity of the oxide layer $(3.453143800 \cdot 10^{-11})$

10.3 Pstar specific items

10.3.1 Syntax

n-channel geometrical model	:	MN_n (D, G, S, B)	<parameters>
p-channel geometrical model	:	MP_n (D, G, S, B)	<parameters>
n-channel electrical model	:	MNE_n (D, G, S, B)	<parameters>
p-channel electrical model	:	MPE_n (D, G, S, B)	<parameters>

n	:	occurrence indicator
<parameters>	:	list of model parameters

D, G, S and B are drain, gate, source and bulk terminals respectively.

10.3.2 Pstar specific values

The default values and clipping values as used by **Pstar** for the parameters of the geometrical MOS model, level 903 (n-channel) are listed below.

No.	Parameter	Units	Default	Clip low	Clip high
1	*LEVEL*	-	903	-	-
2	*LER*	m	1.10×10^{-6}	1.0×10^{-10}	-
3	*WER*	m	20.00×10^{-6}	1.0×10^{-10}	-
4	*LVAR*	m	-0.220×10^{-6}	-	-
5	*LAP*	m	0.100×10^{-6}	-	-
6	*WVAR*	m	-0.025×10^{-6}	-	-
7	*WOT*	m	0.000×10^{-6}	-	-
8	*TR*	°C	21.00	-273.15	-
9	*VTOR*	V	0.730	-	-
10	*STVTO*	VK^{-1}	-1.20×10^{-3}	-	-
11	*SLVTO*	Vm	-0.135×10^{-6}	-	-
12	*SL2VTO*	Vm^2	0.0	-	-
13	*SL3VTO*	V	0.0	-	-
14	*SWVTO*	Vm	0.130×10^{-6}	-	-
15	*KOR*	$V^{1/2}$	0.650	-	-
16	*SLKO*	$V^{1/2}m$	-0.130×10^{-6}	-	-
17	*SL2KO*	$V^{1/2}m^2$	0.0	-	-
18	*SWKO*	$V^{1/2}m$	0.002×10^{-6}	-	-
19	*KR*	$V^{1/2}$	0.110	-	-
20	*SLK*	$V^{1/2}m$	-0.280×10^{-6}	-	-
21	*SL2K*	$V^{1/2}m^2$	0.0	-	-

No.	Parameter	Units	Default	Clip low	Clip high
22	*SWK*	$V^{1/2}m$	0.275×10^{-6}	-	-
23	*PHIBR*	V	0.650	-	-
24	*VSBXR*	V	0.660	-	-
25	*SLVSBX*	Vm	0.000×10^{-6}	-	-
26	*SWVSBX*	Vm	-0.675×10^{-6}	-	-
27	*BETSQ*	AV^{-2}	83.00×10^{-6}	-	-
28	*ETABET*	-	1.600	-	-
29	*LP1*	m	1.0×10^{-6}	1.0×10^{-10}	-
30	*FBET1*	-	0.0	-	-
31	*LP2*	m	1.0×10^{-8}	1.0×10^{-10}	-
32	*FBET2*	-	0.0	-	-
33	*THE1R*	V^{-1}	0.190	-	-
34	*STTHE1R*	$V^{-1}K^{-1}$	0.000×10^{-3}	-	-
35	*SLTHE1R*	$V^{-1}m$	0.140×10^{-6}	-	-
36	*STLTHE1*	$V^{-1}mK^{-1}$	0.000×10^{-3}	-	-
37	*GTHE1*	-	0.0	0.0	1.0
38	*SWTHE1*	$V^{-1}m$	-0.058×10^{-6}	-	-
39	*WDOG*	m	0.0	0.0	-
40	*FTHE1*	-	0.0	-	-
41	*THE2R*	$V^{-1/2}$	0.012	-	-
42	*STTHE2R*	$V^{-1/2}K^{-1}$	0.000×10^{-9}	-	-
43	*SLTHE2R*	$V^{-1/2}m$	-0.033×10^{-6}	-	-
44	*STLTHE2*	$V^{-1/2}mK^{-1/2}$	0.000×10^{-3}	-	-
45	*SWTHE2*	$V^{-1/2}m$	0.030×10^{-6}	-	-

No.	Parameter	Units	Default	Clip low	Clip high
46	*THE3R*	V^{-1}	0.145	-	-
47	*STTHE3R*	$V^{-1}K^{-1}$	-0.660×10^{-3}	-	-
48	*SLTHE3R*	$V^{-1}m$	0.185×10^{-6}	-	-
49	*STLTHE3*	$V^{-1}mK^{-1}$	-0.620×10^{-9}	-	-
50	*SWTHE3*	$V^{-1}m$	0.020×10^{-6}	-	-
51	*GAM1R*	$V^{(1-\eta_{DS})}$	0.145	-	-
52	*SLGAM1*	$V^{(1-\eta_{DS})}$ m	0.160×10^{-6}	-	-
53	*SWGAM1*	$V^{(1-\eta_{DS})}$ m	-0.010×10^{-6}	-	-
54	*ETADSR*	-	0.600	-	-
55	*ALPR*	-	0.003	-	-
56	*ETAALP*	-	0.150	-	-
57	*SLALP*	m^{η_α}	-5.65×10^{-3}	-	-
58	*SWALP*	m	1.67×10^{-9}	-	-
59	*VPR*	V	0.340	-	-
60	*GAMOOR*	-	0.018	-	-
61	*SLGAMOO*	m^2	20.00×10^{-15}	-	-
62	*SL2GAMOO*	-	0.0	-	-
63	*ETAGAMR*	-	2.0	-	-
64	*MOR*	-	0.500	-	-
65	*STMO*	K^{-1}	$0.000 \times 10^{+0}$	-	-
66	*SLMO*	$m^{1/2}$	0.280×10^{-3}	-	-
67	*ETAMR*	-	2.0	-	-
68	*ZET1R*	-	0.420	-	-
69	*ETAZET*	-	0.170	-	-

No.	Parameter	Units	Default	Clip low	Clip high
70	*SLZET1*	m^{η_ζ}	-0.390	-	-
71	*VSBTR*	V	2.10	-	-
72	*SLVSBT*	Vm	-4.40×10^{-6}	-	-
73	*A1R*	-	6.00	-	-
74	*STA1*	K^{-1}	$0.000 \times 10^{+0}$	-	-
75	*SLA1*	m	1.30×10^{-6}	-	-
76	*SWA1*	m	3.00×10^{-6}	-	-
77	*A2R*	V	38.0	-	-
78	*SLA2*	Vm	1.00×10^{-6}	-	-
79	*SWA2*	Vm	2.00×10^{-6}	-	-
80	*A3R*	-	0.650	-	-
81	*SLA3*	m	-0.550×10^{-6}	-	-
82	*SWA3*	m	0.000×10^{-6}	-	-
83	*TOX*	m	25.0×10^{-9}	-	-
84	*COL*	Fm^{-1}	0.320×10^{-9}	-	-
85	*NTR*	J	0.244×10^{-19}	-	-
86	*NFMOD*	-	0	-	-
87	*NFR*	V^2	-	-	-
88	*NFAR*	$V^{-1}m^{-4}$	7.15×10^{22}	10^{-12}	-
89	*NFBR*	$V^{-1}m^{-2}$	2.16×10^{7}	-	-
90	*NFCR*	V^{-1}	0	-	-
91	*L*	m	1.50×10^{-6}	-	-
92	*W*	m	20.0×10^{-6}	-	-
93	*DTA*	°C	0.0	-	-

No.	Parameter	Units	Default	Clip low	Clip high
94	*MULT*	-	1.0	0.0	-

The default values and clipping values as used by **Pstar** for the parameters of the geometrical MOS model, level 903 (p-channel) are listed below.

No.	**Parameter**	**Units**	**Default**	**Clip low**	**Clip high**
1	*LEVEL*	-	903	-	-
2	*LER*	m	1.25×10^{-6}	1.0×10^{-10}	-
3	*WER*	m	20.00×10^{-6}	1.0×10^{-10}	-
4	*LVAR*	m	-0.460×10^{-6}	-	-
5	*LAP*	m	0.025×10^{-6}	-	-
6	*WVAR*	m	-0.130×10^{-6}	-	-
7	*WOT*	m	0.000×10^{-6}	-	-
8	*TR*	°C	21.0	-273.15	-
9	*VTOR*	V	1.100	-	-
10	*STVTO*	VK^{-1}	-1.7×10^{-3}	-	-
11	*SLVTO*	Vm	0.035×10^{-6}	-	-
12	*SL2VTO*	Vm	0.0	-	-
13	*SL3VTO*	V	0.0	-	-
14	*SWVTO*	Vm	0.050×10^{-6}	-	-
15	*KOR*	$V^{1/2}$	0.470	-	-
16	*SLKO*	$V^{1/2}m$	-0.200×10^{-6}	-	-
17	*SL2KO*	$V^{1/2}m^2$	0.0	-	-
18	*SWKO*	$V^{1/2}m$	0.115×10^{-6}	-	-
19	*KR*	$V^{1/2}$	0.470	-	-
20	*SLK*	$V^{1/2}m$	-0.200×10^{-6}	-	-
21	*SL2K*	$V^{1/2}m^2$	0.0	-	-
22	*SWK*	$V^{1/2}m$	0.115×10^{-6}	-	-

No.	Parameter	Units	Default	Clip low	Clip high
23	*PHIBR*	V	0.650	-	-
24	*VSBXR*	V	0.0	-	-
25	*SLVSBX*	Vm	0.0	-	-
26	*SWVSBX*	Vm	0.0	-	-
27	*BETSQ*	AV^{-2}	26.1×10^{-6}	-	-
28	*ETABET*	-	1.6	-	-
29	*LP1*	m	1.0×10^{-6}	1.0×10^{-10}	-
30	*FBET1*	-	0.0	-	-
31	*LP2*	m	1.0×10^{-8}	1.0×10^{-10}	-
32	*FBET2*	-	0.0	-	-
33	*THE1R*	V^{-1}	0.190	-	-
34	*STTHE1R*	$V^{-1}K^{-1}$	0.000×10^{-3}	-	-
35	*SLTHE1R*	$V^{-1}m$	0.70×10^{-6}	-	-
36	*STLTHE1*	$V^{-1}mK^{-1}$	0.000×10^{-3}	-	-
37	*GTHE1*	-	0.0	0.0	1.0
38	*SWTHE1*	$V^{-1}m$	-0.080×10^{-6}	-	-
39	*WDOG*	m	0.0	0.0	-
40	*FTHE1*	-	0.0	-	-
41	*THE2R*	$V^{-1/2}$	0.165	-	-
42	*STTHE2R*	$V^{-1/2}K^{-1}$	0.000×10^{-9}	-	-
43	*SLTHE2R*	$V^{-1/2}m$	-0.075×10^{-6}	-	-
44	*STLTHE2*	$V^{-1/2}mK^{-1/2}$	0.000×10^{-3}	-	-
45	*SWTHE2*	$V^{-1/2}m$	0.020×10^{-6}	-	-
46	*THE3R*	V^{-1}	0.027	-	-
47	*STTHE3R*	$V^{-1}K^{-1}$	0.000×10^{-9}	-	-

No.	Parameter	Units	Default	Clip low	Clip high
48	*SLTHE3R*	$V^{-1}m$	0.027×10^{-6}	-	-
49	*STLTHE3*	$V^{-1}mK^{-1}$	0.000×10^{-3}	-	-
50	*SWTHE3*	$V^{-1}m$	0.011×10^{-6}	-	-
51	*GAM1R*	$V^{(1-\eta_{DS})}$	0.077	-	-
52	*SLGAM1*	$V^{(1-\eta_{DS})}m$	0.105×10^{-6}	-	-
53	*SWGAM1*	$V^{(1-\eta_{DS})}m$	-0.011×10^{-6}	-	-
54	*ETADSR*	-	$0.600 \times 10^{+0}$	-	-
55	*ALPR*	-	0.044	-	-
56	*ETAALP*	-	0.170	-	-
57	*SLALP*	m^{η_α}	9.00×10^{-3}	-	-
58	*SWALP*	m	0.180×10^{-9}	-	-
59	*VPR*	V	0.235	-	-
60	*GAMOOR*	-	0.007	-	-
61	*SLGAMOO*	m^2	11.0×10^{-15}	-	-
62	*SL2GAMOO*	-	0.0	-	-
63	*ETAGAMR*	-	1.0	-	-
64	*MOR*	-	0.375	-	-
65	*STMO*	K^{-1}	$0.000 \times 10^{+0}$	-	-
66	*SLMO*	$m^{1/2}$	0.047×10^{-3}	-	-
67	*ETAMR*	-	1.0	-	-
68	*ZET1R*	-	1.30	-	-
69	*ETAZET*	-	0.03	-	-
70	*SLZET1*	m^{η_α}	-2.80	-	-

No.	Parameter	Units	Default	Clip low	Clip high
71	*VSBTR*	V	100.0	-	-
72	*SLVSBT*	Vm	0.00×10^{-6}	-	-
73	*A1R*	-	10.0	-	-
74	*STA1*	K^{-1}	$0.000 \times 10^{+0}$	-	-
75	*SLA1*	m	-15.0×10^{-6}	-	-
76	*SWA1*	m	30.0×10^{-6}	-	-
77	*A2R*	V	59.0	-	-
78	*SLA2*	Vm	-8.00×10^{-6}	-	-
79	*SWA2*	Vm	15.0×10^{-6}	-	-
80	*A3R*	-	0.520	-	-
81	*SLA3*	m	-0.450×10^{-6}	-	-
82	*SWA3*	m	-0.140×10^{-6}	-	-
83	*TOX*	m	25.0×10^{-9}	-	-
84	*COL*	Fm^{-1}	0.320×10^{-9}	-	-
85	*NTR*	J	0.211×10^{-19}	-	-
86	*NFMOD*	-	0	-	-
87	*NFR*	V^2	-	-	-
88	*NFAR*	$V^{-1}m^{-4}$	1.53×10^{22}	10^{-12}	-
89	*NFBR*	$V^{-1}m^{-2}$	4.06×10^{6}	-	-
90	*NFCR*	V^{-1}	2.92×10^{-10}	-	-
91	*L*	m	1.50×10^{-6}	-	-
92	*W*	m	20.0×10^{-6}	-	-
93	*DTA*	°C	0.0	-	-
94	*MULT*	-	1.0	0.0	-

The default values and clipping values as used by **Pstar** for the parameters of the electrical MOS model, level 903 (n-channel) are listed below.

No.	**Parameter**	Units	**Default**	Clip low	**Clip high**
1	*LEVEL*	-	903	-	-
2	*VTO*	V	7.099154×10^{-01}	-	-
3	*KO*	$V^{1/2}$	6.478116×10^{-01}	1.0×10^{-12}	-
4	*K*	$V^{1/2}$	4.280174×10^{-01}	See note [a]	-
5	*PHIB*	V	6.225999×10^{-01}	1.0×10^{-12}	-
6	*VSBX*	V	6.599578×10^{-01}	1.0×10^{-12}	-
7	*BET*	AV^{-2}	1.418789×10^{-03}	0.0	-
8	*THE1*	V^{-1}	1.923533×10^{-01}	0.0	-
9	*THE2*	$V^{-1/2}$	1.144632×10^{-02}	0.0	1.0
10	*THE3*	V^{-1}	1.381597×10^{-01}	-	-
11	*GAM1*	$V^{(1-\eta_{DS})}$	1.476930×10^{-01}	0.0	-
12	*ETADS*	-	6.000000×10^{-01}	-	-
13	*ALP*	-	2.878165×10^{-03}	0.0	-
14	*VP*	V	3.338182×10^{-01}	1.0×10^{-12}	-
15	*GAM00*	-	1.861785×10^{-02}	0.0	-
16	*ETAGAM*	-	$2.000000 \times 10^{+00}$	-	-
17	*MO*	-	5.024606×10^{-01}	1.0×10^{-12}	-
18	*ETAM*	-	$2.000000 \times 10^{+00}$	-	-
19	*PHIT*	V	2.662680×10^{-02}	0.0	-
20	*ZET1*	-	4.074464×10^{-01}	1.0×10^{-12}	-
21	*VSBT*	V	$2.025926 \times 10^{+00}$	0.0	-

No.	**Parameter**	Units	**Default**	Clip low	**Clip high**
22	*A1*	-	$6.022073 \times 10^{+00}$	0.0	-
23	*A2*	V	$3.801696 \times 10^{+01}$	1.0×10^{-12}	-
24	*A3*	-	6.407407×10^{-01}	0.0	-
25	*COX*	F	2.979787×10^{-14}	0.0	-
26	*CGDO*	F	6.392000×10^{-15}	0.0	-
27	*CGSO*	F	6.392000×10^{-15}	0.0	-
28	*NT*	J	2.563182×10^{-20}	0.0	-
29	*NFMOD*	-	0	-	-
30	*NF*	V^2	-	-	-
31	*NFA*	$V^{-1}m^{-4}$	7.15×10^{22}	10^{-12}	-
32	*NFB*	$V^{-1}m^{-2}$	2.16×10^{7}	-	-
33	*NFC*	V^{-1}	0	-	-
34	*TOX*	m	25×10^{-9}	-	-
35	*MULT*	-	1.0	0.0	-

a. The lower bound for $K = K_0 \cdot \frac{\sqrt{\text{hyp}_1(-V_{SBX}, \varepsilon_2)}}{\sqrt{V_{SBX} + \phi_B}}$

The default values and clipping values as used by **Pstar** for the parameters of the electrical MOS model, level 903 (p-channel) are listed below.

No.	Parameter	Units	Default	Clip low	Clip high
1	*LEVEL*	-	903	-	-
2	*VTO*	V	$1.082125\times10^{+00}$	-	-
3	*KO*	$V^{1/2}$	4.280174×10^{-01}	1.0×10^{-12}	-
4	*K*	$V^{1/2}$	4.280174×10^{-01}	See note [a]	-
5	*PHIB*	V	6.225999×10^{-01}	1.0×10^{-12}	-
6	*VSBX*	V	1.000000×10^{-12}	1.0×10^{-12}	-
7	*BET*	AV^{-2}	4.841498×10^{-04}	0.0	-
8	*THE1*	V^{-1}	2.046809×10^{-01}	0.0	-
9	*THE2*	$V^{-1/2}$	1.492490×10^{-01}	0.0	1.0
10	*THE3*	V^{-1}	3.267633×10^{-02}	-	-
11	*GAM1*	$V^{(1-\eta_{DS})}$	9.905701×10^{-01}	0.0	-
12	*ETADS*	-	6.000000×10^{-01}	-	-
13	*ALP*	-	4.766925×10^{-02}	0.0	-
14	*VP*	V	1.861200×10^{-01}	1.0×10^{-12}	-
15	*GAM00*	-	1.118334×10^{-02}	0.0	-
16	*ETAGAM*	-	$1.000000\times10^{+00}$	-	-
17	*MO*	-	3.801987×10^{-01}	1.0×10^{-12}	-
18	*ETAM*	-	$1.000000\times10^{+00}$	-	-
19	*PHIT*	V	2.662680×10^{-02}	0.0	-
20	*ZET1*	-	$1.270446\times10^{+00}$	1.0×10^{-12}	-
21	*VSBT*	V	$1.000000\times10^{+02}$	0.0	-

No.	Parameter	Units	Default	Clip low	Clip high
22	*A1*	-	$6.858299 \times 10^{+00}$	0.0	-
23	*A2*	V	$5.732410 \times 10^{+01}$	1.0×10^{-12}	-
24	*A3*	-	4.254087×10^{-01}	0.0	-
25	*COX*	F	2.717113×10^{-14}	0.0	-
26	*CGDO*	F	6.358400×10^{-15}	0.0	-
27	*CGSO*	F	6.358400×10^{-15}	0.0	-
28	*NT*	J	2.216522×10^{-20}	0.0	-
29	*NFMOD*	-	0	-	-
30	*NF*	V^2	-	-	-
31	*NFA*	$V^{-1}m^{-4}$	1.53×10^{22}	10^{-12}	-
32	*NFB*	$V^{-1}m^{-2}$	4.06×10^{6}	-	-
33	*NFC*	V^{-1}	2.92×10^{-10}	-	-
34	*TOX*	m	25×10^{-9}	-	-
35	*MULT*	-	1.0	0.0	-

a. The lower bound for $K = K_0 \cdot \frac{\sqrt{\mathrm{hyp}_1(-V_{SBX}, \varepsilon_2)}}{\sqrt{V_{SBX} + \phi_B}}$

10.3.3 The ON/OFF condition

The solution for a circuit involves a process of successive calculations. The calculations are started from a set of 'initial guesses' for the electrical quantities of the non-linear elements. A simplified DCAPPROX mechanism for devices using ON/OFF keywords is mentioned in [9]. By default the devices start in the default state.

n-channel			
	Default	ON	OFF
V_{DS}	2.5	2.5	5.0
V_{GS}	2.5	2.5	0.0
V_{SB}	0.0	0.0	0.0

p-channel			
	Default	ON	OFF
V_{DS}	-2.5	-2.5	-5.0
V_{GS}	-2.5	-2.5	0.0
V_{SB}	0.0	0.0	0.0

10.3.4 Numerical adaptation

To implement the model in a circuit simulator, care must be taken of the numerical stability of the simulation program. A small non-physical conductance, G_{min}, is connected between the nodes *D* and *S*. The value of the conductance is 10^{-15} [1/Ω].

10.3.5 DC operating point

The DC operating point output facility gives information on the state of a device at its operation point. Besides terminal currents and voltages, the magnitudes of linearized internal elements are given. In some cases meaningful quantities can be derived which are then also given (e.g. F_{ug}). The objective of the DCOP-facility is twofold:

- Calculate small-signal equivalent circuit element values.
- Open a window on the internal bias conditions of the device and its basic capabilities (e.g. F_{ug}).

Below the printed items are described. $C_{x(y)}$ indicates the derivate of the charge *Q* at terminal *x* to the voltage at terminal *y*, when all other terminals remain constant.

Quantity	Equation	Description
Level	903	Model level
I_{ds}		Drain current, excluding substrate current
I_{avl}		Substrate current

Quantity	Equation	Description
V_{ds}		Drain-Source voltage
V_{gs}		Gate-Source voltage
V_{sb}		Source-Bulk voltage
V_{TO}		Threshold voltage after geometric and T-scaling
V_{TS}	V_{T1}	V_{T0} including backbias effects
V_{GT}	V_{GT2}	Effective gate drive including backbias and drain effects
V_{dss}	$\lvert V_{DSS1} \rvert$	Saturation voltage at actual bias
V_{sat}	$\lvert V_{ds} \rvert$ - V_{dss}	Saturation limit
g_m	dI_{ds}/dV_{gs}	transconductance (assumed V_{ds}>0)
g_{mb}	dI_{ds}/dV_{bs}	bulk transconductance (assumed V_{ds}>0)
g_{ds}	dI_{ds}/dV_{ds}	output conductance
$C_{d(d)}$	$+CDDS$	$+dQ_d/dV_d$
$C_{d(g)}$	$-CDGS$	$-dQ_d/dV_g$
$C_{d(s)}$	$+CDDS+CDGS-CDSB$	$-dQ_d/dV_s$
$C_{d(b)}$	$+CDSB$	$-dQ_d/dV_b$
$C_{g(d)}$	$-CGDS$	$-dQ_g/dV_d$
$C_{g(g)}$	$+CGGS$	$+dQ_g/dV_g$
$C_{g(s)}$	$+CGDS+CGGS-CGSB$	$-dQ_g/dV_s$
$C_{g(b)}$	$+CGSB$	$-dQ_g/dV_b$
$C_{s(d)}$	$-CSDS$	$-dQ_s/dV_d$
$C_{s(g)}$	$-CSGS$	$-dQ_s/dV_g$
$C_{s(s)}$	$-CSDS-CSGS+CSSB$	$+dQ_s/dV_s$
$C_{s(b)}$	$+CSSB$	$-dQ_s/dV_b$
$C_{b(d)}$	$-CBDS$	$-dQ_b/dV_d$

Quantity	Equation	Description
$C_{b(g)}$	$-CBGS$	$-dQ_b/dV_g$
$C_{b(s)}$	$+CBDS+CBGS-CBSB$	$-dQ_b/dV_s$
$C_{b(b)}$	$-CBSB$	$+dQ_b/dV_b$
C_{GDOL}	$C_{OL}*W_E$	Drain overlap capacitance of the actual transistor
C_{GSOL}	$C_{OL}*W_E$	Gate overlap capacitance of the actual transistor
W_{eff}		Effective channel width for geometrical models
L_{eff}		Effective channel length for geometrical models
u	g_m/g_{ds}	Transistor gain
R_{out}	$1/g_{ds}$	Small signal output resistance
$V_{\mathrm{m\ early}}$	$\lvert I_d \rvert /g_{ds}$	Equivalent Early voltage
K_{eff}	$\frac{(V_{T1} - V_{T0})}{\sqrt{V_{SB} + 2\phi_B} - \sqrt{2\phi_B}}$	Describes body effect at actual bias
B_{eff}	$\frac{2\lvert I_{ds}\rvert}{V_{GT3}^2}$	Effective β at actual bias in the simple MOS model
F_{ug}	$g_m/(2\delta\ C_{in})$	Unity gain frequency at actual bias
$SQRT(S_{fw})$	$\sqrt{S_{th}}/g_m$	input-referred RMS white noise voltage
$SQRT(S_{ff})$	$\sqrt{S_{fl}(1kHz)}/g_m$	input-referred RMS 1/f noise voltage at 1 kHz
F_{knee}	$1Hz \cdot S_{fl}(1Hz)/S_{th}$	Cross-over frequency above which white noise is dominant

Remarks:

- When V_{ds}<0, g_m and g_{mb} are calculated with drain and source terminals interchanged (see section on Channel Type Declarations). The terminal voltages and I_{DS} keep their sign.

- The signs of *VTO* and *VTS* follow the conventions of the model parameter set. The parameter set is always assumed to correspond to an n-channel device.

- The *simple model* mentioned above states that

$$I_d = \begin{cases} \beta_{\mathrm{eff}} \cdot [V_{GT}V_{ds} - V_{ds}^2/2] & V_{ds} \le V_{dss} \\ \beta_{\mathrm{eff}} \cdot V_{GT}^2/2 & V_{ds} > V_{dss} \end{cases}$$

- The calculation of F_{ug} assumes that the total load capacitance on the drain is identical to C_{ox} so that the actual load in the circuit is not taken into account! Intrinsically F_{ug} is related to the transit time

$$T_{tr} = \frac{3}{4}\frac{L^2{}_{\mathrm{eff}}}{\mu_{\mathrm{eff}} V_{GT}}$$

where $\mu_{eff} = B_{eff}/C_{ox}$. However as this transit time has no practical meaning, the rough estimation of the unity gain frequency is preferred.

- The input referred noise power densities S_{fw} and S_{ff} are only defined when g_m>0.

- *W* and *L* are not available for the electrical MOS models.

- *MULT* is a scaling parameter that multiplies all currents and charges by the value of *MULT*. This is equivalent to putting *MULT* (a number) MOS transistors in parallel. And as a consequence *MULT* effects the operating point output.

A non-existent conductance, G_{min}, is connected between the nodes *D* and *S*. This conductance G_{min} does not influence the DC-operating point.

- $C_{in} = C_{g(g)} + C_{gsol} + C_{gdol}$

10.4 Physics

10.4.1 Comments and Physical Background

Current Model

A key parameter in any MOST model is the threshold voltage. Basically this voltage results from a balance between the gate and the substrate charge. The expression (10.5) used in this model has been obtained via calculation of the depletion charge in a substrate with a threshold adjustment implant. In this calculation the Gaussian-type doping profile has been replaced by a box-type profile. Since the depletion charge is determined by the integral substrate doping rather than by the actual profile, such a simplification is allowed in practice [17]. The parameter V_{SBX} is the back-bias value, at which the implanted layer becomes fully depleted. In addition the above result has the advantage that the parameters K_0 and K can be easily determined from the slope of the V_T versus V_{SB} plot. Figure 44 gives a typical result for an implanted p-type substrate.

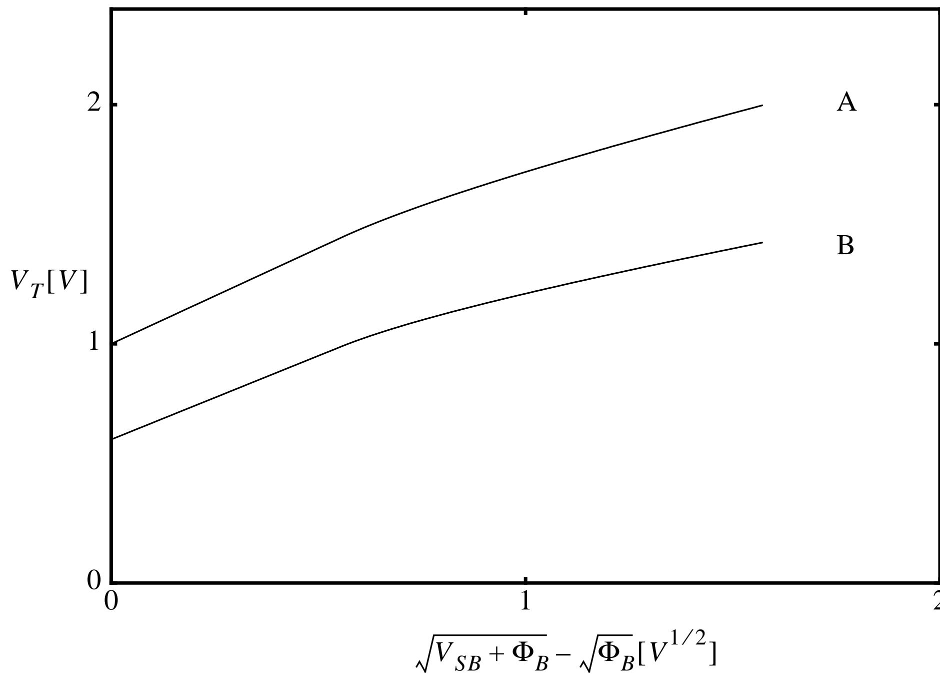

Figure 44: Threshold voltage V_T vs. back bias voltage for two different processes

Furthermore relation (10.5) even holds for a situation, where the substrate doping increases at larger depth. This might occur for a p-channel device in a retrograde

well. However usually the threshold voltage of a p-channel is controlled by a single body coefficient. In this case $K = K_0$ and $\Delta V_{T0} = K_0 \cdot (u_s - u_{s0})$, and Eq. (10.5) has to be used.

The easiest way to implement the single body coefficient in the model is by making $K = K_0$ and giving V_{SBX} a high value (e.g. 100).

In small devices the above threshold voltage usually is changed due to two effects. In short-channel devices depletion from the source and drain junctions causes less gate charge to be required to turn on the transistors. On the other hand in narrow-channel devices the extension of the depletion layer under the isolation causes more gate charge to be required to form a channel. Usually these effects can be modeled by geometrical preprocessing rules:

$$\tilde{V}_{T0} = V_{T0R} + (T_{KD} - T_{KR}) \cdot S_{T;V_{T0}}$$

$$V_{T0} = \tilde{V}_{T0} + \left(\frac{1}{L_E} - \frac{1}{L_{ER}}\right) \cdot S_{L;V_{T0}} + \left(\frac{1}{L_E^2} - \frac{1}{L_{ER}^2}\right) \cdot S_{L;V_{T0}} + \left(\frac{1}{W_E} - \frac{1}{W_{ER}}\right) \cdot S_{W;V_{T0}}$$

$$K = K_R + \left(\frac{1}{L_E} - \frac{1}{L_{ER}}\right) \cdot S_{L;K} + \left(\frac{1}{W_E} - \frac{1}{W_{ER}}\right) \cdot S_{W;K}$$

etc., which follow from physical considerations [17]. When measuring the threshold voltage of p-channel transistors a so called roll-up of this parameter is found as the length decreases. As for the Philips processes this effect is quite significant the pre-processing rule has been altered. For n-channels the advantage is that so called enhanced roll-down of the parameter V_{TO} can now also easily be modelled. Figure 45 is a picture of V_{TO} vs. $1/L_{\mathrm{eff}}$ for a p-channel. At large values of drain bias the drain depletion layer further expands and may affect in case of short channels the potential barrier between the source region and the channel area. Consequently the subthreshold current increases with drain bias. In order to guarantee a smooth transition between the latter operation mode and the strong inversion mode, the above effect is interpreted as an apparent change of the threshold voltage or as an increase of the effective gate drive. This drain bias voltage dependence is expressed in detail, by the first part of Eq. (10.11). At higher back bias voltage the drain-induced effect further increases according to Eq. (10.8). For a uniform substrate doping, the latter expression follows from an approximate solution of the 2-D Poisson equation [17]. In this case $\eta_\gamma = 1$. For an implanted substrate no satisfactory analytic expression has been obtained yet. However empirically it is found that Eq. (10.8) adequately describes measured subthreshold characteristics, the value of $\eta_\gamma = 2$ is used. This is

shown in fig. 46. Once an inversion layer has been formed at higher values of gate bias, an increase of drain bias induces an additional increase if inversion charge at the drain end of the channel (static feedback effect). This can be interpreted as another change of effective gate drive and has been modeled by the second part of Eq. (10.11). From first order calculations and experimental results the exponent η_{DS} is found to have a value of $1/2$. In order to guarantee a smooth transition between subthreshold and strong-inversion mode, the model constant $V_{GTX} = \sqrt{2}/2$ has been introduced in (10.11). When $V_{GT1} \leq V_{GTX}$, the subthreshold effect dominates. However, when $V_{GT1} \geq V_{GTX}$, the latter effect soon is overtaken by the static feedback effect. Note that γ_0 for implanted substrates strongly increases with back bias, while γ_1 does not depend on V_{SB}. This implies that the increase of γ_0 with V_{SB} cannot continue beyond some high V_{SB} value. Otherwise large nonmonotonic behaviour of I_{DS} versus V_{SB} would be observed. Since the limitation of γ_0 usually occurs outside the practical range of V_{SB} values, a simple purely mathematical limiting procedure has been chosen.

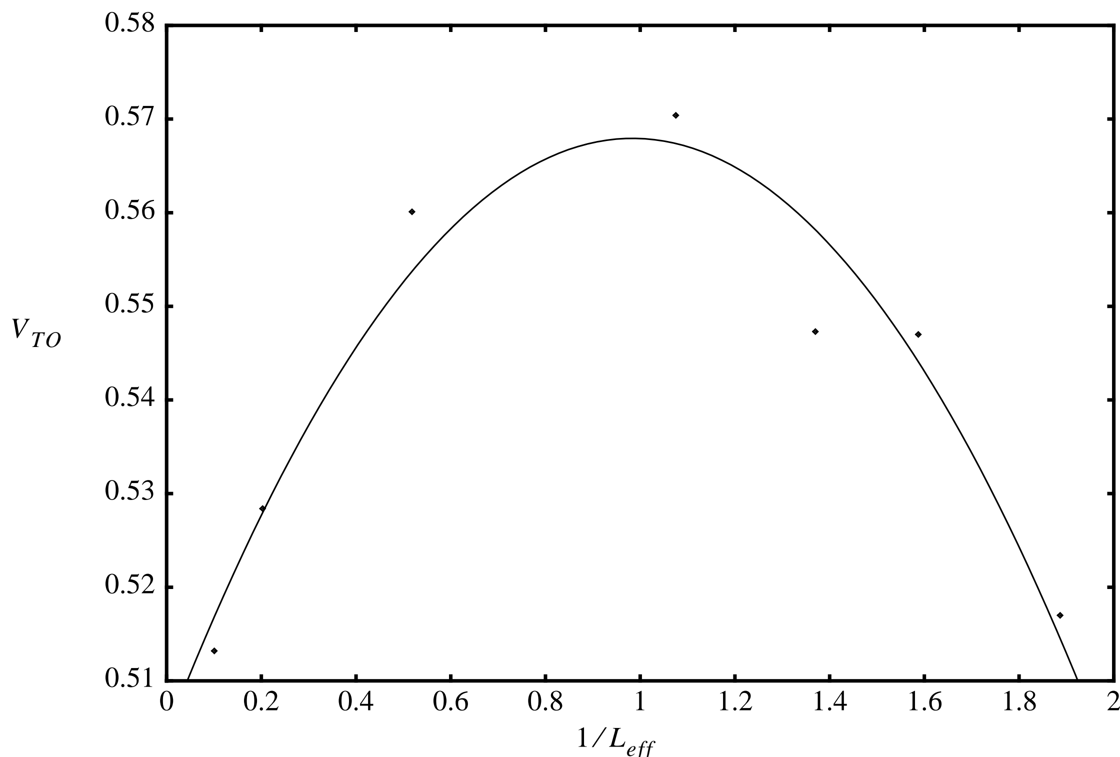

Figure 45: Influence of the effective channel length on V_{T0} for a p-channel device

In fig. 46 it is further shown that the subthreshold slope depends on the back bias applied. This is caused by the fact that the gate control of the potential barrier

between source and channel is affected by the value of the depletion charge [18]. For uniformly doped substrates the slope factor *m* is given by Eq. (10.14), where the exponent η_m equals 1. The latter result follows from a straight forward solution of Poisson's equation. For implanted substrates the situation is more complicated. Empirically it is found that Eq. (10.14) still suffices, provided that the value of η_m is taken 2 (follows from fig. 46 as well).

A smooth transition between the subthreshold current and the current in strong inversion is further guaranteed by the manipulation given in Eqs. (10.15) and (10.16) [19]. When V_{GT2} is negative (subthreshold regime) G_1 becomes small and a Taylor expression of Eq. (10.16) results in an exponential dependence of the drain current on gate bias. On the other hand, when $V_{GT2} = kT/q$, (strong inversion regime), G>>1 and V_{GT3} simply reduces to the linear relation Eq. (10.13).

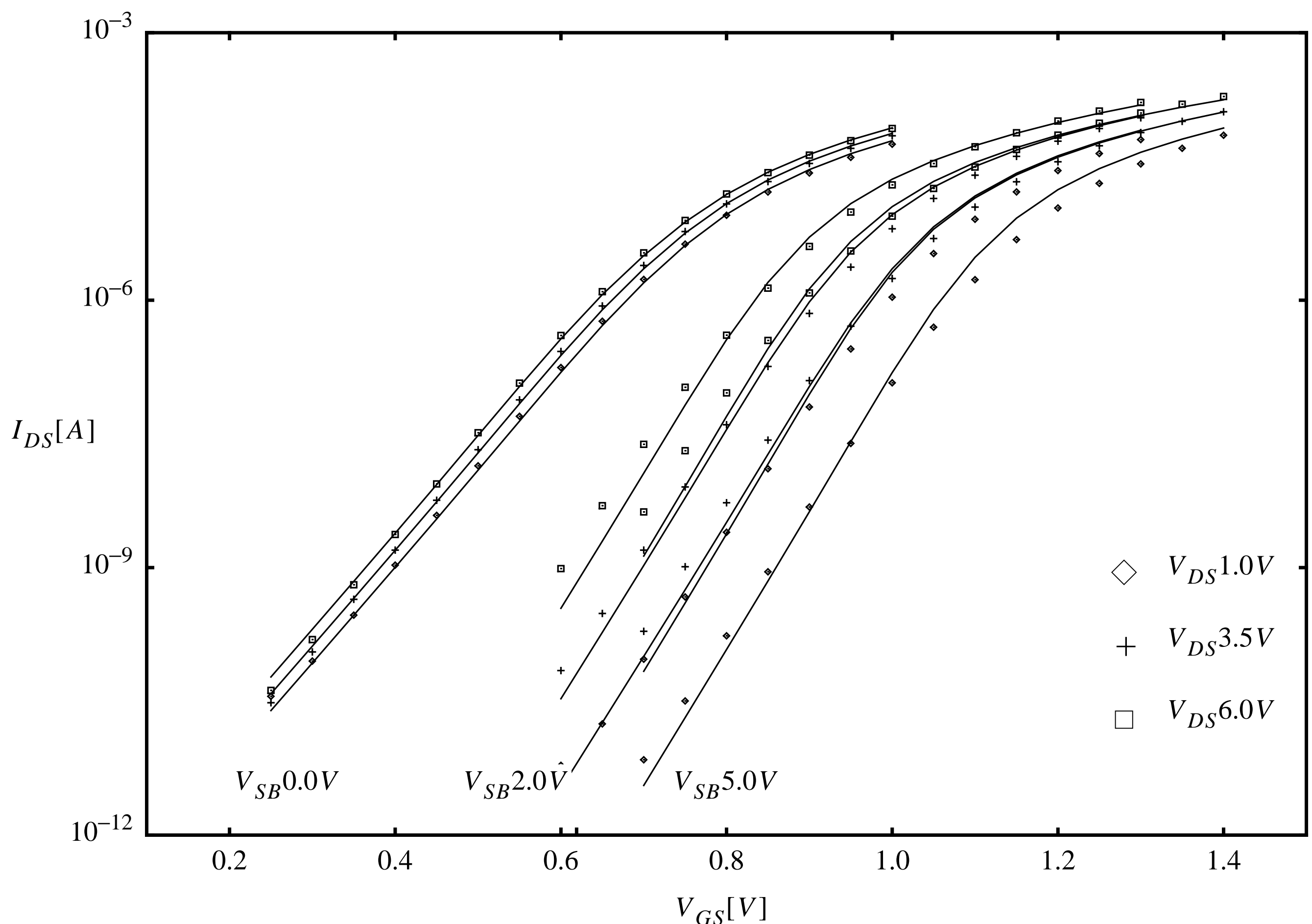

Figure 46: Calculated and measured subthreshold chars. for n-channel transistor, at different back bias voltages (0, 2 and 5 Volts); the calculated characteristics are presented by fully drawn lines, the measured characteristics are presented by marks!

Next comes the effect of the backbias on the I_{DS} - V_{DS} characteristics. When the drain bias is increased, the depletion charge under the drain end of the channel is increased too. Since the latter increase causes a decrease of the mobile carrier charge, the drain current and its saturation voltage are affected too. Taking into account velocity saturation, the saturation voltage expression Eq. (10.20) of model 7 is maintained. However the representation of the depletion charge effect via the δ-term in Eq. (10.19) becomes more complicated in case of implanted substrates. For further details we refer to [17]. Note that if $K = K_0$, Eq. (10.19) reduces to the simple expression used in model 7.

Although the saturation voltage expression Eq. (10.20) from model 7 has been adopted for physics based reasons, for analog application a slight modification is required. If Eq. (10.20) is substituted in the current expression and for instance, the static feedback effect according to Eq. (10.11) is taken into account, the calculated drain conductance agrees very well with the measured values in the linear and the saturation region, but near V_{DSS} large deviations occur. This is shown in Fig. 47.

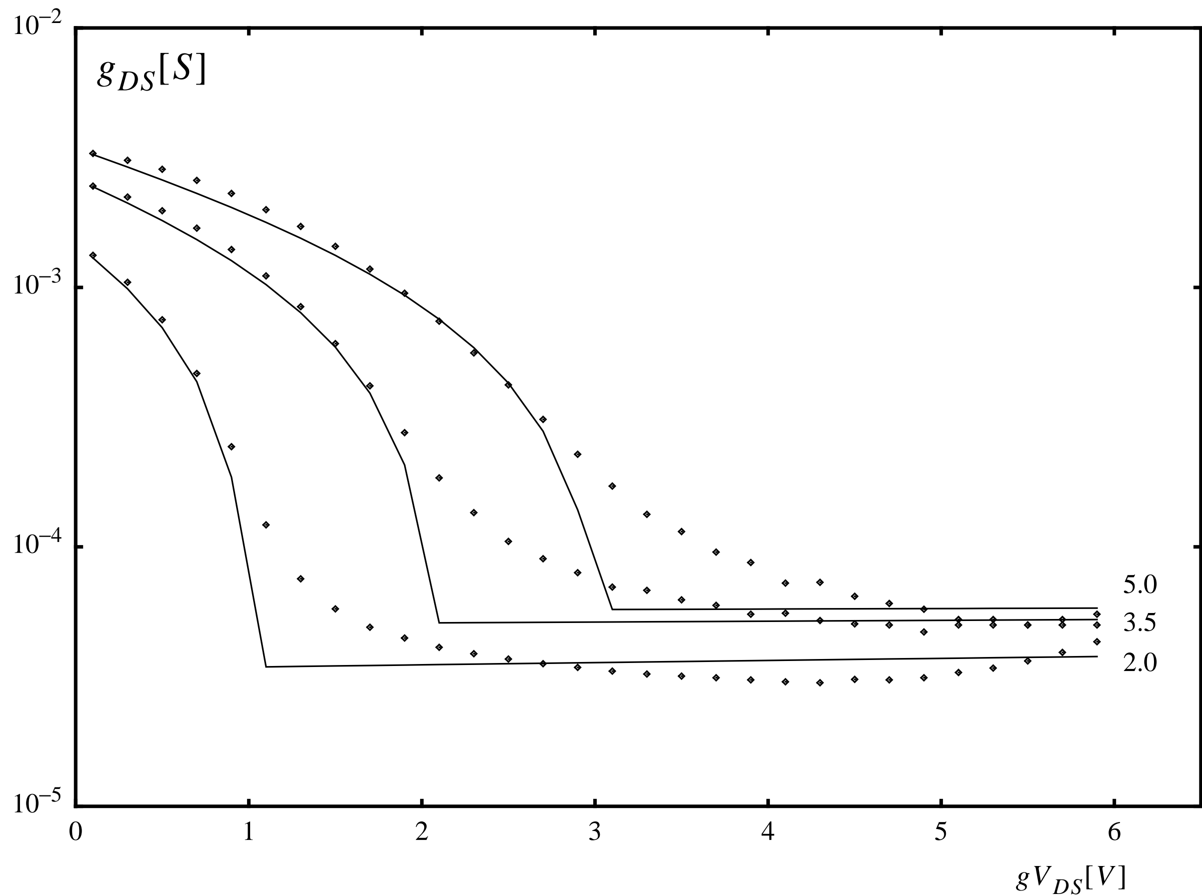

Figure 47: Drain conductance vs. drain-source voltage

These are caused by the fact that the underlying procedure for calculation V_{DSS} does not require continuity of the second derivative of I_{DS}. Since no satisfactory physical arguments can be given to provide this continuity and mathematical arguments lead to too low values of V_{DSS}, continuity of the second derative of I_{DS} has been enforced by introducing Eqs. (10.24) and (10.23). In fact these equations cause a round off of the sudden transition of V_{DSS}, which is controlled by the model constant λ_3. A value $\lambda_3 = 0.3$ has been chosen to compromise between inaccuracies in drain conductance and the current value at small values of V_{DS}. Fig. 48 gives the model variable V_{DS1} as a function of V_{DS}. One of the major shortcomings of model 7 for analog applications is the neglect of channel length reduction at increased values of V_{DS}. This causes the drain conductance calculated according to the static feed back mechanism to depend incorrectly on V_{GS} for long n-channel and p-channel devices.

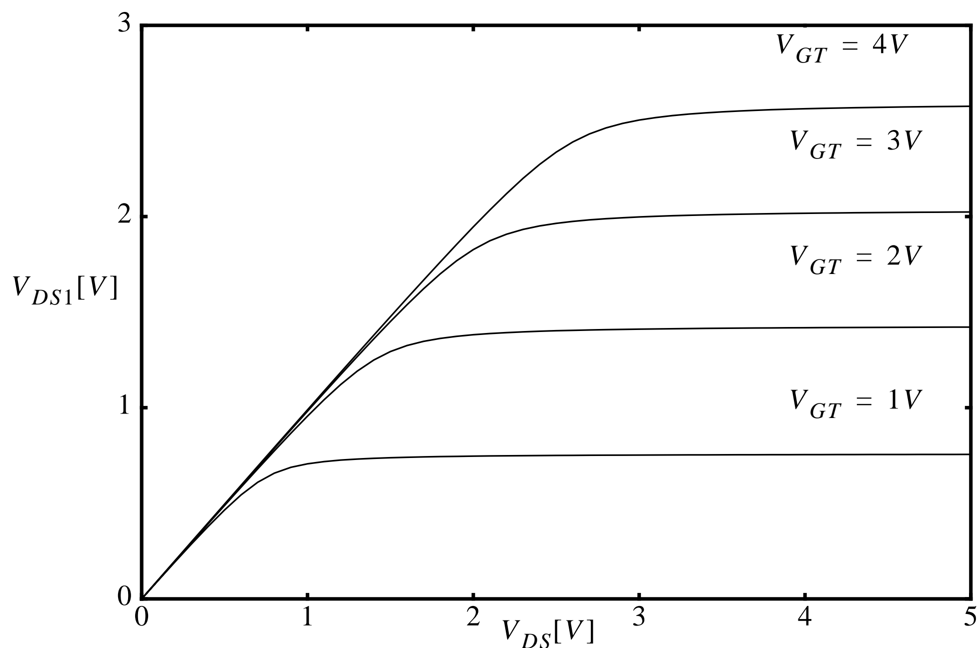

Figure 48: Model variable V_{DS1} as a function of the drain-source voltage V_{DS}

From the many published formulations for channel length shortening, which all lack a strict physics base, Eq. (10.26), which is a modification of one proposal [17], has been found to give the best results in practice. This is shown for the drain conductance of p-channel devices in fig. 49. Although the present formulations give satisfactory results for all practical situations, the measured drain conductance of short-channel n-type devices shows some anomalies, which cannot be explained by the

present model. As shown by fig. 50, the saturated drain conductance increases at high values of V_{DS}, whereas the calculated values decrease with V_{DS}.

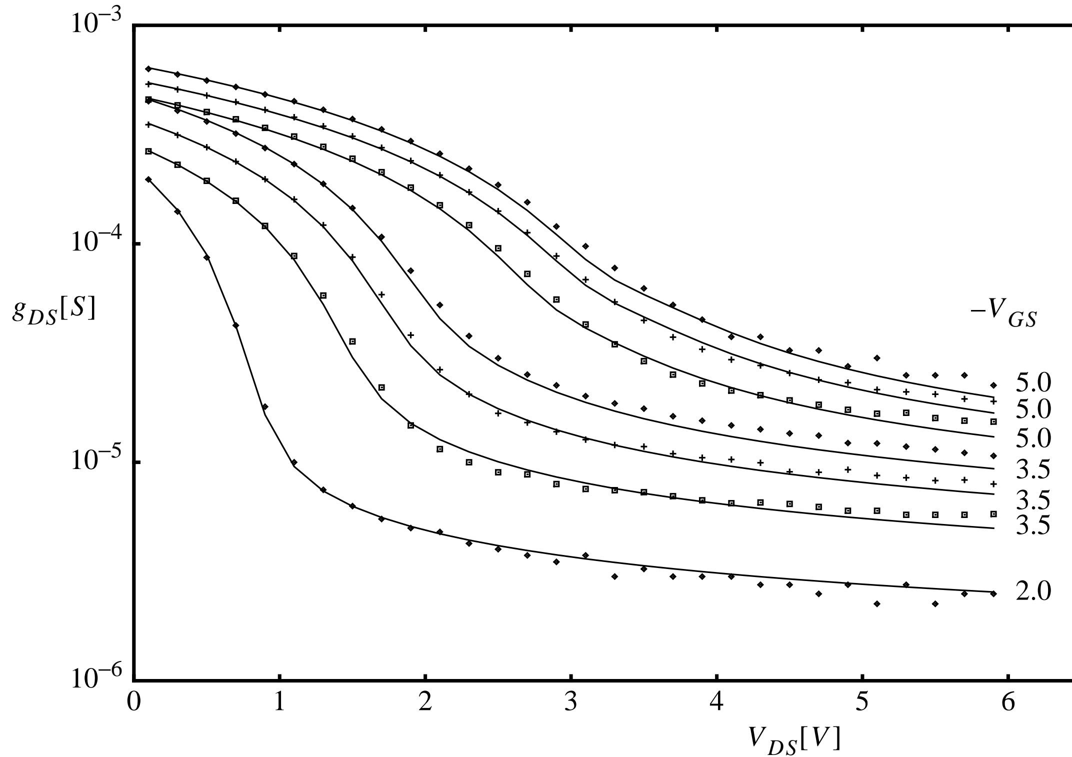

Figure 49: Drain conductance as a function of the drain-source voltage V_{DS} for p-channel transistors at different back bias voltages (0, 2 and 5 Volts); the calculated characteristics are presented by fully drawn lines, the measured characteristics are presented by marks!

A second anomaly appearing only in short-channel n-type transistors, is the increase of g_{DS} at larger values of V_{SB}. In contrast to this, the model forecasts in agreement with experimental findings for p-channel (see fig. 49) and longer n-channel devices a decrease of g_{DS} with V_{SB}.

Since one single expression Eq. (10.27) for the current is used to cover all ranges of bias voltages, the manipulation Eq. (10.26) is needed to obtain a correct saturation of the subthreshold current. While the saturation voltage V_{DSS} increases with V_{GS} in strong inversion, in the subthreshold region the current saturates according to:

$$1 - \exp\left(\frac{-V_{DS}}{\phi_T}\right)$$

This difference in saturation is enforced by the manipulation according to Eq. (10.26).

Despite all the improvements discussed above, the current equation Eq. (10.27) still has the same form as in model 7 with the exception of the mobility reduction term θ_2 (u_s-u_{s0}). The present formulation, which is based on physical arguments [17] has the advantage that its effect on the characteristics disappears, when V_{SB} approaches zero.

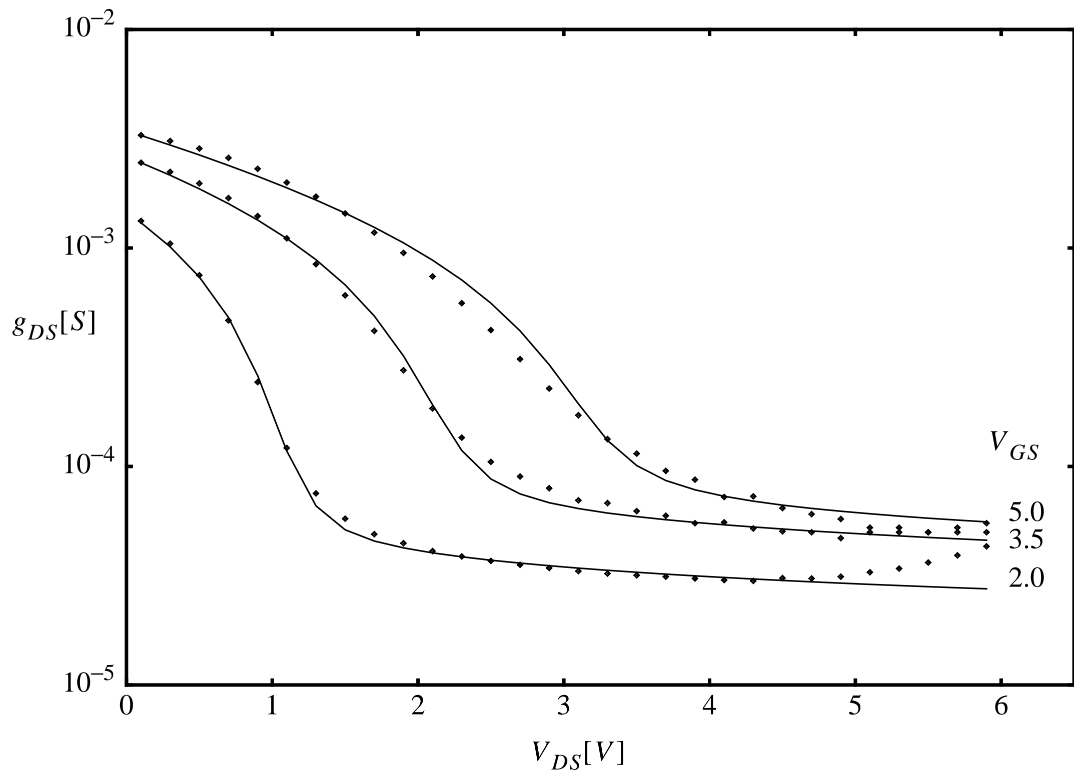

Figure 50: Calculated and measured drain conductance vs. drain-source for n-channel transistor at back bias voltage V_{SB}=0 Volt; the calculated characteristics are presented by fully drawn lines, the measured characteristics are presented by marks!

Therefore the value of θ_2 does not affect the value of β during parameter extraction. Similar to their use in model 7, θ_1 and θ_3 originally represent mobility reduction due the normal and lateral field. However a calculation of the effects of a source and drain series resistance in the characteristics of short-channel devices has shown that Eq. (10.27) can be maintained provided that a much wider significance is assigned to the parameters θ_1 and θ_3 [17]. Generally their value is determined by:

$$\theta_1 = \theta_{10} + (R_S + R_D) \cdot \beta$$

$$\theta_3 \approx \theta_{30} - R_D \cdot \beta$$

In the above relations θ_{10} and θ_{30} are the original mobility reduction parameters, $(R_S + R_D) \cdot \beta$ and $R_D \cdot \beta$ represent the effect of the series resistance. This result makes it possible to take the effects of series resistance into account and leads to geometrical scaling rules for θ_1 and θ_3. Recently, the effect of dogboning (the phenomenon that the contacted area of a narrow device is broader than the channel) on the series resistance, and thus on θ_1 has led to an additional term in the scaling rule for devices that exhibit dogboning [28] and [29].

The inclusion of series resistance in the θ parameters saves internal nodes in the model, thus reducing CPU time during circuit simulation. In addition the form of the model suits the usual measuring procedures. Generally $(R_S + R_D)$ can be obtained from the slope of a plot of θ_1 versus β, using a series of MOSFETs with a fixed width and varying channel length. The intercept with the θ_1-axis yields θ_{10}. An example is given in fig. 51.

New technologies

In new CMOS technologies the dopant concentration varies along the channel due to e.g. pocket implants. Consequently the mobility, and thus the gain factor β_{sq} becomes a function of channel length. To take this effect into account the geometrical scaling rules of the gain factor, the threshold voltage, the drain-induced barrier-lowering parameter γ_{00} and of the mobility reduction parameter θ_1 have been adapted. At the same time a quadratic term in the geometrical scaling rules of the body-effect factors has been added.

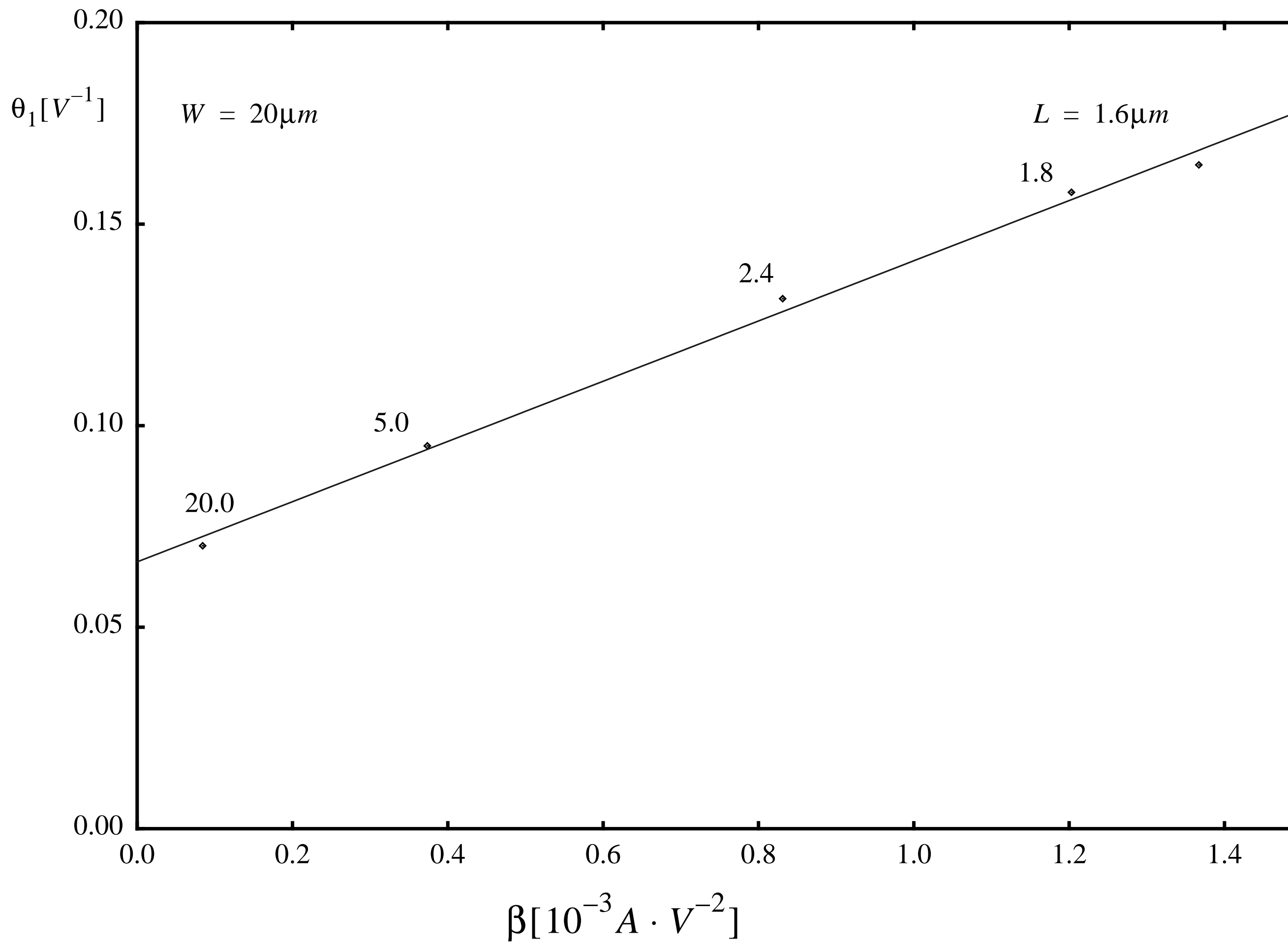

Figure 51: θ_1 *vs.* β *for obtaining* $R_S + R_D$

Charge Model

Compared to model 7 the calculations of the charges Q_S and Q_D is based on a more firm physical basis. In fact the results Eqs. (10.38) and (10.39) are obtained from the definitions:

$$Q_S = -\frac{1}{L}\int_0^L qn(x)\left(1 - \frac{x}{L}\right)dx$$

$$Q_D = -\frac{1}{L}\int_0^L qn(x)\frac{x}{L}dx$$

which have been derived along different lines of approach [19]and [20]. In the above relations the integration with respect to x can be replaced by integrating with respect to the potential V, making use of the current equation. This has the advantage that the charge equations become compatible to the drain current equations. Generally the Eqs. (10.38) and (10.39) produce expressions for the major capacitances, which agree with published measured characteristics. An example is given in fig. 52. However, compared to model 7, Q_S and Q_D and their derivatives do not cause numerical problems, when the transistor switches from the forward to the inverse mode ($V_{DB} \leq V_{SB}$). This is illustrated by the 3-D plot of fig. 53, where the drain charge (normalized with respect to the gate oxide capacitance value) is given as a function of V_D and V_S. Since the $V_S = V_D$ line forms the boundary between the forward and the inverse mode, actually the left-hand part of the figure shows the Q_S expression. At the boundary a smooth transition between Q_S and Q_D is observed. At low values of V_{SB} and V_{DB} the MOSFET operates in the linear mode. Therefore at $V_{SB} = V_{DB} = 0$ Volt the maximum value of Q_D is reached. At low values of V_{SB} and high values of V_{DB}, the transistor operates in the forward saturation mode. In this case Q_D has a lower value than for the inverse saturation mode [17]. When both V_{SB} and V_{DB} are large, the device operates in the subthreshold mode and the active charges are virtually zero within the scale of this figure. Actually the charges considered decrease exponentially towards zero owing to the V_{GT3} term.

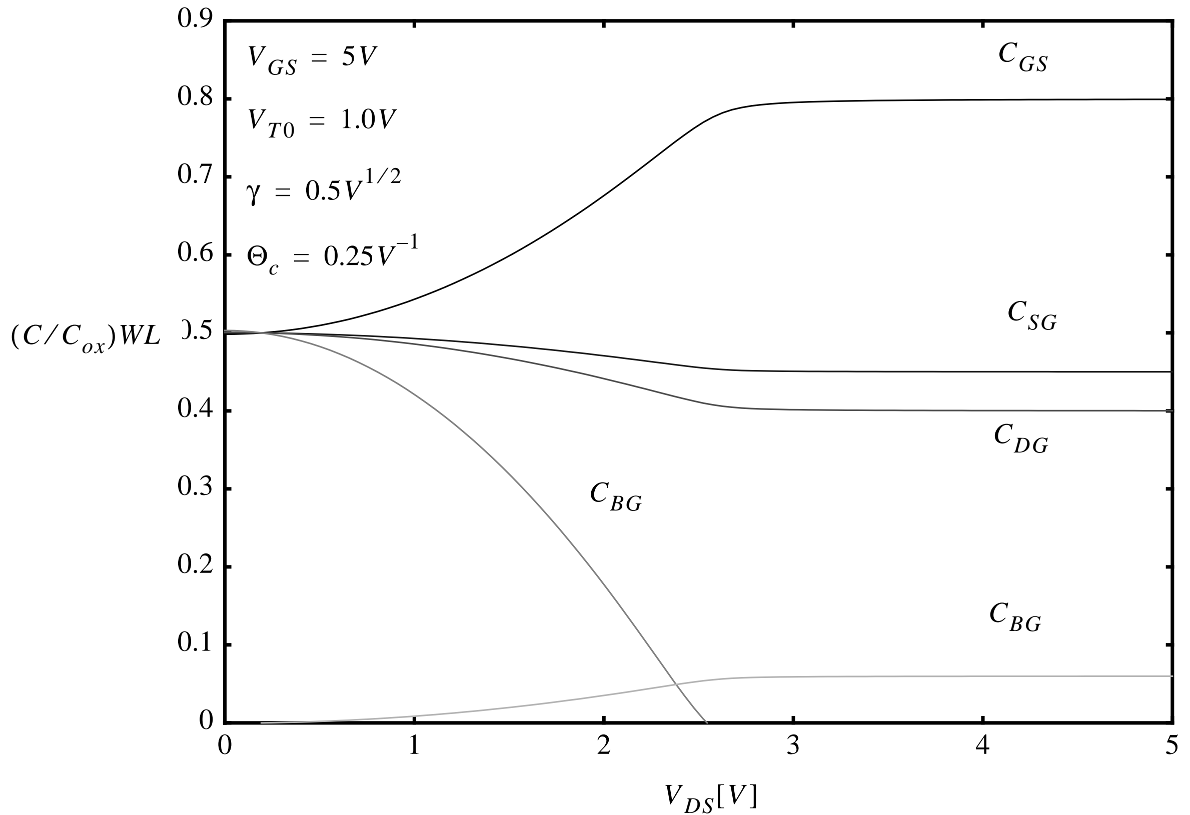

Figure 52: Capacitances as a function of drain-source voltage

Although generally the charges behave in a compatible manner to the drain current, one exception must be emphasized. For reasons of avoiding numerical problems, the δ-expression Eq. (10.19) has to be changed. This is caused by the fact that Eq. (10.19) is not the derivative of the threshold expression Eq. (10.7). This inequality then causes dQ_D / dV_S and dQ_S / dV_D to become discontinuous at $V_{SB} = V_{DB}$. In model 7 this fact has caused major problems. Fortunately, since Q_S and Q_D are hardly dependent on the value of δ, a simple solution can be found by defining for the charge model only:

$$\delta = \frac{dV_T}{dV_S}$$

However this is not the only measure to be taken to guarantee continuity of the charge derivatives at all boundaries of bias conditions. In fact the threshold expression Eq. (10.5) has the problem that its second derivative is discontinuous at V_{SBX}. Therefore if δ is defined according to the above definition, discontinuity problems in

the capacitance expressions have to be expected. Therefore for implementation in a circuit simulator, the physical relations Eq. (10.5) has been replaced by a more smooth mathematical relation, which produces in practice deviations of the threshold voltage less than 5 milli-Volts.

The bulk charge given in Eq. (10.42) has been obtained from a solution of Poisson's equation applied to the depletion layer. The result has been plotted in fig. 54. Compared to model 7, the present Q_B is a more symmetrical function of V_{SB} and V_{DB}. When V_{SB} and V_{DB} are low, an inversion layer exists. In this case the negative charge of Q_B increases with V_{DS}, but does not depend on V_{GB}. At large values of V_{DB}, saturation occurs and Q_D hardly increases further. When a back bias V_{SB} is applied, Q_B increases again due to the expanding depletion layer. Finally at large values of V_{SB} the device operates in the subthreshold mode, where Q_B no longer depends on V_{SB} or V_{DB}, but only on the variable V_{GB} [17], [18].

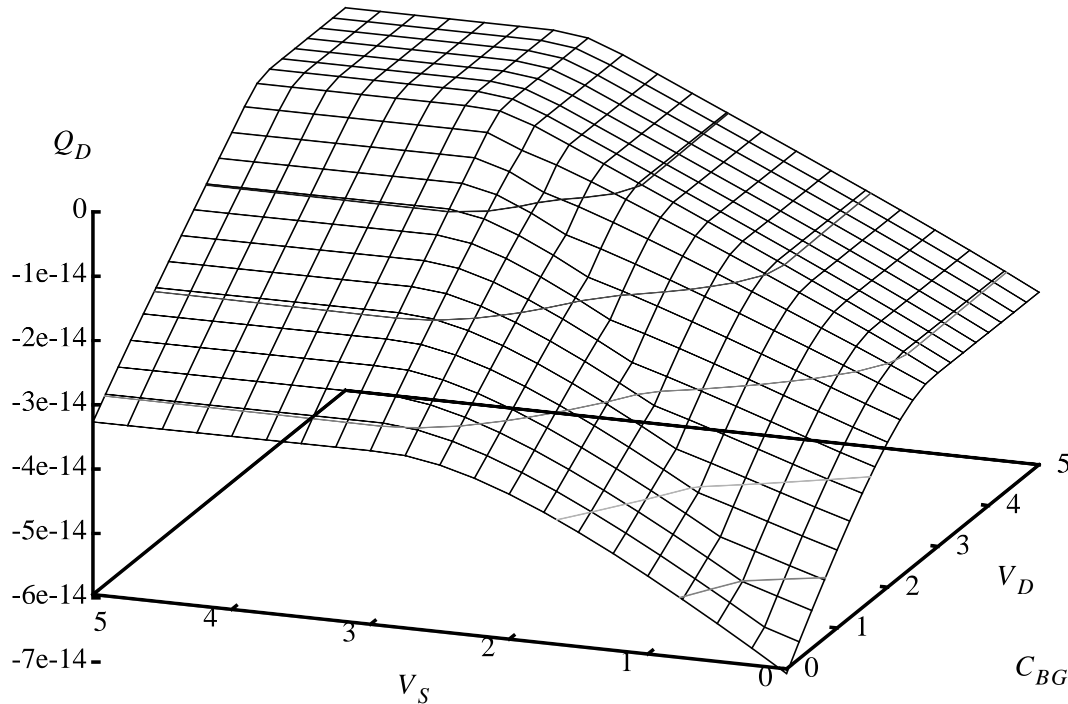

Figure 53: Drain charge as a function of V_D and V_S

Since some derivatives of the physical expressions Eq. (10.42) produce discontinuities at some boundaries, for implementation in a circuit simulator the above equations are modified by applying several hyp-functions. For details we refer to the specific section on this subject.

Finally we remark that the above charge model is quasi-static. A phase-shift between drain current and gate voltage is not taken into account. This implies that for a few applications at high frequencies approaching the cut-off frequency, errors in a.c. calculations have to be expected.

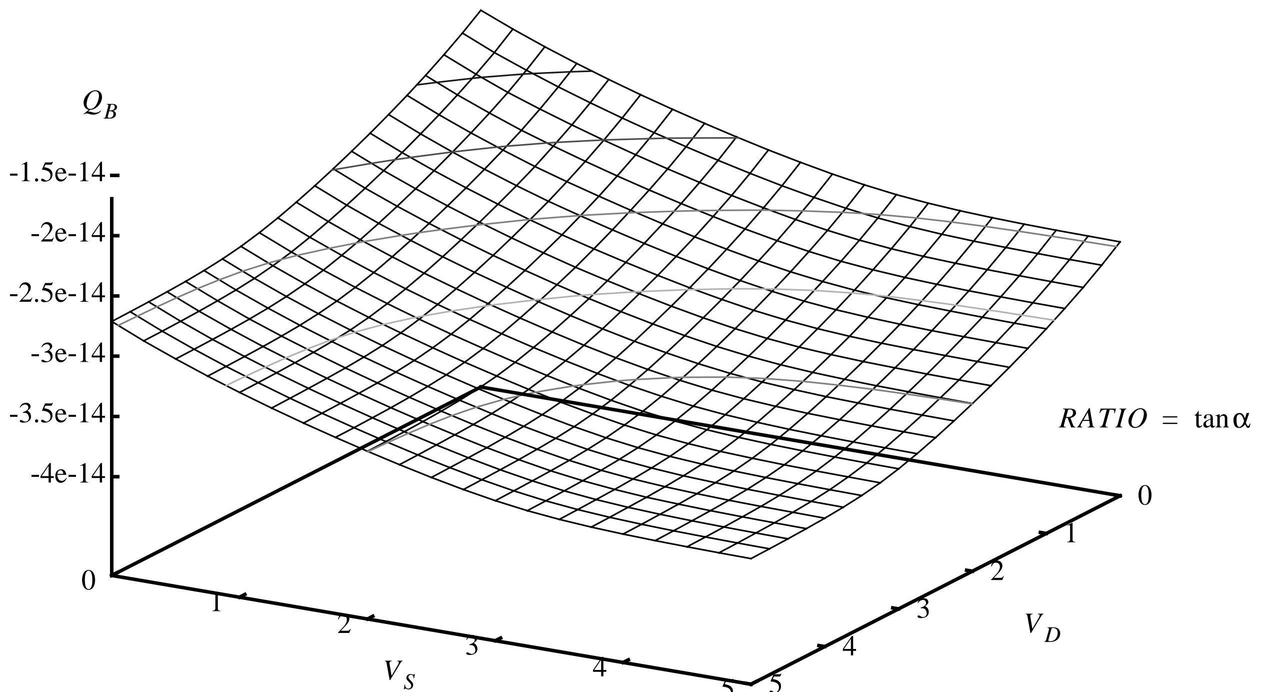

Figure 54: Bulk charge Q_B as a function of V_S and V_D

Noise Model

Since the MOSFET channel can be considered as a non-linear resistor, the channel current is subject to thermal noise. In these equations *f* represents the operation frequency of the transistor. Let thermal-noise current sources be parallel connected to each infinitesimal short element of the channel, it can be shown [17] that the noise spectral density, which is defined by

$$< \Delta I_{th}^2 > = \int_0^\infty S_{th}(f)df,$$

is given by a generalized Nyquist relation:

$$S_{th} = \frac{4 \cdot k \cdot T_{KD}}{L^2} \int_0^L g(x) dx ,$$

where $g(x)$ is the local specific channel conductance. Elaborating the latter integral via a transform of the x-variable into the potential $V(x)$, we obtain the first equation from (10.51). In fact the latter result only applies to the strong inversion mode of operation. In the subthreshold mode the channel is not present and current transport occurs via emission of carriers across the source-channel potential barrier. Therefore in this region shot noise have been observed:

$$S_{sh} = 2 \cdot q \cdot I_{DS}$$

Making use of the generalized gate-drive definition (10.16), we can show that the second equation from (10.51) has the same quantitative value as the shot noise expression. In this way continuity of the noise model is assured along all possible modes of operation. Often a noise level in excess of the Nyquist value is observed. The reason for this is not yet clear! Therefore a parameter N_T has been introduced; usually $4k\,T_{KD} < N_T < 8k\,T_{KD}$. Owing to capacitive coupling between gate and channel, the fluctuating channel current induces noise in the gate terminal at high frequencies. Unfortunately the calculation of this component from first principles is too complicated to provide a result applicable to circuit simulation. It is more practical to derive the desired result from an equivalent circuit presentation given in fig. 55. Owing to the mentioned capacitive coupling, a part of the channel is present as a resistance in series with the gate input capacitance:

$$R_i = \frac{1}{3 \cdot g_m}$$

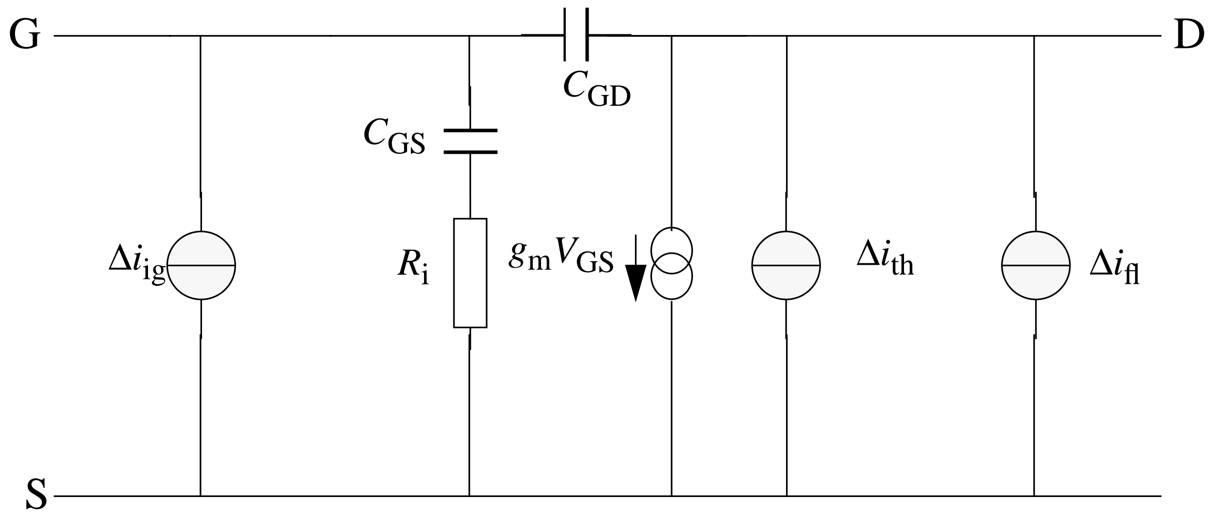

Figure 55: Noise current sources in the electrical scheme of the MOS transistor

It can be easily shown that the latter resistance produces an input noise current with a spectral density given by Eqn. (10.59). In addition, since $\Delta\ i_{th}$ and $\Delta\ i_{ig}$ have the same physical source, both spectral densities are correlated. This is expressed by Eqs. (10.60) and (10.61). Usually thermal noise is not the only source of noise present. At low frequencies flicker (or $1/f$) noise $\Delta\ i_{fl}$ becomes dominant in MOSFETs.

A typical noise spectrum is given in fig. 56.

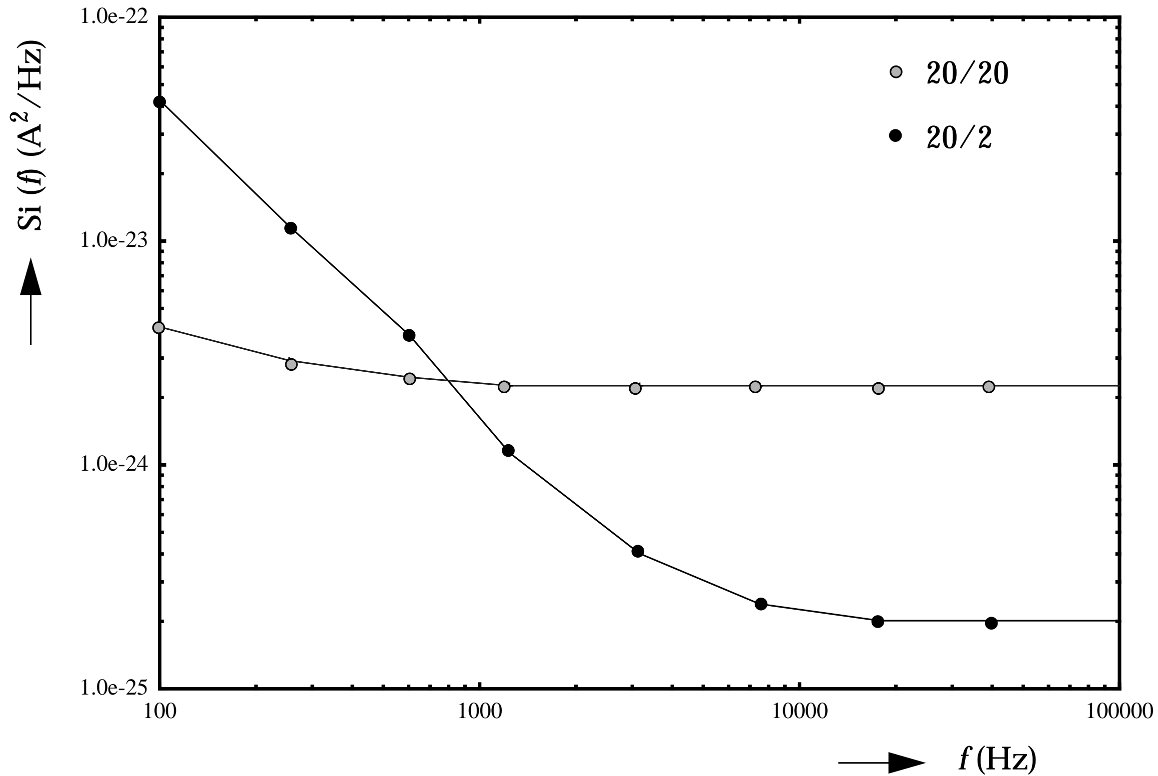

Figure 56: Noise Spectrum for a MOSFET

Generally this type of noise has been interpreted in terms of trapping via surface states or in terms of mobility fluctuation. In MOS MODEL 9, level 903, one can choose between two flicker noise models, selectable via the switch NFMOD.

Selecting NFMOD = 0 activates the flicker noise model of MOS MODEL 9, level 902. This model assumes the input-referred voltage noise:

$$S_{fl}/g_m^2$$

to be bias independent. In practice, however, it was found that there is a bias dependence of this input-referred voltage noise, in particular for p-channels. The noise parameter N_{FR} for this model is determined for the most useful bias condition,

namely $V_T < V_{GS} < V_T + 1.0\text{V}$ and V_{DS} above the saturation voltage. Care should be taken with the outcome of the model at other bias conditions!

NFMOD =1 selects the new flicker noise model, which distinguishes level 903 from level 902. The model, described in detail in [30], [31], [32] assumes trapping of charge carriers in traps located at various depths in the gate oxide. The trapping causes both the mobility and the carrier number to fluctuate in a correlated fashion. Each trapping center is associated with a Lorentzian noise spectral density with a particular knee-frequency. The distribution of trapping depths causes the individual Lorentzians to merge into a $1/f$ spectrum. The model is valid in all operating regions of the MOSFET. Some modelling results are shown in fig. 57.

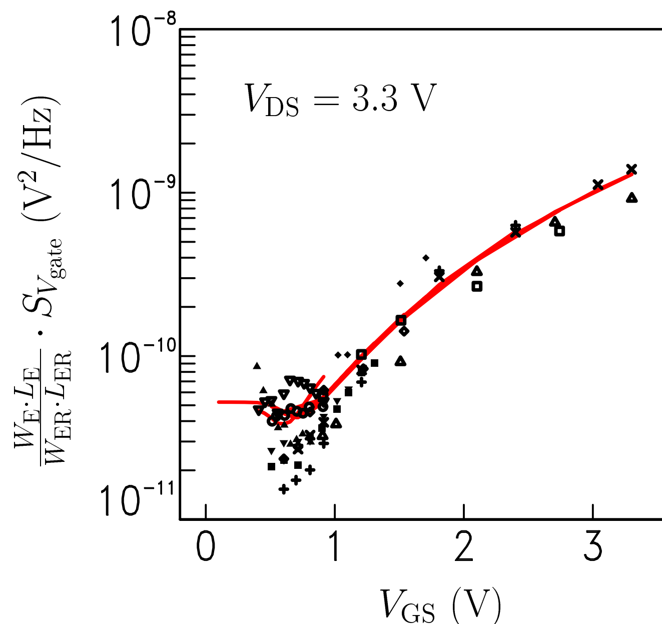

Figure 57: The input-referred 1/f noise at 1 Hz, mutiplied by $W_E L_E/(W_{ER} L_{ER})$, as a function of gate-source voltage, for C075 p-channel MOSFETs. Different symbols correspond to measurements on 11 different geometries. The solid line represents the new 1/f noise model (NFMOD = 1).

This $1/f$ noise model is also found in BSIM3v3. In the subthreshold regime however, the implementation differs slightly from the BSIM3v3 implementation: (i) the correct expression for N" is used, and (ii) the transition between weak and strong inversion regimes has been smoothed. The BSIM3v3 $1/f$ noise parameters NOIA (in $V^{-1}m^{-3}$), NOIB (in $V^{-1}m^{-1}$) and NOIC (in $V^{-1}m$) are found by multiplying the MOS MODEL 9 parameters N_{FAR}, N_{FBR} and N_{FCR} by the factor:

$$0.01 \times W_{ER} \times L_{ER} \times \gamma_{oxide}$$

where $\gamma_{oxide} = 10^{10}\ \mathrm{m}^{-1}$ is the attenuation coefficient of the electron wave function in the gate oxide.

10.4.2 Basic Equations

The equations listed in the following sections, are the basic equations of MOST model 9 without any adaptation necessary for numerical reasons. As such they form the base for parameter extraction. The definitions of the hyp functions, which provide for a smooth clipping, are found in appendix A.

Current Equations

$$u_s = \sqrt{V_{SB} + \phi_B} \tag{10.1}$$

$$u_{s0} = \sqrt{\phi_B} \tag{10.2}$$

$$u_{st} = \sqrt{V_{SBT} + \phi_B} \tag{10.3}$$

$$u_{sx} = \sqrt{V_{SBX} + \phi_B} \tag{10.4}$$

$$\Delta V_{T0} = \begin{cases} K_0 \cdot (u_s - u_{s0})\ , & u_s < u_{sx} \\ \left[1 - \left(\dfrac{K}{K_0}\right)^2\right] \cdot K_0 \cdot u_{sx} - K_0 \cdot u_{s0} & \\ + K \cdot \sqrt{u_s^2 - \left[1 - \left(\dfrac{K}{K_0}\right)^2\right] \cdot u_{sx}^2}\ , & u_s \geq u_{sx} \end{cases} \tag{10.5}$$

$$V_{T1} = V_{T0} + \Delta V_{T0} \tag{10.6}$$

$$u_{s1} = \begin{cases} u_s , & u_s \le u_{st} \\ u_{st} , & u_s > u_{st} \end{cases} \tag{10.7}$$

$$\gamma_0 = \gamma_{00} \cdot \left(\frac{u_{s1}}{u_{s0}}\right)^{\eta_\gamma} \tag{10.8}$$

$$V_{GT1} = \begin{cases} V_{GS} - V_{T1} , & V_{GS} \ge V_{T1} \\ 0 , & V_{GS} < V_{T1} \end{cases} \tag{10.9}$$

$$V_{GTX} = \frac{1}{2} \cdot \sqrt{2} \tag{10.10}$$

$$\Delta V_{T1} = -\gamma_0 \cdot \frac{V_{GTX}^2}{V_{GTX}^2 + V_{GT1}^2} \cdot V_{DS} - \gamma_1 \cdot \frac{V_{GT1}^2}{V_{GTX}^2 + V_{GT1}^2} \cdot V_{DS}^{\eta_{DS}} \tag{10.11}$$

$$V_{T2} = V_{T1} + \Delta V_{T1} \tag{10.12}$$

$$V_{GT2} = V_{GS} - V_{T2} \tag{10.13}$$

$$m = 1 + m_0 \cdot \left(\frac{u_{s0}}{u_{s1}}\right)^{\eta_m} \tag{10.14}$$

$$G_1 = \exp\left(\frac{V_{GT2}}{2 \cdot m \cdot \phi_T}\right) \tag{10.15}$$

$$V_{GT3} = 2 \cdot m \cdot \phi_T \cdot \ln(1 + G_1) \tag{10.16}$$

$$\lambda_1 = 0.3 \tag{10.17}$$

$$\lambda_2 = 0.1 \tag{10.18}$$

$$\delta_1 = \frac{\lambda_1}{u_s} \cdot \left\{ K + \frac{(K_0 - K) \cdot V_{SBX}^2}{V_{SBX}^2 + (\lambda_2 \cdot V_{GT1} + V_{SB})^2} \right\} \tag{10.19}$$

$$V_{DSS1} = \frac{V_{GT3}}{1 + \delta_1} \cdot \frac{2}{1 + \sqrt{1 + \frac{2 \cdot \theta_3 \cdot V_{GT3}}{1 + \delta_1}}} \tag{10.20}$$

$$\lambda_3 = 0.3 \tag{10.21}$$

$$V_{DSSX} = 1 \tag{10.22}$$

$$\varepsilon_3 = \lambda_3 \cdot \frac{V_{DSS1}}{V_{DSSX} + V_{DSS1}} \tag{10.23}$$

$$V_{DS1} = \mathrm{hyp}_5(V_{DS}; V_{DSS1}, \varepsilon_3) \tag{10.24}$$

$$G_2 = 1 + \alpha \cdot \ln\left(1 + \frac{V_{DS} - V_{DS1}}{V_P}\right) \tag{10.25}$$

$$G_3 = \frac{\varsigma_1 \cdot \left\{1 - \exp\left(\frac{-V_{DS}}{\phi_T}\right)\right\} + G_1 \cdot G_2}{\frac{1}{\varsigma_1} + G_1} \tag{10.26}$$

$$I_{DS} = \beta \cdot G_3 \cdot \frac{V_{GT3} \cdot V_{DS1} - \left(\frac{1 + \delta_1}{2}\right) \cdot V_{DS1}^2}{\{1 + \theta_1 \cdot V_{GT1} + \theta_2 \cdot (u_s - u_{s0})\} \cdot (1 + \theta_3 \cdot V_{DS1})} \tag{10.27}$$

$$V_{DSA} = a_3 \cdot V_{DSS1} \tag{10.28}$$

$$I_{AVL} = \begin{cases} 0, & V_{DS} \le V_{DSA} \\ I_{DS} \cdot a_1 \cdot \exp\left(\frac{-a_2}{V_{DS} - V_{DSA}}\right), & V_{DS} > V_{DSA} \end{cases} \tag{10.29}$$

Charge Equations

$$V_{DB} = V_{DS} + V_{SB} \tag{10.30}$$

$$u_d = \sqrt{V_{DB} + \phi_B} \tag{10.31}$$

$$\Delta V_{T0d} = \begin{cases} K_0 \cdot (u_d - u_{s0}) , & u_d < u_{sx} \\ \left[1 - \left(\frac{K}{K_0}\right)^2\right] \cdot K_0 \cdot u_{sx} - K_0 \cdot u_{s0} & \\ + K \cdot \sqrt{u_d^2 - \left[1 - \left(\frac{K}{K_0}\right)^2\right] \cdot u_{sx}^2} , & u_d \ge u_{sx} \end{cases} \tag{10.32}$$

$$V_{T1d} = V_{T0} + \Delta V_{T0d} \tag{10.33}$$

$$\delta_2 = \frac{\partial V_{T2}}{\partial V_{SB}} - \frac{\partial V_{T2}}{\partial V_{GS}} - \frac{\partial V_{T2}}{\partial V_{DS}} \tag{10.34}$$

$$V_{DSS2} = \frac{V_{GT3}}{1+\delta_2} \cdot \frac{2}{1 + \sqrt{1 + \frac{2 \cdot \theta_3 \cdot V_{GT3}}{1+\delta_2}}} \tag{10.35}$$

$$V_{DS2} = \begin{cases} V_{DS}, & V_{DS} \le V_{DSS2} \\ V_{DSS2}, & V_{DS} > V_{DSS2} \end{cases} \tag{10.36}$$

$$F_J = \frac{(1+\delta_2) \cdot (1 + \theta_3 \cdot V_{DS2}) \cdot V_{DS2}}{2 \cdot V_{GT3} - (1+\delta_2) \cdot V_{DS2}} \tag{10.37}$$

$$Q_D = -C_{OX} \cdot \left[\frac{1}{2} \cdot V_{GT3} + (1+\delta_2) \cdot V_{DS2} \cdot \left(\frac{1}{12} \cdot F_J - \frac{1}{60} \cdot F_J^2 - \frac{1}{3}\right)\right] \tag{10.38}$$

$$Q_S = -C_{OX} \cdot \left[\frac{1}{2} \cdot V_{GT3} + (1+\delta_2) \cdot V_{DS2} \cdot \left(\frac{1}{12} \cdot F_J - \frac{1}{60} \cdot F_J^2 - \frac{1}{6}\right)\right] \tag{10.39}$$

$$V_{GB} = V_{GS} + V_{SB} \tag{10.40}$$

$$V_{FB} = V_{T0} - \phi_B - K_0 \sqrt{\phi_B} \tag{10.41}$$

$$Q_{BS} = \begin{cases} -C_{OX} \cdot (V_{GB} - V_{FB}), & V_{GB} < V_{FB} \\ -C_{OX} \cdot K_0 \left\{ -\frac{K_0}{2} + \sqrt{\frac{K_0^2}{4} + (V_{GB} - V_{FB})} \right\}, & V_{FB} \le V_{GB} \le V_{SB} + V_{T1} \\ -C_{OX} \cdot K_0 \left\{ -\frac{K_0}{2} + \sqrt{\frac{K_0^2}{4} + (V_{SB} + V_{T1} - V_{FB})} \right\}, & V_{GB} > V_{SB} + V_{T1} \end{cases} \quad (10.42)$$

$$Q_{BD} = \begin{cases} -C_{OX} \cdot (V_{GB} - V_{FB}), & V_{GB} < V_{FB} \\ -C_{OX} \cdot K_0 \left\{ -\frac{K_0}{2} + \sqrt{\frac{K_0^2}{4} + (V_{GB} - V_{FB})} \right\}, & V_{FB} \le V_{GB} \le V_{DS2} + V_{SB} + V_{T1d} \\ -C_{OX} \cdot K_0 \left\{ -\frac{K_0}{2} + \sqrt{\frac{K_0^2}{4} + (V_{DS2} + V_{SB} + V_{T1d} - V_{FB})} \right\}, & V_{GB} > V_{DS2} + V_{SB} + V_{T1d} \end{cases} \quad (10.43)$$

$$Q_B = \frac{1}{2} \cdot (Q_{BS} + Q_{BD}) \quad (10.44)$$

$$Q_G = -(Q_S + Q_D + Q_B) \quad (10.45)$$

Noise Equations

In these equations f represents the operation frequency of the transistor.

$$g_m = \frac{\partial I_{DS}}{\partial V_{GS}} \quad (10.46)$$

$$F_I = \frac{(1 + \delta_1) \cdot (1 + \theta_3 \cdot V_{DS1}) \cdot V_{DS1}}{2 \cdot V_{GT3} - (1 + \delta_1) \cdot V_{DS1}} \quad (10.47)$$

$$h_3 = \beta \cdot G_3 \cdot \left[\frac{V_{GT3} - \frac{1}{2} \cdot (1 + \delta_1) \cdot V_{DS1}}{\{1 + \theta_1 \cdot V_{GT1} + \theta_2 \cdot (u_s - u_{s0})\} \cdot (1 + \theta_3 \cdot V_{DS1})} \right] \quad (10.48)$$

$$h_4 = 1 + \theta_3 \cdot V_{DS1} + \frac{1}{3} \cdot F_I^2 \quad (10.49)$$

$$h_5 = \frac{V_{DSS1}}{2 \cdot \phi_T} \quad (10.50)$$

$$S_{th} = \begin{cases} N_T \cdot h_3 \cdot h_4 & h_4 < h_5 \\ N_T \cdot h_3 \cdot h_5 & h_4 \geq h_5 \end{cases} \quad (10.51)$$

if NFMOD = 0 then $S_{fl} = N_F \cdot \frac{g_m^2}{f}$ (10.52)

if NFMOD = 1 then eqn.: 10.53, 10.54, 10.55, 10.56, 10.57 and 10.58

$$N_0 = \frac{\varepsilon_{ox}}{qt_{ox}} \cdot V_{GT3} \quad (10.53)$$

$$N_L = \frac{\varepsilon_{ox}}{qt_{ox}} \cdot (V_{GT3} - V_{DS1}) \quad (10.54)$$

$$N'' = \frac{\varepsilon_{ox}}{qt_{ox}} \cdot \phi_T \cdot (m_0 + 1) \quad (10.55)$$

$$S_{wi} = N_{FA} \cdot \frac{\phi_T \cdot I_{DS}^2}{f \cdot N''^2} \tag{10.56}$$

$$S_{si} = \frac{\phi_T \cdot q^2 \cdot I_{DS} \cdot \beta \cdot t_{ox}^2}{f \cdot \varepsilon_{ox}^2 \cdot \{1 + \theta_1 \cdot V_{GT1} + \theta_2 \cdot (u_s - u_{s0})\}} \tag{10.57}$$

$$\cdot \left[N_{FA} \cdot \ln\frac{N_0 + N''}{N_L + N''} + N_{FB} \cdot (N_0 - N_L) + \frac{1}{2} \cdot N_{FC} \cdot (N_0^2 - N_L^2) \right]$$

$$+ \frac{\phi_T \cdot I_{DS}^2}{f} \cdot \frac{G_2 - 1}{G_2} \cdot \left\{ \frac{N_{FA} + N_{FB} \cdot N_L + N_{FC} \cdot N_L^2}{(N_L + N'')^2} \right\}$$

$$S_{fl} = \frac{S_{si} \cdot S_{wi}}{S_{si} + S_{wi}} \tag{10.58}$$

$$S_{ig} = N_T \cdot \frac{(2 \cdot \pi \cdot f \cdot C_{OX})^2}{3 \cdot g_m} \cdot \left\{ 1 + 0.075 \cdot \left(\frac{2 \cdot \pi \cdot f \cdot C_{OX}}{g_m} \right)^2 \right\}^{-1} \tag{10.59}$$

$$\rho_{igth} = 0.4j \tag{10.60}$$

$$S_{igth} = \rho_{igth} \cdot \sqrt{S_{ig} \cdot S_{th}} \tag{10.61}$$

10.5 Accuracy and Validity Range

In order to show the accuracy of the model, we discuss here the measured and calculated characteristics of a 20/1.6 n-channel and a 20/2.4 p-channel device. The first type typically represents the behaviour of short-channel transistors, while the latter already shows long-channel behaviour. Furthermore parallel to the usual manner of parameter determination, we split the characteristics in four parts:

– Linear region
– Saturation region
– Drain conductance
– Subthreshold region

Linear Region

Fig. 58 and fig. 59 give the drain current of the n-channel and p-channel device as a function of the gate-bias voltage. The drain-bias voltage is fixed at 0.10 Volts for n-channel and at -0.10 Volts for p-channel devices. The back-bias and gate voltage have been varied.[1] The deviation between the calculated characteristics (fully drawn lines) and the measured data (dots) gives an impression of the accuracy. The average deviation for both figures amounts 0.40% and 0.60%, respectively, while the maximum deviation amounts 1.5% and 3.0%. The latter value occurs at V_{SB} =-4.5 Volts and the lowest value of V_{GS}. (From these results we conclude that not only the channel resistance characteristics are described very well, but in addition the V_T (V_{SB}) dependence, which is found from extrapolation of the above figures.) In fact this was already shown in fig. 44. The fact that for the p-channel the largest deviation occurs at V_{SB} = -4.5 Volts, is caused by a slight increase of the body coefficient. For reasons of simplicity however only one K-factor was taken into account.

Saturation Region

Figure 60 and fig. 61 give I_{DS} versus V_{DS} for several values of V_{GS} (indicated). In addition for each V_{GS} three values of V_{SB} were taken (0, 2 and 5 Volts). The average deviation amounts 3% for fig. 60 and 2% for fig. 61. In fig. 60 the largest deviations of

1.
Back-bias V_{SB}	$0 \rightarrow 4.5$ *Volts for n-channel*	*step 0.75 Volts*
Back-bias V_{SB}	$0 \rightarrow -4.5$ *Volts for p-channel*	*step -0.75 Volts*
Gate V_{GS}	$0 \rightarrow 6$ *Volts for n-channel*	*step 0.6 Volts*
Gate V_{GS}	$0 \rightarrow -6$ *Volts for p-channel*	*step -0.6 Volts*

6% occur at the transition between the linear and saturation region. This might be an indication that the saturation voltage expression could be improved. In fig. 61 the maximum error of 3% occurs in the saturation region at V_{DS} = -6 Volts. In fact both maximum error figures can be lowered by giving, during parameter extraction, less priority to the modeling of the drain conductance. Nevertheless, since the saturated current values almost perfectly match the V_{GS}-dependence (in particular at V_{SB} = 0 Volts), it can be concluded that the transconductance is modeled within 3%.

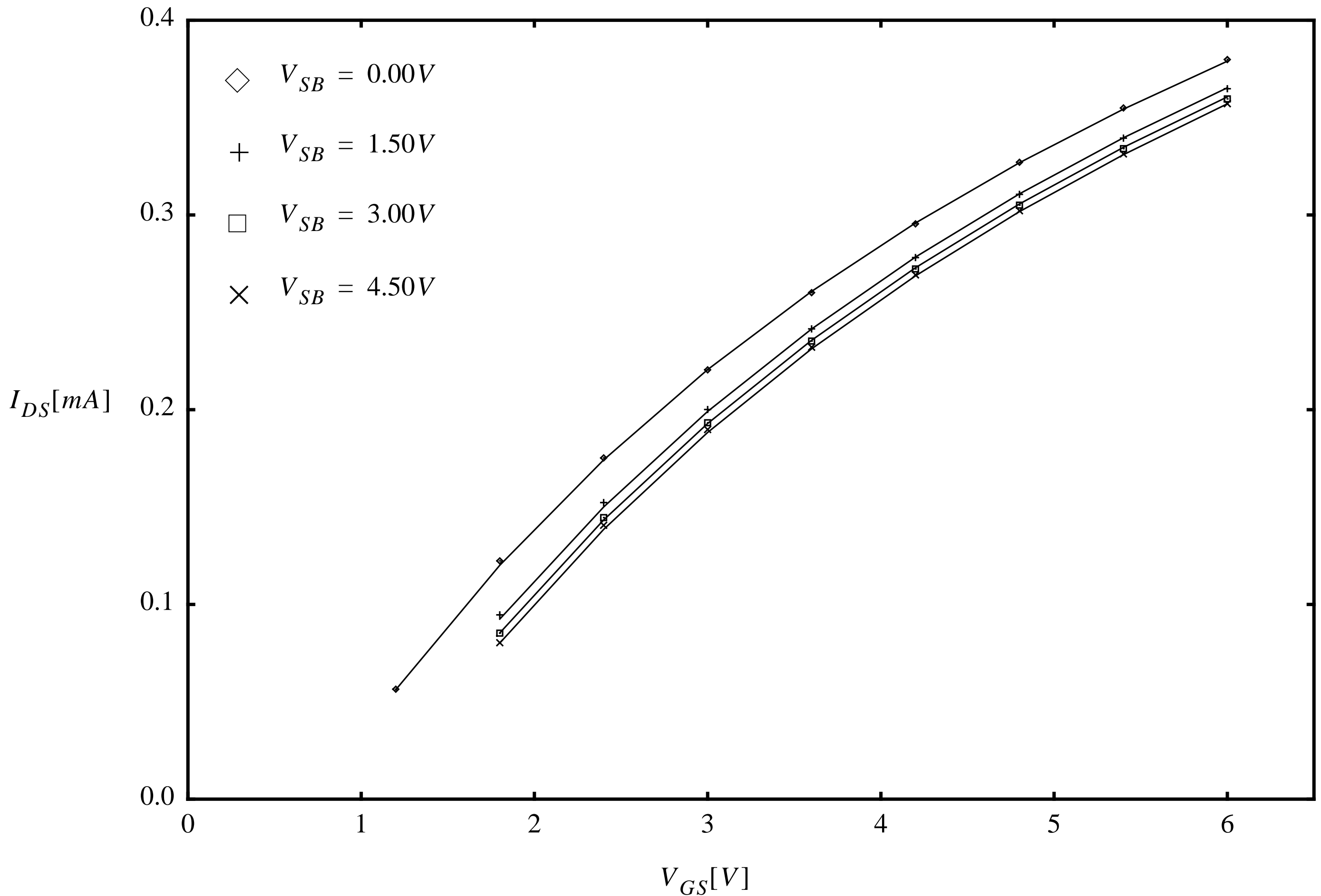

Figure 58: Drain current vs. gate-bias voltage for n-channel transistor at different back-bias voltages

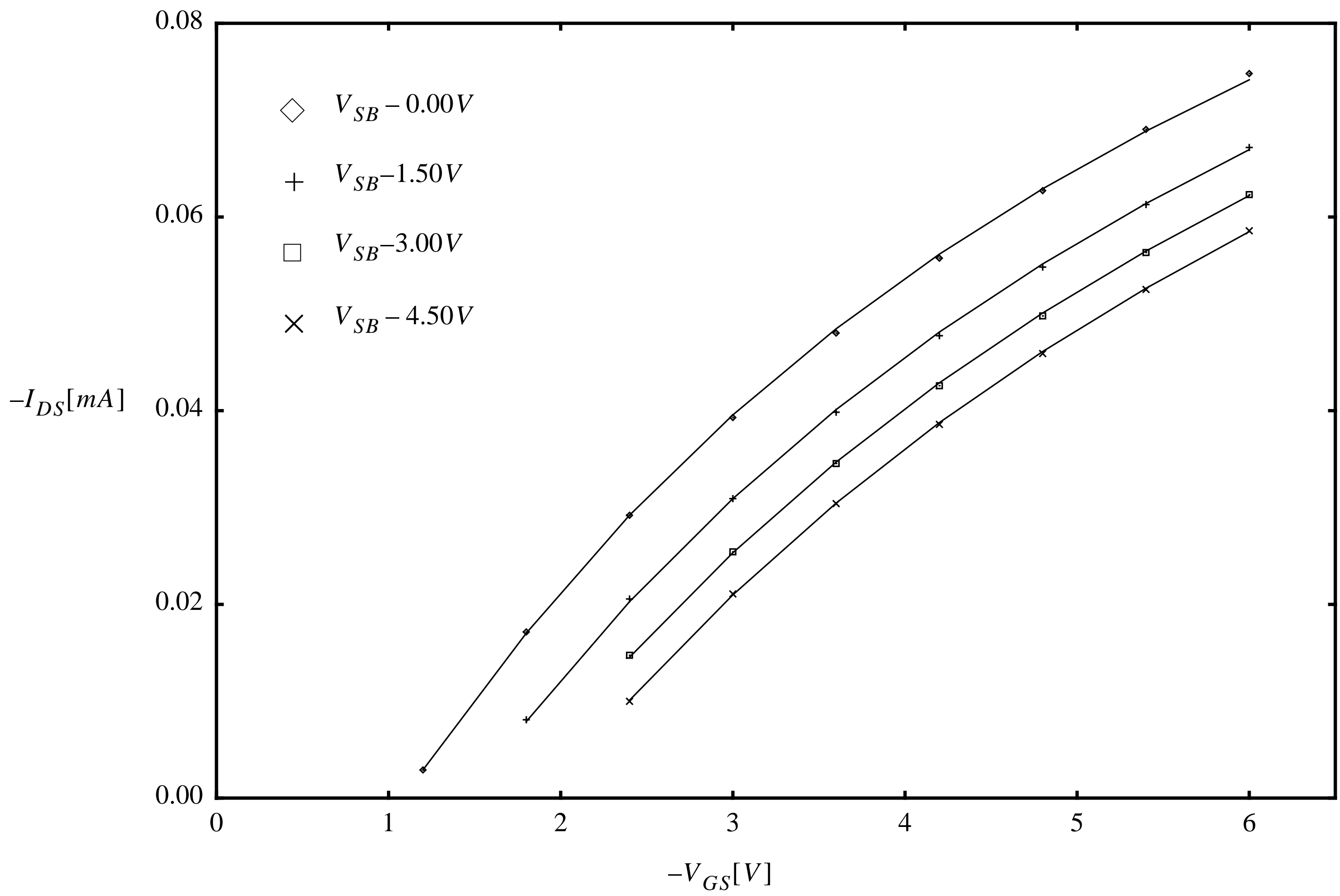

Figure 59: Drain current vs. gate-bias voltage for p-channel transistor at different back-bias voltages

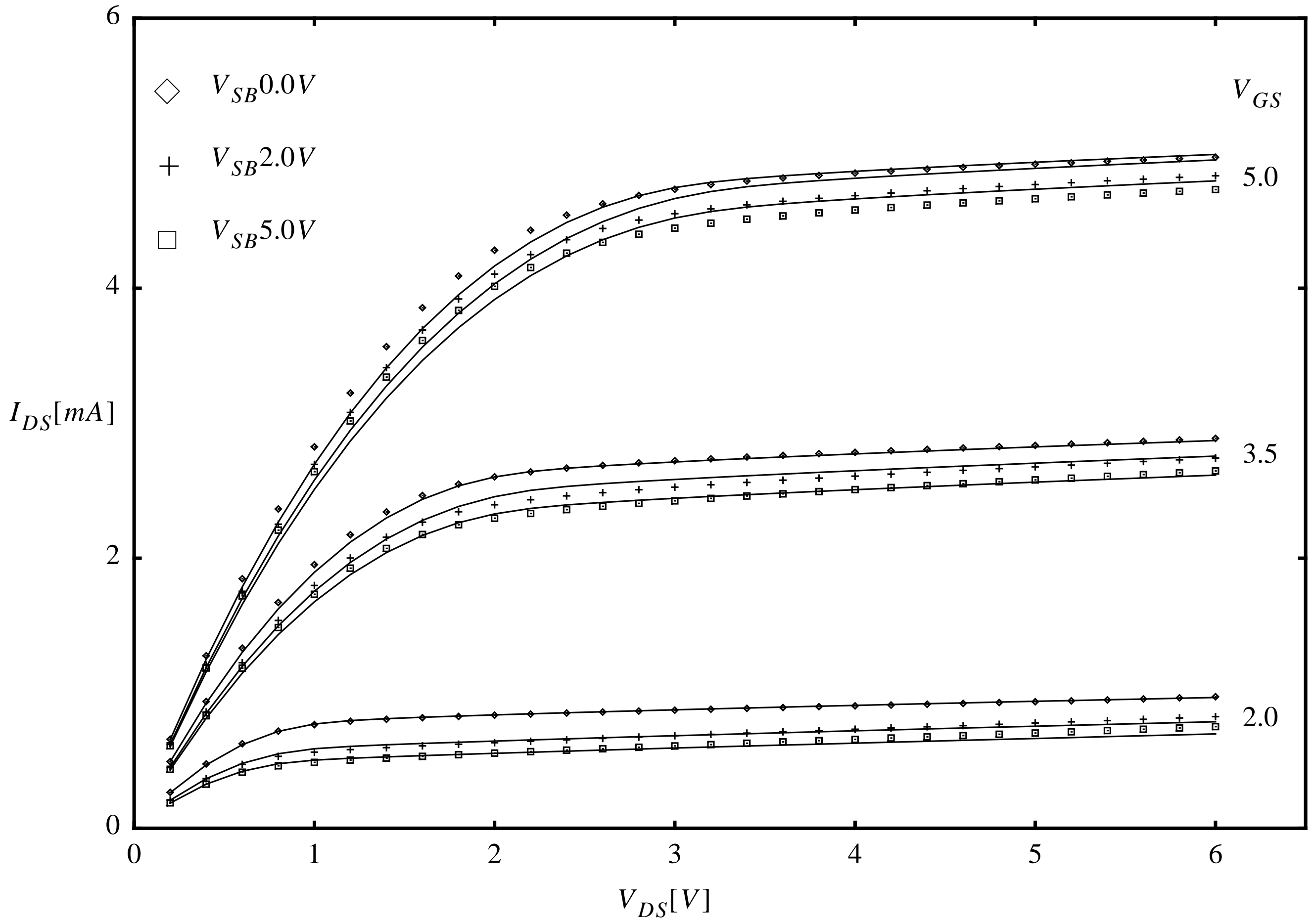

Figure 60: Drain current vs. drain-source voltage for n-channel transistor at different back-bias voltages

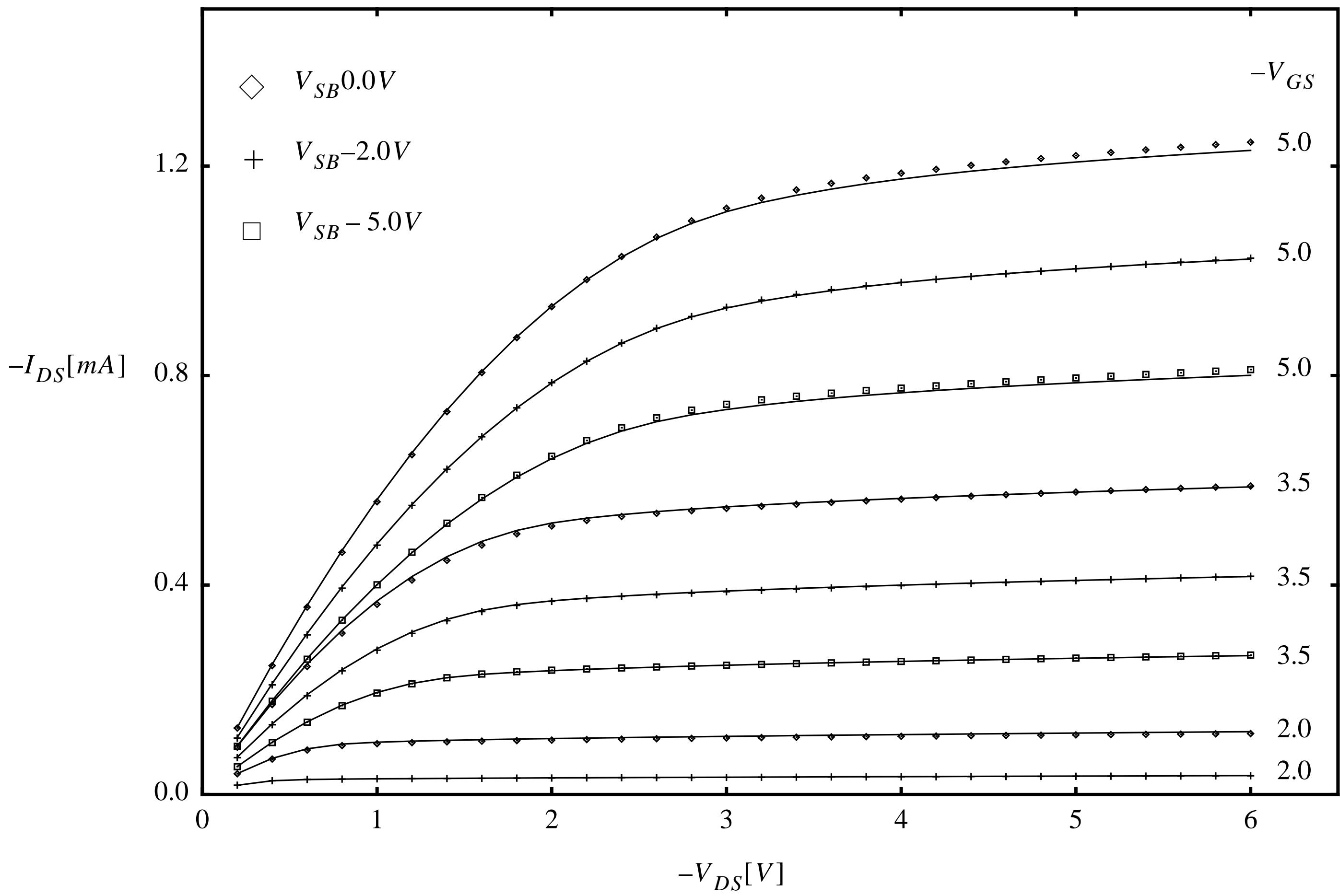

Figure 61: Drain current vs. drain-source voltage for p-channel transistor at different back-bias voltage

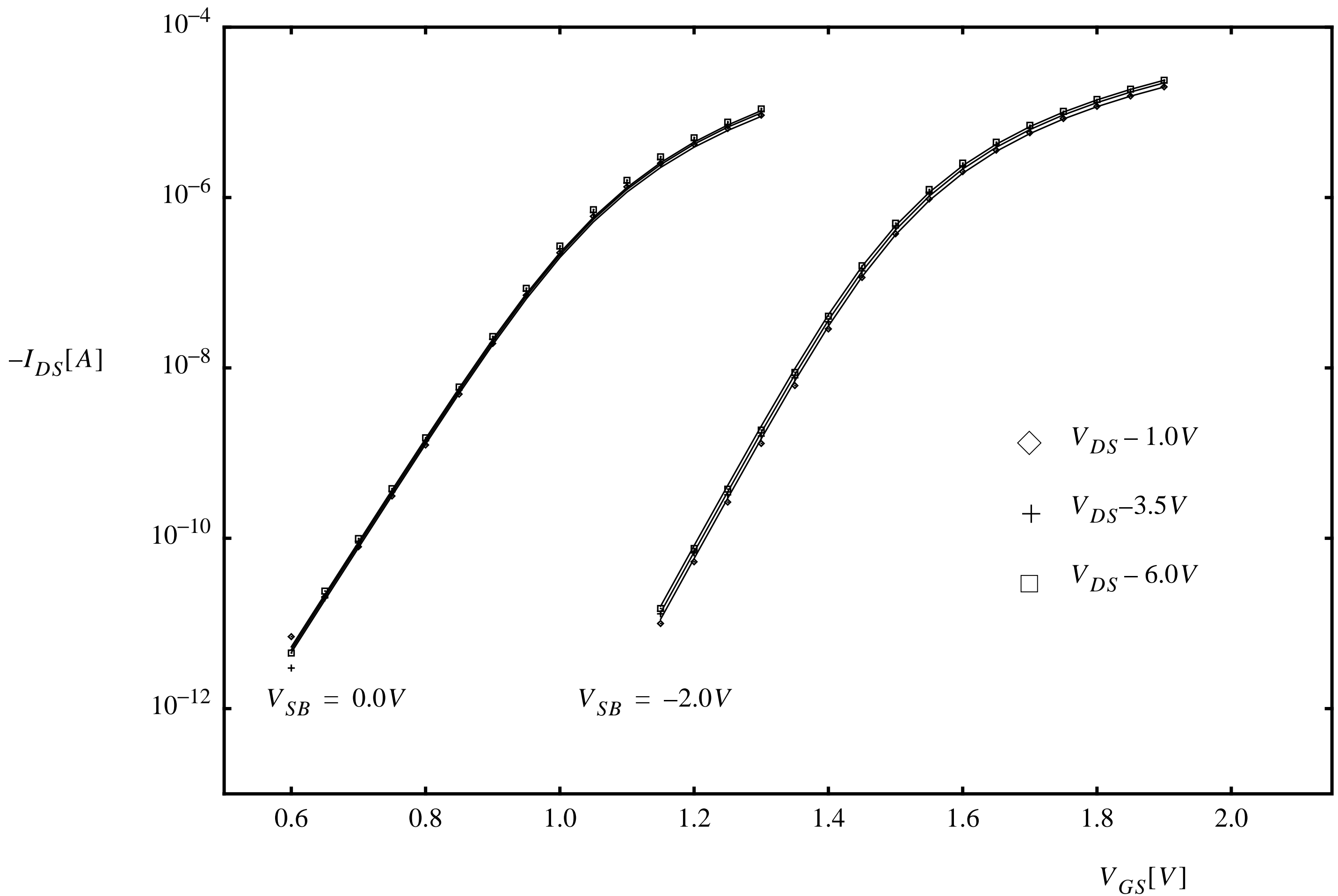

Figure 62: Calculated and measured subthreshold characteristics for p-channel transistor at different back-bias voltages (0 and -2 Volts); the calculated characteristics are presented by fully drawn lines, the measured characteristics are presented by marks!

Drain Conductance

The drain conductance characteristics have already been given in fig. 49 and fig. 50. For the p-channel device the average deviation amounts to 6%, while for the n-channel device the latter has a value of 8%. The largest deviations (21% and 41%, respectively) occur in the transition region between the linear and the saturation mode at a gate voltage of 5 Volts. Very likely the latter results does not cause a problem for practical applications. Furthermore this may not be the case for the deviations in the n-channel device at V_{DS} = 5 Volts with V_{GS} close to the threshold. In fact the close match of the g_{DS} characteristics between $V_{GS} = V_T$ and $V_{GS} = V_T + 2$ Volts indicates that the effects of g_{DS} on amplifier voltage gain can be satisfactorily calculated.

Subthreshold Characteristics

For the n-channel MOST the characteristics have already been given in fig. 46. Figure 62 gives the results for the p-channel transistor. Owing to the large range of current values involved and the fact that a small error in the small-size effects of the threshold voltage causes a large error in the current value, in this case the largest deviations have to be expected. The average deviation amounts to 14% for the n-channel and 5% for the p-channel device. One should realize however that for the latter device the small-size effects upon V_T are minor. This is also the reason that the largest deviations (44%) occur in the n-type device compared to 15% for the p-type device. Fortunately these large deviations occur at a back-bias voltage of 5 Volts in combination with a V_{DS} value of 3 Volts. Such a combination will almost never be met in practice. In fact for practical applications it is important that, in particular at low V_{SB} values, the calculated subthreshold current perfectly tracks the measured gate-bias voltage dependence. Near threshold the deviations are in the order of 10%.

10.6 Parameter scaling

10.6.1 Geometrical scaling and temperature scaling

Calculation of Transistor Geometry

$$L_E = L + \Delta L_{PS} - 2 \cdot \Delta L_{\text{overlap}} \tag{10.62}$$

$$W_E = W + \Delta W_{OD} - 2 \cdot \Delta W_{\text{narrow}} \tag{10.63}$$

WARNING : L_E and W_E after calculation can not be less than 0 !

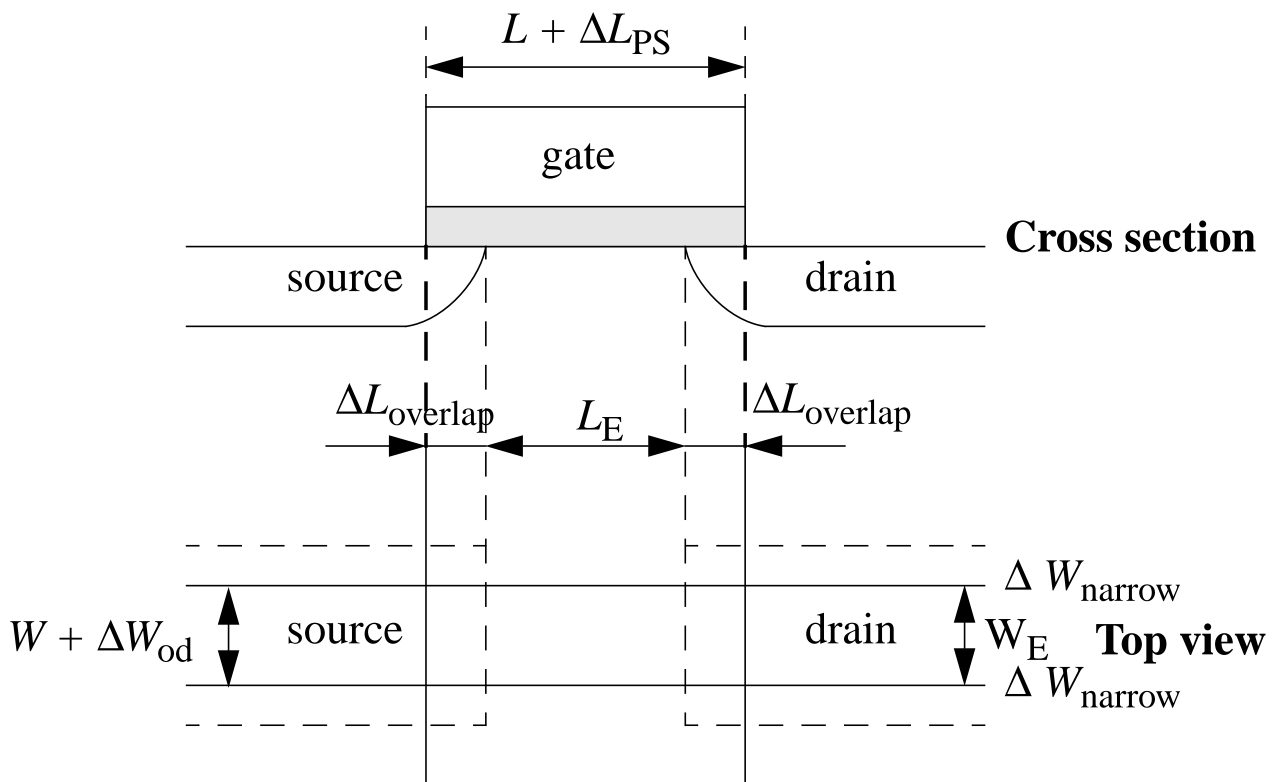

Figure 63: Specification of the dimensions of an MOS transistor

Calculation of Transistor Temperature

T_A is the ambient or the circuit temperature.

$$T_{KR} = T_0 + T_R \tag{10.64}$$

$$T_{KD} = T_0 + T_A + \Delta T_A \tag{10.65}$$

Calculation of Threshold-Voltage Parameters

$$\tilde{V}_{T0} = V_{T0R} + (T_{KD} - T_{KR}) \cdot S_{T;V_{T0}} \tag{10.66}$$

$$G_{P,E} = f_{\beta,1} \cdot \frac{L_{P,1}}{L_E}\left\{1 - \exp\left(-\frac{L_E}{L_{P,1}}\right)\right\} + \tag{10.67}$$

$$f_{\beta,2} \cdot \frac{L_{P,2}}{L_E}\left\{1 - \exp\left(-\frac{L_E}{L_{P,2}}\right)\right\}$$

$$G_{P,ER} = f_{\beta,1} \cdot \frac{L_{P,1}}{L_{ER}}\left\{1 - \exp\left(-\frac{L_{ER}}{L_{P,1}}\right)\right\} + \tag{10.68}$$

$$f_{\beta,2} \cdot \frac{L_{P,2}}{L_{ER}}\left\{1 - \exp\left(-\frac{L_{ER}}{L_{P,2}}\right)\right\}$$

✓ Note

In the circuit simulator care should be taken that

$1 + G_{P,E} \geq 10^{-15}$

$1 + G_{P,ER} \geq 10^{-15}$

$$V_{T0} = \tilde{V}_{T0} + \left(\frac{1}{L_E} - \frac{1}{L_{ER}}\right) \cdot S_{L;V_{T0}} + \left(\frac{1}{L_E^2} - \frac{1}{L_{ER}^2}\right) \cdot S_{L2;V_{T0}} + \tag{10.69}$$

$$(G_{P,E} - G_{P,ER}) \cdot S_{L3;V_{T0}} + \left(\frac{1}{W_E} - \frac{1}{W_{ER}}\right) \cdot S_{W;V_{T0}}$$

$$K_0 = K_{0R} + \left(\frac{1}{L_E} - \frac{1}{L_{ER}}\right) \cdot S_{L;K_0} + \left(\frac{1}{L_E^2} - \frac{1}{L_{ER}^2}\right) \cdot S_{L2;K_0} + \tag{10.70}$$

$$\left(\frac{1}{W_E} - \frac{1}{W_{ER}}\right) \cdot S_{W;K_0}$$

$$K = K_R + \left(\frac{1}{L_E} - \frac{1}{L_{ER}}\right) \cdot S_{L;K} + \left(\frac{1}{L_E^2} - \frac{1}{L_{ER}^2}\right) \cdot S_{L2;K} + \tag{10.71}$$

$$\left(\frac{1}{W_E} - \frac{1}{W_{ER}}\right) \cdot S_{W;K}$$

$$S_{T;\phi_B} = \frac{\phi_{BR} - 1.13 - 2.5 \cdot 10^{-4} \cdot T_{KR}}{300} \tag{10.72}$$

$$\phi_B = \phi_{BR} + (T_{KD} - T_{KR}) \cdot S_{T;\phi_B} \tag{10.73}$$

$$V_{SBX} = V_{SBXR} + \left(\frac{1}{L_E} - \frac{1}{L_{ER}}\right) \cdot S_{L;V_{SBX}} + \left(\frac{1}{W_E} - \frac{1}{W_{ER}}\right) \cdot S_{W;V_{SBX}} \tag{10.74}$$

Calculation of Channel-Current Parameters

$$\tilde{\beta} = \beta_{sq} \cdot \left(\frac{T_{KR}}{T_{KD}}\right)^{\eta_\beta} \tag{10.75}$$

$$\beta = \frac{\tilde{\beta}}{1 + G_{P,E}} \cdot \frac{W_E}{L_E} \tag{10.76}$$

$$\tilde{\theta}_1 = \theta_{1R} + (T_{KD} - T_{KR}) \cdot S_{T;\theta_1,R} \tag{10.77}$$

$$S_{L;\theta_1} = S_{L;\theta_1,R} + (T_{KD} - T_{KR}) \cdot S_{T,L;\theta_1} \tag{10.78}$$

$$W_{EDOG} = W_{DOG} + \Delta W_{OD} - 2 \cdot \Delta W_{\mathrm{narrow}} \tag{10.79}$$

$W_{EDOG} \leq W_{ER}$

$W \geq W_{DOG}$:

$$\theta_1 = \tilde{\theta}_1 + \left\{\frac{1}{L_E \cdot (1 + g_{\theta_1} \cdot G_{P,E})} - \frac{1}{L_{ER} \cdot (1 + g_{\theta_1} \cdot G_{P,ER})}\right\} \cdot S_{L;\theta_1} + \tag{10.80}$$

$$\left(\frac{1}{W_E} - \frac{1}{W_{ER}}\right) \cdot S_{W;\theta_1}$$

$W < W_{DOG}$:

$$\theta_1 = \tilde{\theta}_1 + \left\{ \frac{1}{L_E \cdot (1 + g_{\theta_1} \cdot G_{P,E})} - \frac{1}{L_{ER} \cdot (1 + g_{\theta_1} \cdot G_{P,ER})} \right\} \cdot S_{L;\theta_1} + \tag{10.81}$$

$$\left(\frac{1}{W_E} - \frac{1}{W_{ER}} \right) \cdot S_{W;\theta_1} + \left(\frac{W_E}{W_{EDOG}} - 1 \right) \cdot \frac{f_{\theta_1}}{L_E \cdot (1 + g_{\theta_1} \cdot G_{P,E})} \cdot S_{L;\theta_1}$$

$$\tilde{\theta}_2 = \theta_{2R} + (T_{KD} - T_{KR}) \cdot S_{T;\theta_2,R} \tag{10.82}$$

$$S_{L;\theta_2} = S_{L;\theta_2,R} + (T_{KD} - T_{KR}) \cdot S_{T,L;\theta_2} \tag{10.83}$$

$$\theta_2 = \tilde{\theta}_2 + \left(\frac{1}{L_E} - \frac{1}{L_{ER}} \right) \cdot S_{L;\theta_2} + \left(\frac{1}{W_E} - \frac{1}{W_{ER}} \right) \cdot S_{W;\theta_2} \tag{10.84}$$

$$\tilde{\theta}_3 = \theta_{3R} + (T_{KD} - T_{KR}) \cdot S_{T;\theta_3,R} \tag{10.85}$$

$$S_{L;\theta_3} = S_{L;\theta_3,R} + (T_{KD} - T_{KR}) \cdot S_{T,L;\theta_3} \tag{10.86}$$

$$\theta_3 = \tilde{\theta}_3 + \left(\frac{1}{L_E} - \frac{1}{L_{ER}} \right) \cdot S_{L;\theta_3} + \left(\frac{1}{W_E} - \frac{1}{W_{ER}} \right) \cdot S_{W;\theta_3} \tag{10.87}$$

Calculation of Drain-Feedback Parameters

$$\gamma_1 = \gamma_{1R} + \left(\frac{1}{L_E} - \frac{1}{L_{ER}} \right) \cdot S_{L;\gamma_1} + \left(\frac{1}{W_E} - \frac{1}{W_{ER}} \right) \cdot S_{W;\gamma_1} \tag{10.88}$$

$$\eta_{DS} = \eta_{DSR} \tag{10.89}$$

$$\alpha = \alpha_R + \left(\frac{1}{L_E^{\eta_\alpha}} - \frac{1}{L_{ER}^{\eta_\alpha}}\right) \cdot S_{L;\alpha} + \left(\frac{1}{W_E} - \frac{1}{W_{ER}}\right) \cdot S_{W;\alpha} \tag{10.90}$$

$$V_P = V_{PR} \cdot \left(\frac{L_E}{L_{ER}}\right) \tag{10.91}$$

Calculation of Sub-Threshold Parameters

$$\gamma_{00} = \gamma_{00R} + \left(\frac{1}{L_E^2} - \frac{1}{L_{ER}^2}\right) \cdot S_{L;\gamma_{00}} + (G_{P,E} - G_{P,ER}) \cdot S_{L2;\gamma_{00}} \tag{10.92}$$

$$\eta_\gamma = \eta_{\gamma R} \tag{10.93}$$

$$\tilde{m}_0 = m_{0R} + (T_{KD} - T_{KR}) \cdot S_{T;m_0} \tag{10.94}$$

$$m_0 = \tilde{m}_0 + \left(\frac{1}{\sqrt{L_e}} - \frac{1}{\sqrt{L_{ER}}}\right) \cdot S_{L;m_0} \tag{10.95}$$

$$\eta_m = \eta_{mR} \tag{10.96}$$

$$\phi_T = \frac{k \cdot T_{KD}}{q} \tag{10.97}$$

$$\varsigma_1 = \varsigma_{1R} + \left(\frac{1}{L_E^{\eta_\varsigma}} - \frac{1}{L_{ER}^{\eta_\varsigma}}\right) \cdot S_{L;\varsigma_1} \tag{10.98}$$

$$V_{SBT} = V_{SBTR} + \left(\frac{1}{L_E} - \frac{1}{L_{ER}}\right) \cdot S_{L;V_{SBT}} \tag{10.99}$$

Calculation of Weak-Avalanche Parameters

$$\tilde{a}_1 = a_{1R} + (T_{KD} - T_{KR}) \cdot S_{T;a_1} \tag{10.100}$$

$$a_1 = \tilde{a}_1 + \left(\frac{1}{L_E} - \frac{1}{L_{ER}}\right) \cdot S_{L;a_1} + \left(\frac{1}{W_E} - \frac{1}{W_{ER}}\right) \cdot S_{W;a_1} \tag{10.101}$$

$$a_2 = a_{2R} + \left(\frac{1}{L_E} - \frac{1}{L_{ER}}\right) \cdot S_{L;a_2} + \left(\frac{1}{W_E} - \frac{1}{W_{ER}}\right) \cdot S_{W;a_2} \tag{10.102}$$

$$a_3 = a_{3R} + \left(\frac{1}{L_E} - \frac{1}{L_{ER}}\right) \cdot S_{L;a_3} + \left(\frac{1}{W_E} - \frac{1}{W_{ER}}\right) \cdot S_{W;a_3} \tag{10.103}$$

Calculation of Charge Parameters

$$C_{ox} = \varepsilon_{ox} \cdot \frac{W_E \cdot L_E}{t_{ox}} \tag{10.104}$$

$$C_{GDO} = W_E \cdot C_{ol} \tag{10.105}$$

$$C_{GSO} = W_E \cdot C_{ol} \tag{10.106}$$

Calculation of Noise Parameters

$$N_T = \frac{T_{KD}}{T_{KR}} \cdot N_{TR} \tag{10.107}$$

$$N_F = \frac{W_{ER} \cdot L_{ER}}{W_E \cdot L_E} \cdot N_{FR} \tag{10.108}$$

$$N_{FA} = \frac{W_{ER} \cdot L_{ER}}{W_E \cdot L_E} \cdot N_{FAR} \tag{10.109}$$

$$N_{FB} = \frac{W_{ER} \cdot L_{ER}}{W_E \cdot L_E} \cdot N_{FBR} \tag{10.110}$$

$$N_{FC} = \frac{W_{ER} \cdot L_{ER}}{W_E \cdot L_E} \cdot N_{FCR} \tag{10.111}$$

10.6.2 MULT scaling

The *MULT* factor determines the number of equivalent parallel devices of a specified model. The *MULT* factor has to be applied on the electrical parameters. Hence after the temperature scaling and other parameter processing. Some electrical parameters cannot be specified by the user as parameters but must always be computed from geometrical parameters. They are called electrical quantities here.

The parameters: β, C_{OX}, C_{GDO}, C_{GSO}, *NF, NFA, NFB* and *NFC* are affected by the *MULT* factor:

$$\beta = \beta \times MULT$$

$$C_{OX} = C_{OX} \times MULT$$

$$C_{GDO} = C_{GDO} \times MULT$$

$$C_{GSO} = C_{GSO} \times MULT$$

$$N_F = N_F / MULT$$

$$N_{FA} = N_{FA} / MULT$$

$$N_{FB} = N_{FB} / MULT$$

$$N_{FC} = N_{FC} / MULT$$

Convention:
No distinction is made between the symbol before and after the *MULT* scaling, e.g: the symbol β represents the actual parameter after the *MULT* processing and temperature scaling. This parameter may be used to put several MOSTs in parallel.

10.7 Model Equations

Although the basic equations, given in section Basic Equations, form a complete set of model equations, they are not yet suited for a circuit simulator. Several equations have to be adapted in order to obtain smooth transitions of the characteristics between adjacent regions of operation conditions and to prevent numerical problems during the iteration process for solving the network equations. In the following section a list of numerical adaptations and elucidations is given, followed by the extended set of model equations.

The definitions of the hyp functions are found in the appendix A.

DC current model

$$\varepsilon_1 = 10^{-2} \tag{10.112}$$

$$\lambda_{10} = 0.9 \tag{10.113}$$

$$h_1 = \mathrm{hyp}_1(V_{SB} + \lambda_{10} \cdot \phi_B; \varepsilon_1) + (1 - \lambda_{10}) \cdot \phi_B \tag{10.114}$$

$$u_s = \sqrt{h_1} \tag{10.115}$$

$$u_{s0} = \sqrt{\phi_B} \tag{10.116}$$

$$u_{st} = \sqrt{V_{SBT} + \phi_B} \tag{10.117}$$

$$u_{sx} = \sqrt{V_{SBX} + \phi_B} \tag{10.118}$$

$$\varepsilon_2 = 0.1 \tag{10.119}$$

$$\Delta V_{T0} = K \cdot \left\{ \sqrt{\mathrm{hyp}_4(V_{SB};V_{SBX},\varepsilon_2) + \left(\frac{K}{K_0}\right)^2 \cdot u_{sx}^2} - \left(\frac{K}{K_0}\right) \cdot u_{sx} \right\} + \tag{10.120}$$

$$K_0 \cdot \{ \sqrt{h_1 - \mathrm{hyp}_4(V_{SB};V_{SBX},\varepsilon_2)} - u_{s0} \}$$

$$V_{T1} = V_{T0} + \Delta V_{T0} \tag{10.121}$$

$$\varepsilon_3 = 10^{-2} \tag{10.122}$$

$$u_{s1} = \mathrm{hyp}_2(u_s;u_{st},\varepsilon_3) \tag{10.123}$$

$$\gamma_0 = \gamma_{00} \cdot \left(\frac{u_{s1}}{u_{s0}}\right)^{\eta_\gamma} \tag{10.124}$$

$$\varepsilon_4 = 5 \cdot 10^{-4} \tag{10.125}$$

$$V_{GT1} = \mathrm{hyp}_1(V_{GS} - V_{T1};\varepsilon_4) \tag{10.126}$$

$$\lambda_1 = 0.1 \tag{10.127}$$

$$\lambda_2 = 10^{-4} \tag{10.128}$$

$$V_{GTX} = \frac{1}{2} \cdot \sqrt{2} \tag{10.129}$$

$$\Delta V_{T1} = \left[-\gamma_0 - \left\{\gamma_1 \cdot (V_{DS} + \lambda_2)^{\eta_{DS} - 1} - \gamma_0\right\} \cdot \frac{V_{GT1}^2}{V_{GTX}^2 + V_{GT1}^2}\right] \cdot \frac{V_{DS}^2}{V_{DS} + \lambda_1} \quad (10.130)$$

$$V_{T2} = V_{T1} + \Delta V_{T1} \quad (10.131)$$

$$m = 1 + m_0 \cdot \left(\frac{u_{s0}}{u_{s1}}\right)^{\eta_m} \quad (10.132)$$

$$V_{GT2} = V_{GS} - V_{T2} \quad (10.133)$$

$$\lambda_7 = 37 \quad (10.134)$$

$$V_{GTA} = 2 \cdot m \cdot \phi_T \cdot \lambda_7 \quad (10.135)$$

$$G_1 = \begin{cases} \exp\left(\dfrac{V_{GT2}}{2 \cdot m \cdot \phi_T}\right), & V_{GT2} < V_{GTA} \\ \text{No assignment is necessary}, & V_{GT2} \geq V_{GTA} \end{cases} \quad (10.136)$$

$$\lambda_3 = 10^{-8} \quad (10.137)$$

$$V_{GT3} = \begin{cases} 2 \cdot m \cdot \phi_T \cdot \ln(1 + G_1) + \lambda_3, & V_{GT2} < V_{GTA} \\ V_{GT2} + \lambda_3, & V_{GT2} \geq V_{GTA} \end{cases} \quad (10.138)$$

$$\lambda_4 = 0.3 \quad (10.139)$$

$$\lambda_5 = 0.1 \quad (10.140)$$

$$\delta_1 = \frac{\lambda_4}{u_s} \cdot \left\{ K + \frac{(K_0 - K) \cdot V_{SBX}^2}{V_{SBX}^2 + (\lambda_5 \cdot V_{GT1} + V_{SB})^2} \right\} \tag{10.141}$$

$$\lambda_9 = 0.1 \tag{10.142}$$

$$\varepsilon_8 = 0.001 \tag{10.143}$$

$$V_{DSS1} = \frac{V_{GT3}}{1 + \delta_1} \cdot \frac{2}{1 + \sqrt{\lambda_9 + \mathrm{hyp}_1 \cdot \left(1 - \lambda_9 + \frac{2 \cdot \theta_3 \cdot V_{GT3}}{1 + \delta_1}; \varepsilon_8\right)}} \tag{10.144}$$

$$\lambda_6 = 0.3 \tag{10.145}$$

$$V_{DSSX} = 1 \tag{10.146}$$

$$\varepsilon_5 = \lambda_6 \cdot \frac{V_{DSS1}}{V_{DSSX} + V_{DSS1}} \tag{10.147}$$

$$V_{DS1} = \mathrm{hyp}_5(V_{DS}; V_{DSS1}, \varepsilon_5) \tag{10.148}$$

$$G_2 = 1 + \alpha \cdot \ln\left(1 + \frac{V_{DS} - V_{DS1}}{V_P}\right) \tag{10.149}$$

$$G_3 = \begin{cases} \dfrac{\varsigma_1 \cdot \left\{1 - \exp\left(\dfrac{-V_{DS}}{\phi_T}\right)\right\} + G_1 \cdot G_2}{\dfrac{1}{\varsigma_1} + G_1}, & V_{GT2} < V_{GTA} \\ G_2, & V_{GT2} \geq V_{GTA} \end{cases} \tag{10.150}$$

$$I_{DS} = \beta \cdot G_3 \tag{10.151}$$

$$\cdot \frac{V_{GT3} \cdot V_{DS1} - \left(\dfrac{1 + \delta_1}{2}\right) \cdot V_{DS1}^2}{\{1 + \theta_1 \cdot V_{GT1} + \theta_2 \cdot (u_s - u_{s0})\} \cdot (\lambda_9 + \mathrm{hyp}_1 \cdot (1 - \lambda_9 + \theta_3 \cdot V_{DS1}; \varepsilon_8))}$$

$$V_{DSA} = a_3 \cdot V_{DSS1} \tag{10.152}$$

$$I_{AVL} = \begin{cases} 0, & V_{DS} \leq V_{DSA} \\ I_{DS} \cdot a_1 \cdot \exp\left(\dfrac{-a_2}{V_{DS} - V_{DSA}}\right), & V_{DS} > V_{DSA} \end{cases} \tag{10.153}$$

Charge model

$$V_{DB} = V_{DS} + V_{SB} \tag{10.154}$$

$$h_2 = \text{hyp}_1(V_{DB} + \lambda_{10} \cdot \phi_B;\varepsilon_1) + (1 - \lambda_{10}) \cdot \phi_B \tag{10.155}$$

$$\Delta V_{T0d} = K \cdot \left\{ \sqrt{\text{hyp}_4(V_{DB};V_{SBX},\varepsilon_2) + \left(\frac{K}{K_0}\right)^2 \cdot u_{sx}^2} - \left(\frac{K}{K_0}\right) \cdot u_{sx} \right\} + \tag{10.156}$$

$$K_0 \cdot \{ \sqrt{h_2 - \text{hyp}_4(V_{DB};V_{SBX},\varepsilon_2)} - u_{s0} \}$$

$$V_{T1d} = V_{T0} + \Delta V_{T0d} \tag{10.157}$$

$$\delta_2 = \frac{\partial V_{T2}}{\partial V_{SB}} - \frac{\partial V_{T2}}{\partial V_{GS}} - \frac{\partial V_{T2}}{\partial V_{DS}} \tag{10.158}$$

$$\Delta_2 = \frac{\partial V_{GT3}}{\partial V_{SB}} + \frac{\partial V_{GT3}}{\partial V_{GS}} + \frac{\partial V_{GT3}}{\partial V_{DS}} \tag{10.159}$$

$$V_{DSS2} = \frac{V_{GT3}}{1 + \delta_2} \cdot \frac{2}{1 + \sqrt{\lambda_9 + \text{hyp}_1 \cdot \left(1 - \lambda_9 + \frac{2 \cdot \theta_3 \cdot V_{GT3}}{1 + \delta_2};\varepsilon_8\right)}} \tag{10.160}$$

$$\lambda_8 = 0.1 \tag{10.161}$$

$$\varepsilon_7 = \lambda_8 \cdot \frac{V_{DSS2}}{V_{DSSX} + V_{DSS2}} \tag{10.162}$$

$$V_{DS2} = \text{hyp}_5(V_{DS}; V_{DSS2}, \varepsilon_7) \tag{10.163}$$

$$F_J = \frac{(1+\delta_2)\cdot\{\lambda_9 + \text{hyp}_1\cdot(1-\lambda_9+\theta_3\cdot V_{DS2};\varepsilon_8)\}\cdot V_{DS2}}{2\cdot V_{GT3}-(1+\delta_2)\cdot V_{DS2}} \tag{10.164}$$

$$Q_D = -C_{OX}\cdot\left[\frac{1}{2}\cdot V_{GT3} + \Delta 2\cdot V_{DS2}\cdot\left(\frac{1}{12}\cdot F_J + \frac{1}{60}\cdot F_J^2 - \frac{1}{3}\right)\right] \tag{10.165}$$

$$Q_S = -C_{OX}\cdot\left[\frac{1}{2}\cdot V_{GT3} + \Delta 2\cdot V_{DS2}\cdot\left(\frac{1}{12}\cdot F_J - \frac{1}{60}\cdot F_J^2 - \frac{1}{6}\right)\right] \tag{10.166}$$

$$\varepsilon_6 = 0.03 \tag{10.167}$$

$$V_{GB} = V_{GS} + V_{SB} \tag{10.168}$$

$$V_{FB} = V_{T0} - \phi_B - K_0\sqrt{\phi_B} \tag{10.169}$$

$$Q_{BS} = \begin{cases} -C_{OX}\cdot\text{hyp}_3(V_{GB}-V_{FB}; V_{SB}+V_{T1}-V_{FB}, \varepsilon_6), & V_{GB} < V_{FB} \\ -C_{OX}\cdot K_0\left[-\frac{K_0}{2} + \right. \\ \left.\left[\sqrt{\left(\frac{K_0}{2}\right)^2 + \text{hyp}_3(V_{GB}-V_{FB}; V_{SB}+V_{T1}-V_{FB}, \varepsilon_6)}\right]\right], & V_{GB} \ge V_{FB} \end{cases} \tag{10.170}$$

$$Q_{BD} = \begin{cases} -C_{OX}\cdot\text{hyp}_3(V_{GB}-V_{FB}; V_{DS2}+V_{SB}+V_{T1d}-V_{FB}, \varepsilon_6), & V_{GB} < V_F \\ -C_{OX}\cdot K_0\left[-\frac{K_0}{2} + \right. \\ \left.\sqrt{\left(\frac{K_0}{2}\right)^2 + \text{hyp}_3(V_{GB}-V_{FB}; V_{DS2}+V_{SB}+V_{T1d}-V_{FB}, \varepsilon_6)}\right], & V_{GB} \ge V_{FB} \end{cases} \tag{10.171}$$

$$Q_B = \frac{1}{2} \cdot (Q_{BS} + Q_{BD}) \tag{10.172}$$

$$Q_G = -(Q_D + Q_S + Q_B) \tag{10.173}$$

Noise model

In these equations f represents the operation frequency of the transistor.

$$g_m = \frac{\partial I_{DS}}{\partial V_{GS}} \tag{10.174}$$

$$F_I = \frac{(1+\delta_1)\cdot\{\lambda_9 + \mathrm{hyp}_1\cdot(1-\lambda_9+\theta_3\cdot V_{DS1};\varepsilon_8)\}\cdot V_{DS1}}{2\cdot V_{GT3}-(1+\delta_1)\cdot V_{DS1}} \tag{10.175}$$

$$h_3 = \beta\cdot G_3 \tag{10.176}$$

$$\cdot\left[\frac{V_{GT3}-\frac{1}{2}\cdot(1+\delta_1)\cdot V_{DS1}}{\{1+\theta_1\cdot V_{GT1}+\theta_2\cdot(u_s-u_{s0})\}\cdot\{\lambda_9+\mathrm{hyp}_1\cdot(1-\lambda_9+\theta_3\cdot V_{DS1};\varepsilon_8)\}}\right]$$

$$h_4 = \lambda_9 + \mathrm{hyp}_1\cdot(1-\lambda_9+\theta_3\cdot V_{DS1};\varepsilon_8) + \frac{1}{3}\cdot F_I^2 \tag{10.177}$$

$$h_5 = \frac{V_{DSS1}}{2\cdot\phi_T} \tag{10.178}$$

$$h_6 = \begin{cases} h_3\cdot h_4, & h_4 < h_5 \\ h_3\cdot h_5, & h_4 \ge h_5 \end{cases} \tag{10.179}$$

$$S_{th} = N_T\cdot h_6 \tag{10.180}$$

if NFMOD = 0 then $$S_{fl} = N_F \cdot \frac{g_m^2}{f} \tag{10.181}$$

if NFMOD = 1 then eqn.: 10.182, 10.183, 10.184, 10.185, 10.186 and 10.187

$$N_0 = \frac{\varepsilon_{ox}}{qt_{ox}} \cdot V_{GT3} \tag{10.182}$$

$$N_L = \frac{\varepsilon_{ox}}{qt_{ox}} \cdot (V_{GT3} - V_{DS1}) \tag{10.183}$$

$$N'' = \frac{\varepsilon_{ox}}{qt_{ox}} \cdot \phi_T \cdot (m_0 + 1) \tag{10.184}$$

$$S_{wi} = N_{FA} \cdot \frac{\phi_T \cdot I_{DS}^2}{f \cdot N''^2} \tag{10.185}$$

$$S_{si} = \frac{\phi_T \cdot q^2 \cdot I_{DS} \cdot \beta \cdot t_{ox}^2}{f \cdot \varepsilon_{ox}^2 \cdot \{1 + \theta_1 \cdot V_{GT1} + \theta_2 \cdot (u_s - u_{s0})\}} \cdot \left[N_{FA} \cdot \ln\frac{N_0 + N''}{N_L + N''} + N_{FB} \cdot (N_0 - N_L) + \frac{1}{2} \cdot N_{FC} \cdot (N_0^2 - N_L^2)\right] + \frac{\phi_T \cdot I_{DS}^2}{f} \cdot \frac{G_2 - 1}{G_2} \cdot \left\{\frac{N_{FA} + N_{FB} \cdot N_L + N_{FC} \cdot N_L^2}{(N_L + N'')^2}\right\} \tag{10.186}$$

$$S_{fl} = \frac{S_{si} \cdot S_{wi}}{S_{si} + S_{wi}} \tag{10.187}$$

$$S_{ig} = N_T \cdot \frac{(2 \cdot \pi \cdot f \cdot C_{OX})^2}{3 \cdot g_m} \cdot \left(1 + 0.075 \cdot \left(\frac{2 \cdot \pi \cdot f \cdot C_{OX}}{g_m}\right)^2\right)^{-1} \tag{10.188}$$

$$\rho_{igth} = 0.4j \tag{10.189}$$

$$S_{igth} = \rho_{igth} \cdot N_T \cdot 2 \cdot \pi \cdot f \cdot C_{OX} \cdot \sqrt{\frac{g_m \cdot h_6}{3 \cdot (g_m^2 + 0.075 \cdot (2 \cdot \pi \cdot f \cdot C_{OX})^2)}}$$

$$g_m \geq 0 \tag{10.190}$$

10.7.1 Numerical adaptations

The electrical equations of MOS model 9 to be implemented are essentially based on the physical description in section 10.4. Because in circuit design equal parallel circuited transistors are frequently applied the specification of one transistor together with a multiplication factor N_{MULT} in the circuit description is convenient and saves computation time. The general and safe method to implement this mechanism into the model is to evaluate the currents, charges, noise spectral densities and their derivatives with respect to the external voltages and, at the end, to multiply them by N_{MULT}. In MOS model 9 it is allowed to circumvent these multiplications for each model evaluation during circuit simulation by adjusting some parameters.

- The dependence of the threshold voltage on the back-bias voltage is described by the Eqs. (10.1) through (10.7). Because this description is valid for $V_{SB} \geq 0$ V, and negative values of V_{SB} can occur during the iteration process of the circuit simulator, Eq. (10.1) has been replaced by the Eqs. (10.112), (10.114) and (10.115). The difference between u_s calculated according to Eq. (10.115) and u_s of Eq. (10.1) does not exceed $2 \cdot 10^{-4}$ V$^{1/2}$ for $V_{SB} \geq 0$ V.

- The threshold-voltage shift V_{T0} of Eq. (10.5) yields satisfactory results for the channel current. It is desirable to use the same threshold-voltage shift for the charge equations, which causes a problem. Because all differential capacitances have to be continuous functions of the nodal voltages, it is obvious that via Eq. (10.34) the second derivative of ΔV_{T0} with respect to V_{SB} has to be continuous. Unfortunately this does not hold for $V_{SB} = V_{SBX}$. Therefore Eq. (10.5) has been replaced by Eq. (10.120). For $V_{SB} = 0$ V the results of Eq. (10.5) and of Eq. (10.120) are equal, while the largest deviation (< 4 mV) is obtained at $V_{SB} = V_{SBX}$.

- The threshold-voltage shift ΔV_{T1}, described in Eq. (10.11), contains two parts, the first part dominates for $V_{GT1} < V_{GTX}$ and the second part for $V_{GT2} > V_{GTX}$. To balance these parts for a monotonic behaviour of I_{DS} versus V_{SB} γ_0 should not increase unlimited with V_{SB}. This clipping: Eqs. (10.7) and (10.8), occurs at $V_{SB} = V_{SBT}$, which is far out of the practical region of operation. For mathematical reasons a smooth clipping, Eq. (10.123), has to be implemented instead of Eq. (10.7).

- The equation of the threshold-voltage shift ΔV_{T1}, Eq. (10.11), provides first and second derivative functions with respect to V_{DS}, which are not well-behaved functions for $V_{DS} = 0$ V due to $\eta_{DS} \approx 0.6$. Therefore Eq. (10.11) has to be replaced by

$$\Delta V_{T1} = \left\{-\gamma_0 \frac{V_{GTX}^2}{V_{GTX}^2 + V_{GT1}^2} - \gamma_1 \frac{V_{GT1}^2}{V_{GTX}^2 + V_{GT1}^2}(V_{DS} + \lambda_2)^{\eta_{DS} - 1}\right\} \cdot \left(\frac{V_{DS}^2}{V_{DS} + \lambda_1}\right)$$

in which λ_1 and λ_2 are model constants. This equation can be simplified. The expression between braces smoothly transists from $-\gamma_0$ to $-\gamma_1 \cdot (V_{DS} + \lambda_2)^{\eta_{DS} - 1}$ which is controlled by the two weighting functions of V_{GT1} which sum equals one. Using one of these functions only, we obtain Eq. (10.130).

- The voltage V_{GS} controls via V_{GT2}, Eq. (10.14), and G_1, Eq. (10.15), the functional behaviour of V_{GT3}, Eq.(10.16) and G_3, Eq. (10.26). For the subthreshold region

$$V_{GT3} \approx 2 \cdot m \cdot \phi_T \cdot \exp\left(\frac{V_{GT2}}{2 \cdot m \cdot \phi_T}\right)$$

and

$$G_3 \approx \varsigma_1^2 \cdot \left\{1 - \exp\left(\frac{-V_{DS}}{\phi_T}\right)\right\} \quad ,$$

and for large values of V_{GS} $V_{GT3} \approx V_{GT2}$ and $G_3 \approx G_2$. Although the Eqs. (10.16) and (10.26) are well-behaved analytical functions of G_1, they will cause numerical problems due to the limited value range of the numbers, which can be represented by the computer. If x exceeds the allowed maximum value of the argument range of the exp-function $\ln\{\exp(x)\} \neq x$ and $\exp(x) \cdot y / \exp(x) \neq y$ with $y>1$. To prevent this a maximum value for the argument range λ_7 has been specified, which is the lowest-value of the computer implementations of the circuit simulator, Eq. (10.134). For small values of the arguments i.e. $V_{GT2} < V_{GTA}$, Eq. (10.135), G_1, V_{GT3} and G_3 are calculated according to Eqs. (10.15), (10.16) and (10.26). But for $V_{GT2} \geq V_{GTA}$ no assignment is done to G_1, Eq. (10.136), calculated asymptotic values are assigned to V_{GT3} and G_3 Eqs. (10.138) and (10.150).

- As V_{GT3} decreases to zero the denominator of Eq. (10.37) approaches zero. The addition of a small constant to the denominator is not a good solution for this problem because the first derivatives of Q_D and Q_S will become discontinuous functions. Therefore a small constant λ_3 has been added to V_{GT3}, Eq. (10.138).

- At the outset the charge equations for Q_D and Q_S has been derived for $V_{GS}>V_{T2}$. To extend the validity range of these original equations to the subthreshold region V_{GT3} has been introduced. The remaining problem, the discontinuous transition between the derivatives dQ_D / dV_S and dQ_S / dV_D around $V_{DS} = 0$, can be solved by replacing $1 + \delta$ in Eqs. (10.38) and (10.39) by Δ_2, Eq. (10.159). This yields the Eqs. (10.165) and (10.166).

- The derivation of the equation for the bulk charges Q_{BS} and Q_{BD}, Eqs. (10.42) and (10.43), had to be performed for three successive ranges of V_{GB}. Unfortunately, the first derivatives of Q_{BS} and Q_{BD} with respect to V_{GB} are not continuous at the boundaries $V_{SB} + V_{T2}$ and $V_{DB} + V_{T1d}$, respectively. A simple remedy is the introduction of the smoothing function hyp_3 into Eqs. (10.42) and (10.43), leading to Eqs. (10.170) and (10.171).

- Calculating the value of the spectral densities for frequency zero leads to a division by zero in Eq. (10.181) and also in Eqs. (10.188), (10.190) when $g_m = 0$. For these exceptional cases the noise spectral densities should be put to zero.

10.8 Model embedding in a circuit simulator

Although CMOS processes support n- and p-channel MOS's, Model 9 only knows n-channel devices. This can easily be circumvented by mapping a p-channel device with its bias conditions and parameter set onto an equivalent n-channel device with appropriately changed bias conditions and parameters. The criterion is that the equivalent model plus bias conditions plus parameter set should attribute the same charge and the same current value and current direction (DC, AC and noise) to any physical node involved when compared to a hypothetical model that supports both device types.

As said earlier, any circuit simulator internally identifies the terminals of a MOS transistor by a number. However, designers are used to the standard terminology of source, drain, gate and bulk. Therefore, in the context of a circuit simulator it is traditionally possible to address, say, the drain of MOS number 17, even if in reality the corresponding source is at a higher potential (n-channel case). More strongly, most circuit simulators provide for model evaluation a so-called V_{DS}, V_{GS}, and V_{SB} based on an a priori assignment of source, drain and bulk that is independent of the actual bias conditions. The basic Model 903 cannot cope with bias conditions that correspond to $V_{DS} < 0$. Again a transformation of the bias conditions is necessary. In this case, the transformation corresponds to internally reassigning source and drain, applying the standard electrical model, and then reassigning the currents and charges to the original terminals. Especially in combination with weak avalanche and with noise calculations, enormous care should be taken in incorporating these changes.

In detail, in order to embed Model 903 correctly into a circuit simulator, the following procedure, illustrated in fig. 64 should be followed.

We have assumed that indeed the simulator provides the nodal potentials V^e_D, V^e_G, V^e_S and V^e_B based on an a priori assignment of drain, gate, source and bulk.

Step 1 Calculate the voltages V_{DS}'', V_{GS}'' and V_{SB}'', and the additional voltages V_{DG}'' and V_{SG}''. The latter are used for calculating the charges associated with overlap capacitances.

Step 2 Based on n- or p-channel devices, calculate the modified voltages V'_{DS}, V'_{GS} and V'_{SB}. From here onwards only n-channel behaviour needs to be considered.

Step 3 Based on a positive or negative V'_{DS}, calculate the internal nodal voltages. At this level, the voltages - and the parameters, see below - comply to all the requirements for input quantities of Model 9.

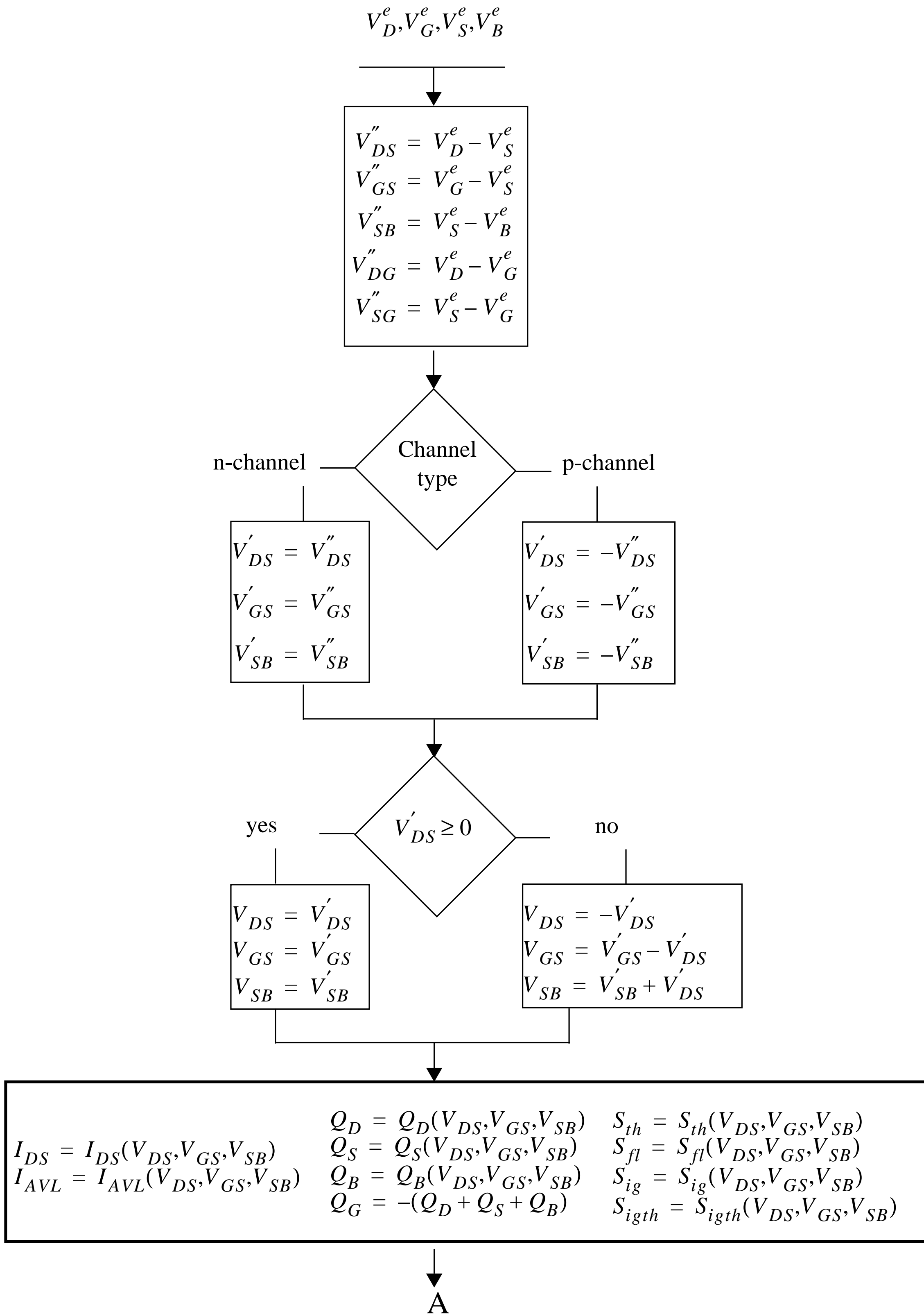
$V^e_D, V^e_G, V^e_S, V^e_B$
$V''_{DS} = V^e_D - V^e_S$
$V''_{GS} = V^e_G - V^e_S$
$V''_{SB} = V^e_S - V^e_B$
$V''_{DG} = V^e_D - V^e_G$
$V''_{SG} = V^e_S - V^e_G$
Channel type
n-channel
p-channel
$V'_{DS} = V''_{DS}$
$V'_{GS} = V''_{GS}$
$V'_{SB} = V''_{SB}$
$V'_{DS} = -V''_{DS}$
$V'_{GS} = -V''_{GS}$
$V'_{SB} = -V''_{SB}$
$V'_{DS} \geq 0$
yes
no
$V_{DS} = V'_{DS}$
$V_{GS} = V'_{GS}$
$V_{SB} = V'_{SB}$
$V_{DS} = -V'_{DS}$
$V_{GS} = V'_{GS} - V'_{DS}$
$V_{SB} = V'_{SB} + V'_{DS}$
$I_{DS} = I_{DS}(V_{DS}, V_{GS}, V_{SB})$
$I_{AVL} = I_{AVL}(V_{DS}, V_{GS}, V_{SB})$
$Q_D = Q_D(V_{DS}, V_{GS}, V_{SB})$
$Q_S = Q_S(V_{DS}, V_{GS}, V_{SB})$
$Q_B = Q_B(V_{DS}, V_{GS}, V_{SB})$
$Q_G = -(Q_D + Q_S + Q_B)$
$S_{th} = S_{th}(V_{DS}, V_{GS}, V_{SB})$
$S_{fl} = S_{fl}(V_{DS}, V_{GS}, V_{SB})$
$S_{ig} = S_{ig}(V_{DS}, V_{GS}, V_{SB})$
$S_{igth} = S_{igth}(V_{DS}, V_{GS}, V_{SB})$
A

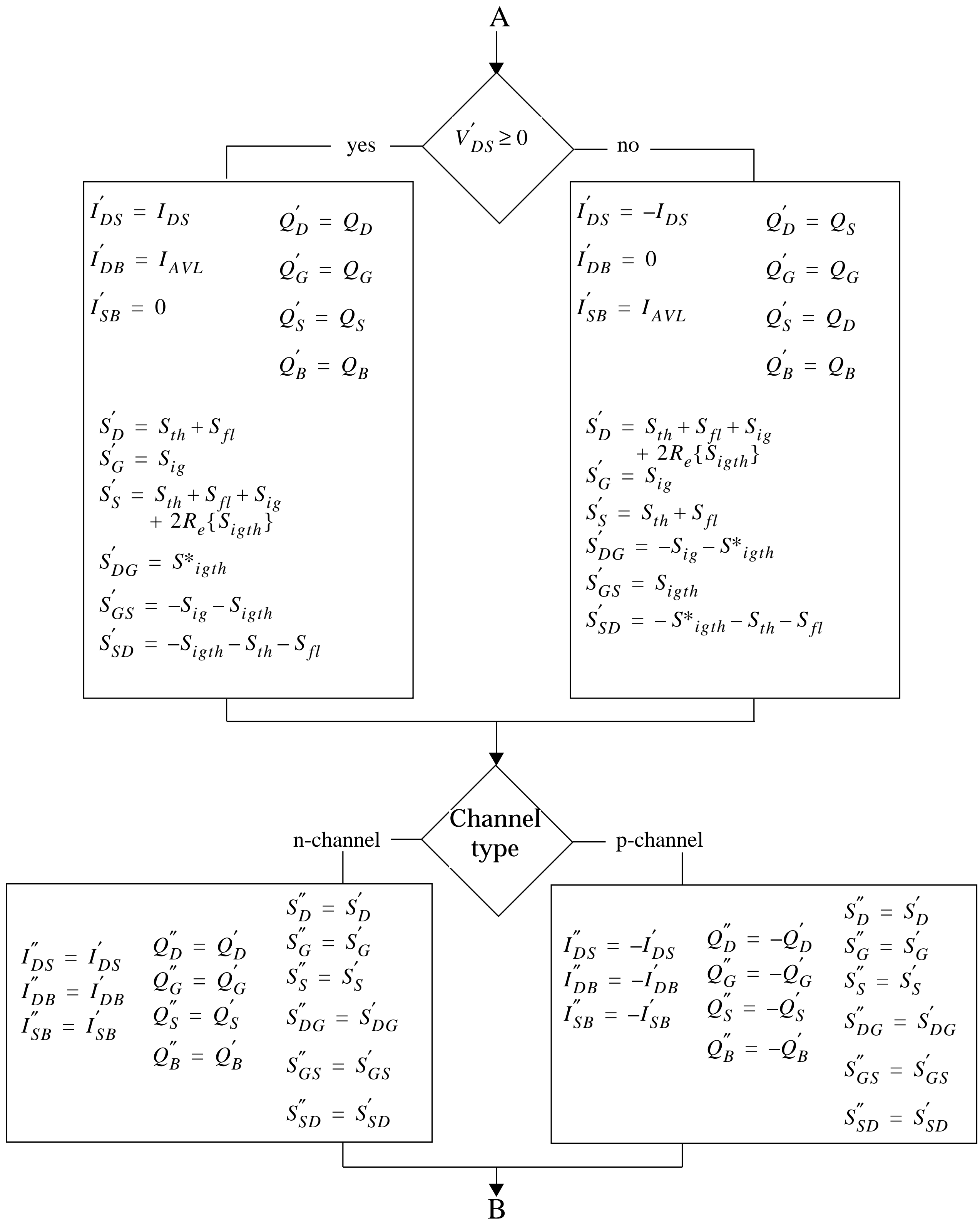
A
$V'_{DS} \geq 0$
yes
no
$I'_{DS} = I_{DS}$
$I'_{DB} = I_{AVL}$
$I'_{SB} = 0$
$Q'_D = Q_D$
$Q'_G = Q_G$
$Q'_S = Q_S$
$Q'_B = Q_B$
$S'_D = S_{th} + S_{fl}$
$S'_G = S_{ig}$
$S'_S = S_{th} + S_{fl} + S_{ig} + 2R_e\{S_{igth}\}$
$S'_{DG} = S^*_{igth}$
$S'_{GS} = -S_{ig} - S_{igth}$
$S'_{SD} = -S_{igth} - S_{th} - S_{fl}$
$I'_{DS} = -I_{DS}$
$I'_{DB} = 0$
$I'_{SB} = I_{AVL}$
$Q'_D = Q_S$
$Q'_G = Q_G$
$Q'_S = Q_D$
$Q'_B = Q_B$
$S'_D = S_{th} + S_{fl} + S_{ig} + 2R_e\{S_{igth}\}$
$S'_G = S_{ig}$
$S'_S = S_{th} + S_{fl}$
$S'_{DG} = -S_{ig} - S^*_{igth}$
$S'_{GS} = S_{igth}$
$S'_{SD} = -S^*_{igth} - S_{th} - S_{fl}$
Channel type
n-channel
p-channel
$I''_{DS} = I'_{DS}$
$I''_{DB} = I'_{DB}$
$I''_{SB} = I'_{SB}$
$Q''_D = Q'_D$
$Q''_G = Q'_G$
$Q''_S = Q'_S$
$Q''_B = Q'_B$
$S''_D = S'_D$
$S''_G = S'_G$
$S''_S = S'_S$
$S''_{DG} = S'_{DG}$
$S''_{GS} = S'_{GS}$
$S''_{SD} = S'_{SD}$
$I''_{DS} = -I'_{DS}$
$I''_{DB} = -I'_{DB}$
$I''_{SB} = -I'_{SB}$
$Q''_D = -Q'_D$
$Q''_G = -Q'_G$
$Q''_S = -Q'_S$
$Q''_B = -Q'_B$
$S''_D = S'_D$
$S''_G = S'_G$
$S''_S = S'_S$
$S''_{DG} = S'_{DG}$
$S''_{GS} = S'_{GS}$
$S''_{SD} = S'_{SD}$
B

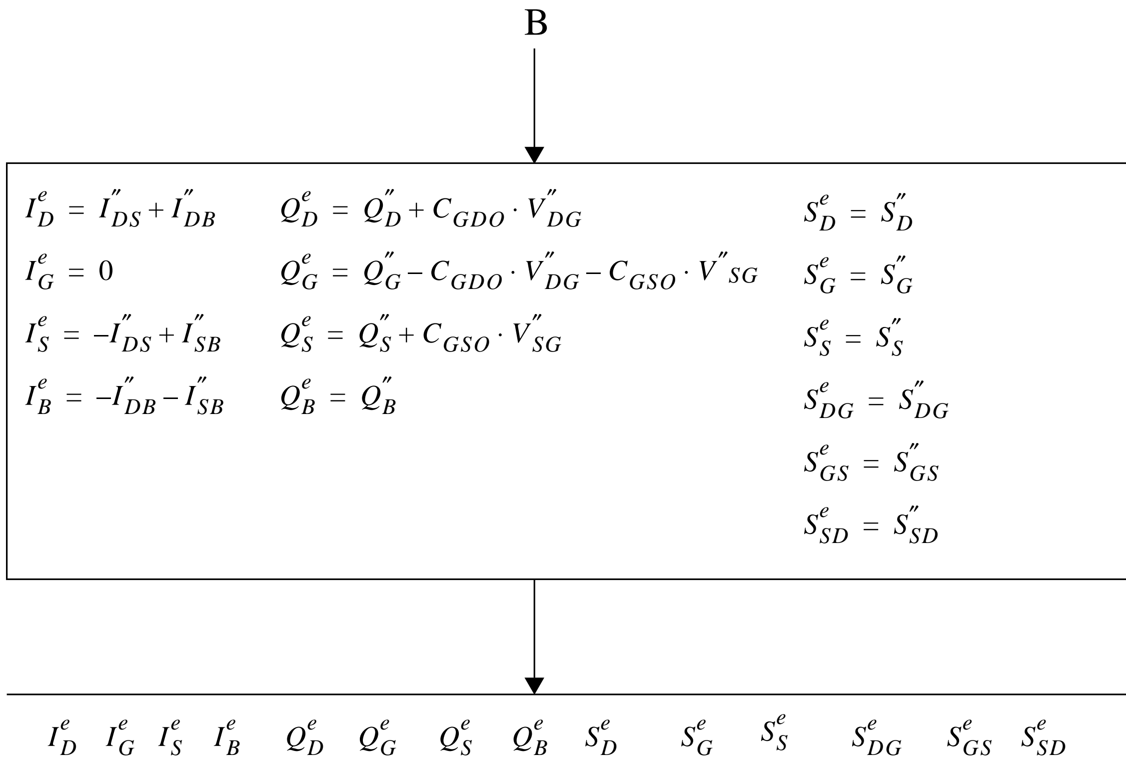

Figure 64: Transformation scheme

Step 4 Evaluate all the internal output quantities - channel current, weak-avalanche current, nodal charges, and noise-power spectral densities - using the standard Model 9 equations and the internal voltages.

Step 5 Correct the internal output quantities for a possible source-drain interchange. In fact, this directly establishes the external noise-power spectral densities.

Step 6 Correct for a possible p-channel transformation.

Step 7 Change from branch current to nodal currents, establishing the external current output quantities. Calculate the overlap charges that are related to the physical regions and add them to the nodal charges, thus forming the external charge output quantities.

It is customary to have separate user models in the circuit simulators for p- and n-channel transistors. In that manner it is easy to use different "maxi-set" parameters for the two channel types. As a consequence, the changes in the parameter values necessary for a p-channel-type transistor are normally already included in the parameter sets on file. The changes should not be included in the simulator. It is the responsibility of the persons that do the parameter determination to do so!

10.8.1 Cross spectral densities of noise currents in MOS MODEL 9

The cross spectral densities as mentioned in the figure 64 are found in the following way (See also fig. 55, [25] and [26]):

The noise currents i_s, i_d and i_g, (all in $A/\sqrt{Hz}$) are defined as in figure below:

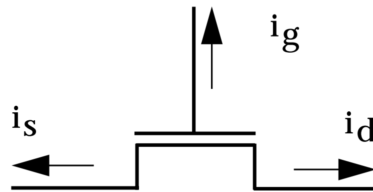

Figure 65: Noise currents in a MOSFET

Here i_d consists of two (uncorrelated) parts $i_{D,\,th}$ and $i_{D,\,fl}$, describing the thermal noise and flicker noise respectively:

$$i_D = i_{D,\,th} + i_{D,\,fl} \tag{10.191}$$

Conservation of current and no noise current flowing to the bulk, leads to:

$$i_S = -i_D - i_G \tag{10.192}$$

Noise spectral densities are defined by:

$$S_{th} \equiv \langle i_{D,\,th} i^*{}_{D,\,th} \rangle \tag{10.193}$$

$$S_{fl} \equiv \langle i_{D,\,fl} i^*{}_{D,\,fl} \rangle \tag{10.194}$$

$$S_{ig} \equiv \langle i_G i^*{}_G \rangle \tag{10.195}$$

where $\langle\ \rangle$ denotes the time average. Gate current amd drain current thermal noise are correlated. The correlation is given by the complex spectral density S_{igth}:

$$S_{igth} \equiv \langle i_G i^*_{D,\,th} \rangle \tag{10.196}$$

$$S_S \equiv \langle i_S i^*_S \rangle$$

$$= \langle (-i_D - i_G)(-i_D - i_G)^* \rangle$$

$$= \langle i_D i^*_D \rangle + \langle i_G i^*_G \rangle + \langle i_D i^*_G \rangle + \langle i_G i^*_D \rangle \tag{10.197}$$

$$= S_{th} + S_{fl} + S_{ig} + 2Re \cdot (S_{igth}) \tag{10.198}$$

The noise spectral densities S_D and S_G are simply:

$$S_D = S_{th} + S_{fl} \tag{10.199}$$

$$S_G = S_{ig} \tag{10.200}$$

Now we turn to the cross-spectral densities and calculate S_{DG}:

$$S_{DG} = \langle i_D i^*_G \rangle$$

$$= \langle i_{D,\,th} i^*_G \rangle + \langle i_{D,\,fl} i^*_G \rangle$$

$$= S^*_{igth} \tag{10.201}$$

S_{GD} is the complex conjugate of S_{DG}:

$$S_{GD} = \langle i_G i^*_D \rangle = S_{igth}$$

Similarly, S_{GS} is given by:

$$S_{GS} = \langle i_G i^*{}_S \rangle$$

$$= \langle i_G(-i_D - i_G)^* \rangle$$

$$= -\langle i_G i^*{}_D \rangle - \langle i_G i^*{}_G \rangle$$

$$= -\langle i_G i^*{}_{D,\,th} \rangle - \langle i_G i^*{}_{D,\,fl} \rangle - \langle i_G i^*{}_G \rangle$$

$$= -S_{igth} - S_{ig} \quad (10.202)$$

S_{SG} is the complex conjugate of S_{GS} :

$$= -S^*{}_{igth} - S_{ig} \quad (10.203)$$

$$S_{SD} = \langle i_S i^*{}_D \rangle$$

$$= \langle (-i_D - i_G) i^*{}_D \rangle$$

$$= S_{th} - S_{fl} - S_{igth} \quad (10.204)$$

$$S_{DS} = -S_{th} - S_{fl} - S^*{}_{igth} \quad (10.205)$$

It is convenient to summarize the results in matrix form:

$$\bar{\bar{S}} = \begin{bmatrix} S_D & S_{DG} & S_{DS} \\ S_{GD} & S_G & S_{GS} \\ S_{SD} & S_{SG} & S_S \end{bmatrix}$$

$$= \begin{bmatrix} S_{th} + S_{fl} & S^*_{igth} & -S_{th} - S_{fl} - S^*_{igth} \\ S_{igth} & S_{ig} & -S_{igth} - S_{ig} \\ -S_{th} - S_{fl} - S_{igth} & -S^*_{igth} - S_{ig} & S_{th} + S_{fl} + S_{ig} + 2Re \cdot (S_{igth}) \end{bmatrix} \quad (10.206)$$

The above applies to the case $V_{DS} \geq 0$. In case $V_{DS} < 0$ we obtain the right equations from equation 10.206 by switching colums 1 and 3 and then switching rows 1 and 3:

$$\bar{\bar{S}} = \begin{bmatrix} S_D & S_{DG} & S_{DS} \\ S_{GD} & S_G & S_{GS} \\ S_{SD} & S_{SG} & S_S \end{bmatrix}$$

$$= \begin{bmatrix} S_{th} + S_{fl} + S_{ig} + 2Re \cdot (S_{igth}) & -S^*_{igth} - S_{ig} & -S_{th} - S_{fl} - S_{igth} \\ -S_{igth} - S_{ig} & S_{ig} & S_{igth} \\ -S_{th} - S_{fl} - S^*_{igth} & S^*_{igth} & S_{th} + S_{fl} \end{bmatrix} \quad (10.207)$$

10.9 Parameter Extraction Method

The parameter extraction for MOST model 9 using an **optimisation method** is described step-by-step in the scheme below. The equations used for the parameter extraction are the basic equations of section 10.4. The simultaneous determination of all parameters is not possible, because the value of some parameters can be wrong due to suboptimisation. Therefore it is more practical to split the parameters into five groups, and, for each group, to measure the characteristics according to the indicated conditions and to determine the particular parameters. It should be noticed that for the p-channel MOST all voltage and current values have to change sign upon entering the optimisation programme as a p-MOST is treated as an equivalent n-MOST.

The bias conditions to be used for the measurements are dependent on the supply voltage of the process. Of course it is advisable to restrict the range of voltages to this supply voltage V_{sup}. Otherwise physical effects, atypical for normal transistor operation and therefore less well described by MOST model 9, may dominate the characteristics. This can lead for certain processes to parameter values dependent on the selected range of voltages.

Before the optimisation starts a parameter set has to be determined which contains a first estimation of the parameters to be extracted and the parameters which remain constant. The values of ϕ_B and ϕ_T are calculated from the device temperature T_{KD} and ϕ_{BR} according eqn. Eq. (10.73) and Eq. (10.96). From our experience with different processes η_{DS} is set to 0.6. The values of η_γ and η_m which characterise the subthreshold behaviour, are 2 for the double *k*-factor model and 1 for the single *k*-factor model.

With this parameter set a first optimisation following the scheme below, is performed. After this the new parameter set serves as an estimation for the second optimisation, which is performed following the same scheme. This method yields a proper set of parameters after the second optimisation. Experiments with transistors of different processes show that the parameter set does not change very much after a third optimisation.

The parameter extraction contains the following steps:

- I_D-V_{GS} :

n-channel	:	$V_{GS} = 0 \ldots V_{sup}$ (at least 10 steps). $V_{DS} = 0.1$ V $V_{BS} = 0$ V
p-channel	:	$V_{GS} = 0 \ldots -V_{sup}$ (at least 10 steps). $V_{DS} = -0.1$ V $V_{BS} = 0$ V

Determination of V_{T0}, β and θ_1.

- I_D-V_{GS}:

n-channel	:	$V_{GS} = 0 \ldots V_{sup}$ (at least 10 steps). $V_{DS} = 0.1$ V $V_{BS} = 0 \ldots -V_{sup}$
p-channel	:	$V_{GS} = 0 \ldots -V_{sup}$ (at least 10 steps). $V_{DS} = -0.1$ V $V_{BS} = 0 \ldots V_{sup}$

Determination of θ_2, k, k_0 and V_{SBX} for a n-channel and determination of θ_2 and k for a p-channel.

It is recommended not to incorporate the subthreshold description in the optimisation of the parameters for the I_D-V_{GS} behaviour in the linear region because suboptimisations may result in wrong values and strange characteristics. So during such an optimisation, values of I_D with V_{GS} under V_T have to be neglected.

Normally the value of k_o is larger than the value of k. But for certain processes the value of V_T versus V_{BS} shows a different behaviour and the value of k_o is smaller than the value of k. This behaviour can also be described with the model, but the parameters for this description are very difficult to determine from the above measurements. Therefore these parameters have to be determined from the measurements in the subthreshold region.

- Subthreshold:

n-channel	:	$V_{GS} = V_{GS1} \dots V_{GS2}$ with $I_{DS}(V_{GS1}) \approx 10$ pA and $V_{GS2} > V_{T1}$. V_{DS} = 3 values starting from 1 V to V_{sup} V_{BS} = 0V
p-channel	:	$V_{GS} = -V_{GS1} \dots -V_{GS2}$ with $I_{DS}(-V_{GS1}) \approx -10$ pA and $V_{GS2} > V_{T1}$. V_{DS} = 3 values starting from -1 V to $-V_{sup}$ V_{BS} = 0 V

Determination of γ_{00}, m_0 ,ζ_1.
For short-channel transistors V_{SBT} also has to be determined. Therefore three V_{BS} are used starting from 0 V to $-V_{sup}$ (for n-channel transistors) or V_{sup} (for p-channel transistors).

If V_{SBT} is not important, this parameter has to be large! In this case its value is set 100 V. In the subthreshold region it is in principle possible to determine the values of η_γ and η_m. It is also possible to verify in the subthreshold region the correctness of the values of k and k_0. If necessary these parameters can be corrected in order to obtain a better subthreshold behaviour fit.

The output conductance values are extracted from the measurements of I_D-V_{DS} by calculating in a numerical way the derivative of I_D to V_{DS}.

- Output conductance:

n-channel	:	$V_{DS} = 0.1 \dots V_{sup}$ (step 0.2 V). V_{GS} = 3 values starting above threshold, not above V_{sup} V_{BS} = 3 values starting from 0 V to $-V_{sup}$
p-channel	:	$V_{DS} = -0.1 \dots -V_{sup}$ (step -0.2 V). V_{GS} = 3 values starting below threshold, not below $-V_{sup}$ V_{BS} = 3 values starting from 0 V to V_{sup}

For analogue purposes the behaviour of the output conductance for values at V_T + 100 mV is also important.

Determination of γ_1, α. For long-channel transistors, V_P is also determined.

Because $V_P \sim L_E$, it is difficult to determine this parameter for short-channel transistors. Therefore the proportionality factor for a long-channel transistor is determined and then V_P for a short-channel transistor is calculated. With this calculated value of V_P, the values of α and γ_1 are determined for a short-channel transistor.

If there is no long-channel transistor available one can determine the parameters γ_1, α and V_P from the measurements of the output conductance at V_{BS} = 0 V. Experiments with C300 transistors show that these values are in good agreement with the values, obtained with calculation and optimisation.

Measurements with V_{GS} near threshold, can be used to check the value of γ_{00} after the optimisation of V_P, γ_1 and α.

Especially for short-channel transistors, the weak avalanche parameters also affect the behaviour of the output conductance for large V_{DS} values. The output conductance will increase again when the weak avalanche parameters are taken into account. If these parameters are not available, these output conductance values have to be neglected. Also the values in the corresponding I_D-V_{DS} characteristic have to be neglected to eliminate their influence on the value of θ_3.

- I_D-V_{DS}:

n-channel	:	V_{DS} = 0 ... V_{sup} (step 0.2 V). V_{GS} = 3 values starting above threshold, not above V_{sup} V_{BS} = 3 values starting from 0 V to $-V_{sup}$
p-channel	:	V_{DS} = -0 ... $-V_{sup}$ (step -0.2 V). V_{GS} = 3 values starting below threshold, not below $-V_{sup}$ V_{BS} = 3 values starting from 0 V to V_{sup}

Determination of θ_3.

10.9.1 Scaling of Parameters.

Using the formulae of chapter 10.4 it is possible to calculate a parameter set for a process, given the parameter set of typical transistors of this process. To accomplish this, transistors of different lengths, widths and at different temperatures have to be measured. With the results of these measurements the sensitivities of the parameters on length, width and temperature can be found. In the formulae Eq. (10.90) (for α) and Eq. (10.98) the length dependence term contains an exponent. This exponent

was introduced to be able to distinguish n- and p-channels. Out of measurements in C3DM a different behaviour of these parameters with the length was found.
For n-channels : $\eta_\alpha = 0$ and $\eta_\zeta = 0.5$
For p-channels : $\eta_\alpha = 1$ and $\eta_\zeta = 1$
During the determination of a parameter set the exponents of the two formulae are best kept constant. Optimising these exponents can lead to strange results and can become very time consuming.

Using the new parameters W_{DOG} and f_{θ_1} generally results in better modelling accuracy. A good strategy is to keep W_{DOG} fixed at the value calculated from the minimum design rules, i.e. the contact dimension plus two times the minimum OD-CO spacing. The parameter f_{θ_1} must be optimized. Care must be taken that the reference transistor is chosen in such a way that $W_{ER} \geq W_{EDOG}$.

For the determination of a geometry-scaled parameter set a three-step procedure is recommended:

1. determine minisets (V_{T0}, β, ...) for all measured devices, as explained above.

2. the width and length sensitivity coefficients are optimized by fitting the appropriate scaling rules to these miniset parameters.

3. finally the width and length sensitivity coefficients are optimized by fitting the result of the scaling rules and current equations to the measured currents of all devices simultaneously.

Note that this extraction procedure is implemented in IC-CAP, which is the standard parameter extraction tool within Philips.

Since the development of MOST model 9, parameter sets have been determined for several processes (e.g. C200, C150, C100 and C075). These can be found in the Design Manuals. For all processes good results have been obtained.

10.9.2 Parameter extraction 1/f noise

Devices

Selection of geometries suitable for the 1/f noise measurements is done as follows:

- because of the sample-to-sample spread, inherent to 1/f noise in MOSFETS, one always has to measure a large number of devices.

- because this sample-to-sample spread increases inversely proportional to the device area, one should use sufficiently large devices (area larger than $\sim 50\mu$ m^2).

- use wide and short devices to keep the noise measurable (the measured noise is proportional to W/L^3).

- "very wide" devices (eg. 100/1, 400/0.25, etc.) may be used to get some data around or even below V_{TO}, where it is difficult to perform measurements on standard geometries.

- especially when the devices are to be packaged, a gate protection is recommended.

Bias conditions

It suffices to measure data as a function of V_{GS} in the staturation regime, with $V_{DS} = V_{supply}$, because the saturation region is the most important region for circuit simulation. But of course data in the linear regime may also be taken into account in parameter extraction.

Parameter extraction

The parameter extraction strategy is as follows:

- Fit a $A \cdot \frac{1}{f} + B$ relationship to the measured drain current noise spectra. This yields, for every spectrum, the coefficient A, which is the (modelled) drain current noise spectral density at $f = 1$ Hz.

- Use the measured g_m to calculate the input-referred noise voltage spectral density at 1 Hz by dividing A by g_m^2.

- Adjust the three noise parameters N_{FAR}, N_{FBR}, and N_{FCR} to fit the data of the input-referred noise of all measured geometries simultaneously. For $NFMOD = 0$, the N_{FR} parameter should be fitted to the measurements at low gate overdrive and in saturation. For $NFMOD = 1$, one should be able to fit the entire bias range.